CHARACTERIZATION AND TRIBO-MECHANICAL ANALYSIS FOR FABRICATED ALUMINIUM ALLOY FOAM

Thesis Submitted to the Delhi Technological University, Delhi in Partial Fulfilment of the Requirements for the Award of Degree of

DOCTOR OF PHILOSOPHY

In

MECHANICAL ENGINEERING

By

ALI NAWAZ

(Roll. No. 2K18/PHD/ME/502)

Under the Supervision of

Dr. SUSHILA RANI

Associate Professor, Department of Mechanical Engineering, DTU, Delhi

Department Of Mechanical Engineering

DELHI TECHNOLOGICAL UNIVERSITY

(Formerly Delhi College of Engineering)

Shahbad Daulatpur, Main Bawana Road, Delhi-110042, India

January, 2025

ACKNOWLEDGEMENTS

I express my profound gratitude to **Dr. Sushila Rani, Associate Professor (supervisor), Department of Mechanical Engineering, Delhi Technological University, Delhi,** for her inspiring guidance, encouragement, motivation, constructive criticism and valuable suggestions throughout the course of the investigation, which paved way for the completion of my Ph.D. work.

I would like to express my sincere gratitude to **Prof. B.B Arora,** Head, Mechanical Engineering Department and **Prof. Atul Kumar Agarwal**, Chairman, DRC, Mechanical Engineering Department, Delhi Technological University, for their valuable help, motivation and extending all the necessary processing and experimental facilities during my research work. I am extremely thankful to **Prof. Qasim Murtaza** (DTU, Delhi), **Dr. Paras Kumar** (DTU, Delhi), and **Dr. Sanjay Kumar** (DTU, Delhi) for their whole hearted cooperation, allowing me to use their testing and production facility, suggestions and for making my research works a delightful experience. My sincere thanks to all the staff members of Mechanical Engineering Department, Delhi Technological University, for their support during my entire research work. I am very grateful to **Mr. Tek Chand, Mr. Phool Singh, Mr. Virender Sharma, Mr. Net Ram** and **Mr. Lallan Singh** for their valuable technical support.

I also convey my sincere thanks to **Mr. Mohd Bilal** (Research Scholars DTU) for his technical support. It will be very difficult for me to carry the whole research work without the support of my whole family, especially my father, **Mr. Ashraf Ali,** and my wife, **Mrs. Safiya Rizwan**, who all the way have supported me to proceed my research work beside all constraints and its only with their blessings and moral support that enabled me to finish this difficult task. I am always grateful and thankful to **ALMIGHTY GOD** in providing me with good health and patience in every best and worst situation, during this research work.

(Ali Nawaz)

DELHI TECHNOLOGICAL UNIVERSITY

(Formerly Delhi College of Engineering)

Shahbad Daulatpur, Main Bawana Road, Delhi-42

CANDIDATE'S DECLARATION

I hereby certify that the work which is being presented in the thesis entitled **"Characterization and Tribo-mechanical Analysis for fabricated Aluminium alloy Foam"** in partial fulfillment of the requirements for the award of the Degree of Doctor of Philosophy, submitted in the Department of Mechanical Engineering, Delhi Technological University is an authentic record of my work carried out during the period from January 2019 to March 2024 under the supervision of Dr. Sushila Rani, Associate Professor, Department of Mechanical Engineering, Delhi Technological University, Delhi. The matter presented in the thesis has not been submitted by me for the award of any other degree of this or any other university or institute. The thesis has been prepared in conformity with the rules and regulations of the Delhi Technological University, Delhi.

ALI NAWAZ

DELHI TECHNOLOGICAL UNIVERSITY

(Formerly Delhi College of Engineering)
Shahbad Daulatpur, Main Bawana Road, Delhi-42

CERTIFICATE BY THE SUPERVISOR

Certified that **Mr. ALI NAWAZ** (2K18/PHD/ME/502) has carried out the research work presented in this thesis entitled **"Characterization and Tribo-mechanical Analysis for fabricated Aluminium alloy Foam"** for the award of the degree of Doctor of Philosophy from Department of Mechanical Engineering, Delhi Technological University, Delhi, under my supervision. The thesis embodies results of original work, and studies are carried out by the student himself and the contents of the thesis do not form the basis for the award of any other degree to the candidate or to anybody else from this or any other University.

Dr. SUSHILA RANI
(Associate Professor)
Department of Mechanical Engineering
Delhi Technological University, Delhi

Date:

ABSTRACT

Aluminium alloy foam is a light-weight and porous material characterized by its unique combination of mechanical, structural, and functional properties. Aluminium alloy foams can be fabricated through various conventional and non-conventional foaming methods. In this research work, aluminium 6063 alloy foam was fabricated using stir casting method with aluminium 6063 alloy as the base metal and titanium hydride as a foaming agent. The structural and mechanical properties of the fabricated aluminium alloy foam were evaluated experimentally. The foam fabrication process was optimized through the Taguchi method coupled with grey relational analysis. The optimized process parameter setting for the foam fabrication was 2 wt.% titanium hydride, 650 °C titanium hydride mixing temperature, and 8 minutes of stirring time. The corresponding values of the optimized response variables were 53.15% porosity, 33.3 MJ/m^3 energy absorption, and 25.97 MPa flexural strength. In order to optimize the effect of wear parameters on the tribological properties of stir-cast aluminium 6063 alloy foam, the $L_9 3^3$ orthogonal array (OA) was designed and modeled statistically. The tribological properties of stir-cast aluminium 6063 alloy and its foam were evaluated by pin-on-disc tests. The optimal tribological properties of the synthesized foam are 0.29 coefficient of friction, 8.6 N frictional force, and 0.00025 mm^3/N-m specific wear rate. The tribological properties of stir-cast aluminium 6063 alloy foam are superior to those of aluminium 6063 alloy and comparable to other aluminium foams described in the literature.

Aluminium alloy foams play a vital role in the automotive, aviation, marine, and defense sectors as they are light in weight and have better mechanical, physical, and tribological properties. The fabricated aluminium 6063 alloy foam is the efficient replacement for solid materials used in vehicle frames to achieve improved drivability, stability, crashworthiness, and mileage. Also, the synthesized aluminium 6063 alloy foam is highly suitable replacement for solid materials used in loading and unloading packaged goods in the shipping industry, which involves sliding and rubbing with other surfaces.

LIST OF PUBLICATIONS

Research Papers Published/ Accepted In Journals

[1] Nawaz, Ali, and Sushila Rani. "Fabrication methods and property analysis of metal foams–a technical overview." *Materials Science and Technology* (2023):1-26. DOI:10.1080/02670836.2023.2186068. **(SCIE Indexed Journal)**.

[2] Nawaz, Ali, and Sushila Rani. "Fabrication, properties evaluation, and process optimization of aluminium 6063 alloy foam: Fabrication, évaluation des propriétés et optimisation du procédé de mousse en alliage d'aluminium 6063." *Canadian Metallurgical Quarterly* (2023): 1-16. DOI: 10.1080/00084433.2023.2233737. **(SCIE Indexed Journal)**.

[3] Nawaz, Ali, and Sushila Rani. "Microstructure and Wear Behavior Characterization of Stir-Cast Aluminium 6063 Alloy and its Foam: A Comparative Study." *Surface Review and Letters* (2024): https://doi.org/10.1142/S0218625X24500707. **(SCIE Indexed Journal)**.

Research Papers Presented in International Conferences

[1] Ali Nawaz, Sushila Rani. A review on fabrication methods and analysis of mechanical properties of metal foams. "2nd International Conference on Recent Trends in Engineering and Scientific Technology" held on 21St March 2020 at Rathinam Technical Campus, Coimbatore, India.

[2] Ali Nawaz, Sushila Rani. Fabrication and evaluation of percent porosity and density reduction of aluminium alloy foam. 1st International Conference on "Technology Innovation in Mechanical Engineering" (TIME-2021) organized by the Department of Mechanical Engineering, Sagar Institute of Science & Technology, Gandhi Nagar, Bhopal, India during 10-11 May 2021.

TABLE OF CONTENTS

Description **Page No.**

LIST OF TABLES

Table No. **Description** **Page No.**

LIST OF FIGURES

Figure No. **Description** **Page No.**

LIST OF ABRIVIATIONS

Symbol	Description
OA	Orthogonal Array
IEDs	Improvised Explosive Devices
UV	Ultra-Violet
GASARS	Solid-gas-eutectic Solidification Process
AM	Additive Manufacturing
CAD	Computer Aided Design
PBF	Powder Bed Fusion
DED	Direct Energy Deposition
SLM	Selective Laser Melting
DMLS	Direct Metal Laser Sintering
DMP	Direct Metal Printing
DMLS	Direct Metal Laser Sintering
EBM	Electron Beam Melting
LENS	Laser Engineered Net Shaping
DMD	Direct Metal Deposition
EBAM	Electron Beam Additive Manufacturing
PBF	Powder Bed Fusion
BJAM	Binder Jet Additive Manufacturing
L-PBF	Laser Powder Bed Fusion
EB-PBF	Electron Beam Powder Bed Fusion
PM	Powder Metallurgy
MWCNTs	Multi-walled Carbon Nano Tubes
CNT/AL	Carbon Nano Tube/Aluminium
CVD	Chemical Vapor Deposition
PU	Polyurethane
MSFs	Metallic Syntactic Foams
MMSFs	Metal Matrix Syntactic Foams
EP-MSF	Extended Perlite Metallic Syntactic Foam
AC-MSF	Activated Carbon Metallic Syntactic Foam
ANOVA	Analysis of Variance
AL-6063	Aluminium Alloy 6063
EDX	Energy Dispersive X-ray Analysis
SEM	Scanning Electron Microscopy
EDM	Electric Discharge Machining
UTM	Universal Testing Machine

Chapter 1
Introduction

1.1 Introduction

Metal foam is a type of cellular structure made from solid metal, commonly aluminum, featuring gas-filled pores that occupy a significant portion of its volume. These pores can either be sealed, creating a closed-cell foam, or inter-connected, resulting in an open-cell foam. Metal foams are characterized by high porosity. Metal foams retain their base metal physical properties and can be recycled back into the base metals. The coefficient of thermal expansion for metal foams remains consistent with that of the base metal. However, their thermal conductivity is lower compared to the base metal. Foams made from non-flammable metals retain their non-flammable properties and can typically be recycled back into their original base material. Various metals, including magnesium, lead, zinc, copper, bronze, titanium, steel, and gold, can be processed into foams. Due to research and process development, many metal foams are available nowadays and will increase in coming years. Metal foams available in the market are mostly aluminum or nickel-based.

At the beginning of 20^{th} century, researchers paid their attention to porous composite materials, and the patent by French researchers in 1925AD initialized the path towards the fabrication of porous materials *[1]*. Between 1950s and 1970s, numerous patents were granted, and various types of foaming processes were discovered and proposed *[2]*. In the late 1980s, researchers re-established

some of the old techniques of metal foam fabrication and discovered new ones. In the beginning, many companies conducted in house research in their laboratories and published their work. In 1990, Fraunhofer-Institute in Bremen worked in the field of metal foam fabrication and re-established old powder-based foam fabrication technique *[3, 4]*. The advent of 21st century brought new advancements in metal foam fabrication techniques. It was established that the foremost fabrication methods of metal foams are based on liquid state, solid state, vapor deposition, and electro-deposition processing techniques *[5]*. It was suggested that the quality of metal foams depends on many factors such as porosity, density, cell structure and distribution, grain size and distribution and foaming process involved and so on *[6, 7]*. The main problem encountered was to understand how metal foams are stabilized and how their stability can be enhanced to produce reliable metal foams. The stabilization mechanism of metal foams during foaming is studied under the term high-temperature colloid chemistry in the field of aqueous foam physics *[8]*. Recent developments, applications, new methods of metal foam characterization, and property analysis have been discussed in detail *[9]*.

The improved foam production methods paved the way for significant enhancement in the physical and mechanical properties of metal foams. The metallic foam of light weight metals', especially aluminium alloy foams exhibit superior mechanical and structural properties, including high porosity, low relative density, crashworthiness, high toughness and energy absorption capability *[10]*. Due to these attractive mechanical properties, metal foams are employed in various industrial sectors, including construction, automotive,

naval, aviation, defense, acoustics, and healthcare. Major application sectors of metal foams are illustrated in Fig. 1.1.

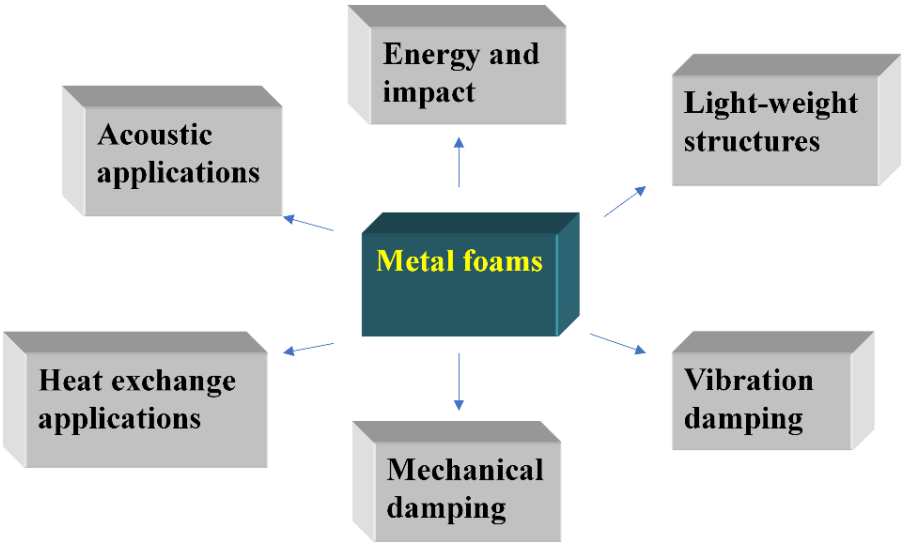

Fig. 1. 1: Major industrial applications sectors of metal foams

Metal foam manufacturing methods are based on two primary strategies. The first strategy is based on direct foaming, in which metal melt is prepared, and some non-metallic stabilizer particles are uniformly mixed for viscosity enhancement; finally, the metal melt is foamed by injecting some gases or adding foaming agents. The second strategy is based on the indirect foaming method in which precursor composite material is prepared; this precursor material contains uniformly distributed blowing agent particles. On melting of the metal matrix, expansion takes place, and foam is produced *[5]*. The five primary stages followed during metal foam fabrication through the powder compaction process (indirect foaming) are preparation of precursor material, pore initiation, pore inflation, metal foam degradation, and foam solidification *[11]*.

Although the available methods of foam production provide surety of base metal's topological structures and their constituents, researchers are trying to develop more sophisticated methods of metal foam fabrication for commercial use. Many fields of research are associated with metal foams such as microstructural characterization, mechanical property analysis and modeling of metal foam structures. Modeling metal foam structure is crucial to analyze the data collected experimentally and to help engineers in the application field. In modeling, foam structure is usually depicted by simple geometry, and the foam is represented as an effective medium. Efforts have been made to model foamed structures at various levels, ranging from micro-modeling to the modeling of fundamental components *[7, 12]*.

1.2 Classification of Metal Foams

The International Union of Pure and Applied Chemistry (IUPAC) defines foam as *"a dispersion in which a large proportion of gas by volume is dissolved in the form of gas bubbles in a liquid, solid, or gel." [13]*.The properties of metal foams mainly depend on their cell morphology, leading to their broad classification into open-pore and closed-pore foams. Open-pore foams have randomly distributed pores that are interconnected, whereas closed-pore foams contain small voids separated by well-defined membranes. Due to their high stiffness, closed-pore metal foams are utilized in structural applications. Open-pore metal foams are utilized in thermal applications like heat exchangers as they have a large surface area and internally connected highly porous structures *[14-16]*. Recently, metal syntactic foams comprising hollow particles such as

cenosphere, alumina, and aluminide hollow spheres embedded inside the metal matrix also joined the metal foams. The mechanical properties of metal syntactic foams are superior to gas foamed metal structures *[17, 18]*. Metal syntactic foams are utilized in automobile, construction, naval, and healthcare sectors *[19]*. Classification of metal foams based on pore structure is shown in Fig. 1.2.

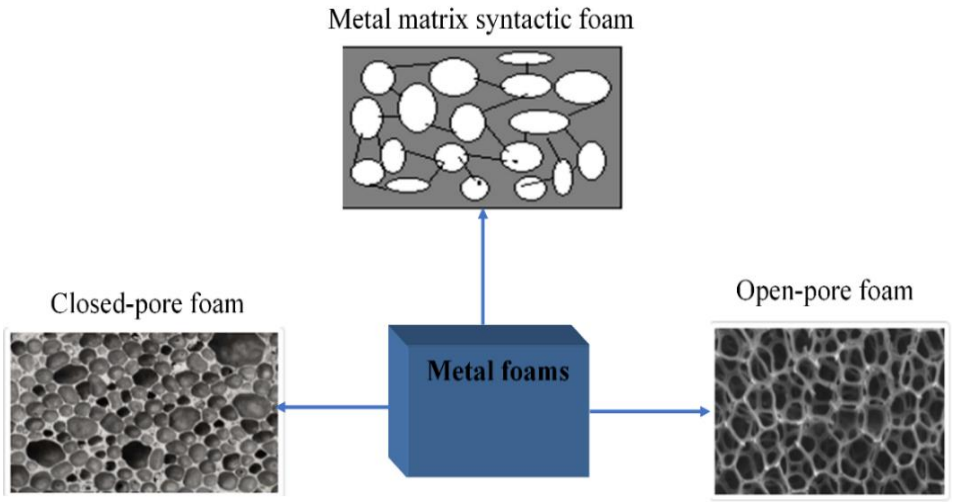

Fig. 1. 2: Classification of metal foams (Source- www.metalfoam.net)

1.3 Metal Foam Manufacturing Techniques

Metal foams, in particular, can be processed by both liquid and solid-state metal through direct or indirect foaming methods. In liquid-state processing, the foaming rate is high, with the processing temperature exceeding the melting point of the base material. In contrast, the processing temperature in solid-state processing remains below the melting point of the base material. The difference between the two manufacturing strategies, their merits, and demerits are elaborated in Table 1.1.

Table 1. 1: Differences between the metal foam manufacturing strategies

Metal Foam Manufacturing Techniques	
Direct foaming	**Indirect foaming**
In the direct foaming technique, foam is achieved by introducing gases like air, nitrogen, or argon or by adding some foaming agent, such as TiH_2, ZrH_2, MgH_2, $CaCO_3$ etc. into the molten melt.	In indirect foaming, precursor material is prepared and foamed subsequently, or molten metal is poured over inorganic granulates.
Foaming or blowing agents are directly introduced into previously blended metals in order to attain intrinsic porosity.	Extrinsic porosity can be attained by collecting metal matrix composite around pre-processed foam templates followed by subsequent foaming.
The process lacks stability and control and needs advancement in processing technology.	Foams produced by this process are more stable and reliable but costly.
A few materials are available which can be processed by this technique.	In the near future, commercial foam manufacturing industries may find this method valuable.

1.4 Motivation

Aluminium alloy foams have many interesting mechanical and physical properties including high resistance to deformation (stiffness), low specific gravity (specificweight), high compression strength, high toughness and energy absorption characteristics. Hence they are utilized in various applications ranging from structural applications to the defense sector. Aluminium foams serve key functions in vehicles, such as enhancing sound damping, reducing its weight, improving energy absorption during crashes, and mitigating the impact of IEDs in military applications. For instance, foam-filled tubes can be utilized as anti-intrusion bars. Aluminium alloy foams are of particular interest due to

their low density (0.4–0.9 g/cm^3). In particular, as compared to hollow components these foams are characterized by their stiffness, fire resistance, non-toxicity, recyclability, higher energy absorption, lower thermal conductivity, reduced magnetic permeability, and superior sound damping. In hollow car components, aluminium foams address common weaknesses related to crashes and vibrations. They are also economical to fabricate through the powder metallurgy process in comparison to the fabrication of other hollow parts through casting.

Compared to polymer foams used in vehicles, aluminium foams offer greater stiffness, strength, energyabsorption, and resistance to fire, UV light, humidity, and temperature. However, polymer foams are lighter, cheaper, and possess insulating properties. Typically, closed-cell aluminium foams reinforce structures without adding significant weight. Foam sections are pasted onto the aluminium panels to create a durable composite sandwich that provides local rigidity and longitudinal stiffness depending on the foam's thickness. One of the key advantages of aluminium foams is their consistent response to forces irrespective of their direction of application, with constant plateau stress maintained through up to 80% of the deformation process.

After the fabrication of aluminium alloy foam it is most important to analyze its microstructure and mechanical properties experimentally. In recent years, there has been growing interest in metallic foams, particularly aluminium alloy foams. These materials offer exceptional stiffness-to-weight ratios, impact energy absorption, vibration damping, noise attenuation, and electromagnetic shielding, all at relatively low densities (300 - 900 kg/m^3). Cellular materials,

including metallic, polymer and ceramic foams, provide highly attractive options for a wide range of applications such as filters, light-weight structures, biomedical implants, heat exchangers, sound absorbers, mechanical damping devices, electrodes, sensors and catalyst substrates. Although relative density has traditionally been considered the main factor affecting the stiffness and strength of foams, other characteristics such as cell packing, distribution and shape, also play a crucial role in determining their mechanical properties. The results obtained by the experimental analysis should be validated with the help of computational results.

Due to excellent and promising mechanical properties of metal foams researchers are interestedin their customized production, especially aluminium alloy foams. Theresearchers are trying to stabilize the properties of aluminium alloy foams with respect to their utilization. It is expected that metal foam market will rise all over the world in future with maximum demand in Asia-Pacific region as shown in the graph in Fig. 1.3 (Markets and Markets survey reports).

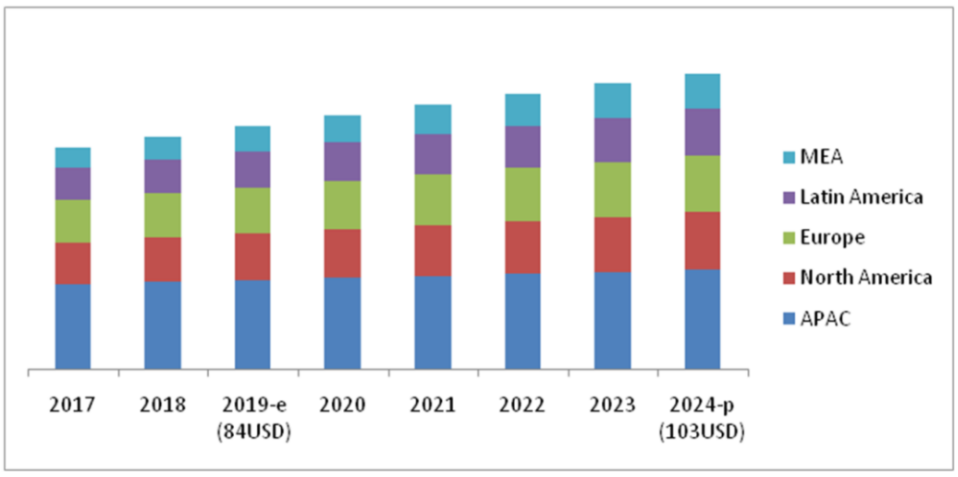

Fig. 1. 3: Metal foam market by region and USD in million

Chapter 2
Literature Review

2.1 Literature Review

Decades of research have resulted in various methods of foam production; however, some of them are feasible for mass production, keeping in mind the environmental aspects. The methods used to process metal foams have undergone various iterations. The manufacturing process employed for metal foam fabrication decides foam anatomy or pore distribution, properties, and finally its application. It is impossible to discuss all manufacturing methods suggested and incorporated by researchers and manufacturers; however, a detailed overview of traditional to advanced manufacturing techniques, which are being used for manufacturing of metal foams, is provided in the section 2.2 and 2.3 under direct and indirect foaming techniques, respectively.

2.2 Direct Foaming Techniques

Direct foaming is accomplished by introducing gases like air, argon, or nitrogen into the molten metal or by incorporating some foaming agent such as TiH_2, ZrH_2, MgH_2, $CaCO_3$, etc. To achieve intrinsic porosity, foaming or blowing agents are directly introduced into previously blended metals. The section 2.2.1 and 2.2.2 presents a brief review of conventional and technologically advanced methods of metal foam fabrication, respectively based on direct foaming techniques.

2.2.1 Conventional Foaming Methods Based on Direct Foaming Technique

In conventional foaming, the metal melts are foamed by injecting gas or mixing foaming agents. Solid-gas eutectic solidification (GASARS) is a traditional process based on direct foaming, where hydrogen is introduced into the molten metal under elevated pressure, and the mixture solidifies in a specific direction. A brief review of conventional foaming methods based on the direct foaming technique is presented in sub-sections 2.2.1.1 and 2.2.1.2.

2.2.1.1 Foaming of metal melts by injecting gas or by mixing foaming agents

In the direct foaming method, metal melt is initially prepared, with ceramic particles like silicon carbide, aluminium oxide and boron carbide mixed into it, making the composite alloy amenable for foaming. The proportion of reinforced ceramic particles generally falls between 10 - 20%, with an average particle size varying from 5 - 20 μm. A flowchart containing steps for foaming of melts by gas injection is shown in Fig. 2.1. Foam is usually obtained by injecting a gas or air directly into the molten metal alloy with the help of specially designed capillaries or frits, which are made to rotate or vibrate. As gas or air is injected into the molten alloy, bubbles are formed, which have an upward-lifting tendency. The rising bubbles accumulate with the particles in the molten alloy; some particles are attached to the melt-bubble interface. The particles in the melt-bubble interface prevent bubbles from bursting until they reach the top surface of the molten alloy. As the melt-bubble interface reaches the top surface a foamed layer is formed, which can be separated with the help of a conveyor

belt or can be guided directly into the pre-specified molds. After solidification, the foam can be cut into desired shapes. The main advantage of this process is that a large volume of low-density metal foam can be produced easily and economically. Many researchers have patented this process *[20-22]* and presently companies like Hydro Aluminium and Cymat are utilizing it.

When molten metal melts containing thickening agents such as $CaCO_3$, SiC, and Al_2O_3 are foamed by injecting gas or air, metal oxides or metal silicates are formed due to the diffusion of gas or oxygen into the metal lattice. Gases like CO_2 or H_2 is evolved, as shown in Eq. 2.1. The porosity of produced metal foam primarily depends on the gas diffusion phenomenon, which depends on metal melt temperature and the reaction rate between the reactants.

$$Metal\ melt + Thickening\ agent(CaCO_3\ or\ SiC\ or\ Al_2O_3) + Gas \rightarrow$$
$$Metal\ foam\ compounds(metal\ oxides\ or\ silicates) + gases\ (CO_2 or\ H_2)$$

Eq. 2.1

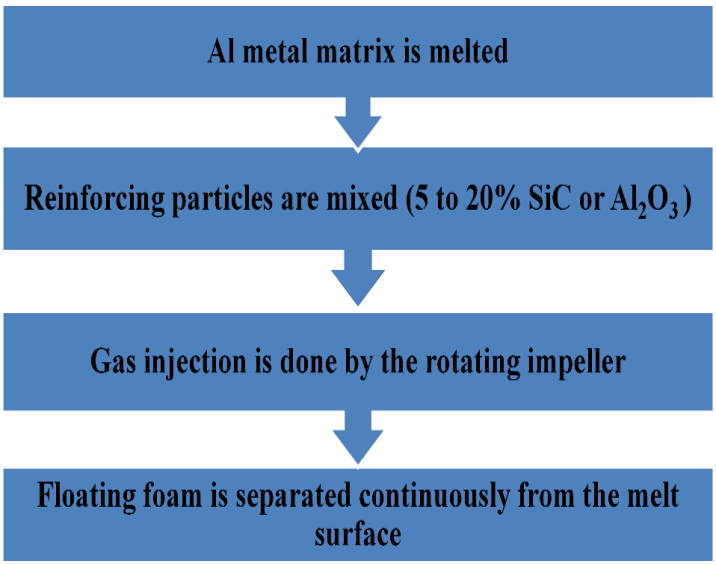

Fig. 2. 1: Flowchart for producing foams through gas infusion

The molten metal could be easily bubbled with the introduction of a blowing agent. Dissociation of the blowing agent occurs due to higher temperature, and gas is evolved; for example, titanium hydride (TiH_2), when added to the molten metal, emits hydrogen gas, and the foaming process begins. Shinko Wire Company in Amagasaki, Japan, has been fabricating foams since 1986, with a daily production of about 1,000 kg. For aluminium alloy foam fabrication, first aluminium alloy is melted and 1.5 wt. % calcium (Ca) is mixed into it at about 680°C. This molten mixture is stirred for a few minutes, forming calcium oxide (CaO), calcium aluminium oxide ($CaAl_2O_4$), or intermetallics such as Al_4Ca. This increases its viscous resistance up to five times as compared to the initial level. Titanium hydride (TiH_2) is mixed as a foaming agent into the viscous melt alloy, as the agent begins to dissociate, hydrogen gas is evolved, due to which the molten alloy begins to expand at constant pressure and finally occupies the entire volume of the foaming container. The liquid aluminium alloy foam is cooled down to achieve solid aluminium alloy foam. This solid foam can be processed further to make it suitable for desired applications. This method of foam fabrication is well known as the ALPORAS process, and this result in uniform structure metal foam.

The steps of the ALPORAS process are shown through the flowchart in Fig. 2.2. The pore structure of this type of metal foam was found to be more uniform with better mechanical properties. Table 2.1 contains a brief literature review of direct foaming methods of metal melts by gas injection or foaming agents.

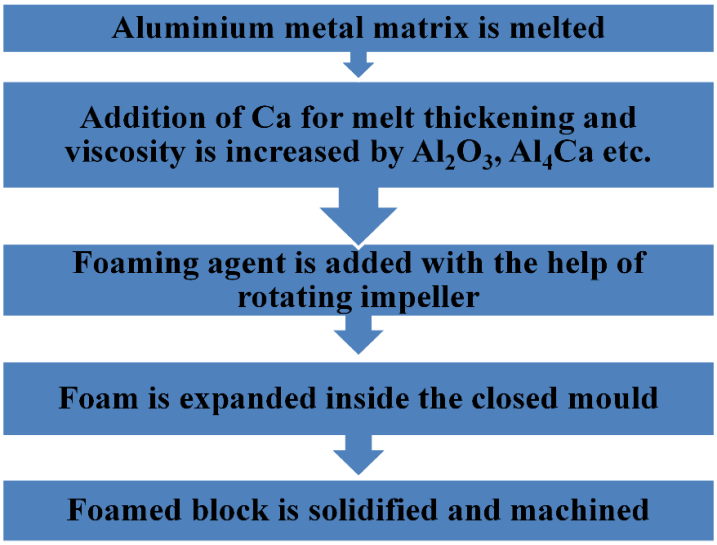

Fig. 2. 2: Flowchart for direct foaming of melts by the foaming agent

When molten metal melts are foamed by mixing blowing agents like TiH_2, the reaction mechanism between metal melt and TiH_2 is controlled by the reaction between titanium and metal melt and the hydrogen atom diffusion into the titanium lattices as shown in Eq. 2.2. The reaction mechanism is controlled by a chemical reaction at lower temperatures, and by chemical reaction and diffusion mechanism at higher temperatures.

$$3Al + TiH_2 \rightarrow Al_3Ti + H_2 \qquad \text{Eq. 2.2}$$

Table 2. 1: Brief literature review of direct foaming methods

Authors	Materials Used	Foaming Technique	Results & Findings
Lloyd et al. [23]	Metal matrix Reinforcing particles Blowing gases	Direct foaming method by gas injection.	This process's advantage is producing large volume of aluminium foam at low price with low density and porosities ranging from 80% to 97%.

Prakash et al. [24]	Aluminium matrix Reinforcing particles Blowing gases	Direct foaming method by gas injection.	Deformation in a compressive strength test occurs in a band and travels outward, whereas deformation in an indentation test arises around the indenter and proceeds radially outward. Cell membranes cracks are linked to a wide damage zone, which increases the particular impact strength.
Akiyama et al. [25]	Metal melt Reinforcing particles (Ca metal) Blowing agent (TiH_2)	The decomposition of the foaming agent produces gases that accelerate the bubbling operation.	In Japan, this process is used for small-scale production. Calcium is used to stabilize the metal and titanium hydride is utilized as a gas-releasing agent. The size of the foamed aluminium samples is approximately 2000x1000x600 mm. The density of foamed samples varies from 0.25 to 0.33 g/cm^3.
Miyoshi et al.[26]	Metal melt 1-2% Calcium(Ca) as a thickening agent 1–2% TiH_2 or CaH_2 as a foaming agent	ALPORAS process	The quality of metal foam relies on the extent of consistent blending of gas-releasing and thickening agents, mixing temperature, and the rate at which melt cools. The relative densities of metal foam produced by this method range from 0.2 to 0.9
Banhart, J. [5]	-	Review paper	Direct foaming methods are cost-efficient in terms of initial setup and material costs. ALPORAS foams are comparatively more expensive

	than metal matrix composite (MMC) foams. MMC foams are likely more cost-effective than other porous materials.

2.2.1.2 Solid-gas eutectic solidification process (GASARS)

Some metals have a eutectic relationship with gaseous hydrogen therefore, when these metals are melted in the presence of hydrogen at elevated pressure, molten metal uniformly charged with hydrogen is obtained. On cooling, this charged melt passes through a eutectic transition and results in a two phase heterogeneous system, as shown in Eq. 2.3.

$$Metals\ (L) \xrightarrow[and\ directional\ solidification]{heating\ at\ higher\ pressure\ in\ presence\ of\ H_2} \alpha + \beta \qquad \text{Eq. 2.3}$$

When the molten metal is allowed to cool, directional solidification takes place at an average front velocity between 0.05 and 5 mm/s, ultimately, hydrogen accumulates near the solidification front, leading to the formation of gas bubbles *[27]*. These bubbles remain intact with molten metal, and the pores are formed. The pore's shape, size and structure largely depend on the quantity of hydrogen, pressure above the molten metal surface, direction of solidification, rate of heat removal and the composition of molten metal alloy. The process in which metal melt is produced in a refractory crucible, hydrogen at high pressure is dissolved into the molten metal, and the mixture is solidified directionally is termed GASARS. The Steps for making GASARS are shown in Fig. 2.3, and Table 2.2 contains a brief literature review of GASARS processes.

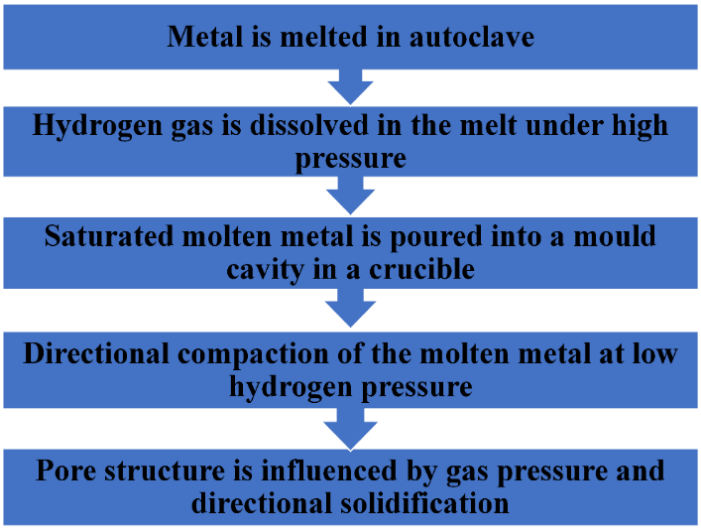

Fig. 2. 3: Steps for foaming of metals by GASAR process

Table 2. 2: Brief literature review of GASARS processes

Authors	Materials Used	Foaming Technique	Results & Findings
Shapovalov [28]	Metal melts in a hydrogen environment at high pressure.	GASARS technique	Pore structure mainly depends on the solidification method; the casting crucible may be of any shape.
Zheng et al.[29]	Metal melts in a hydrogen environment at high pressure.	GASARS technique	Directional solidification of the melt helps to fabricate foams containing large pores. Radial and axial pores are obtained by using the cylindrical vessels. The porosities ranging from 5% to 75% are achieved by this method, and this method can be used to foam metals having moderate melting points.

Simone et al. [30]	Metal melts in a hydrogen environment at high pressure.	GASARS technique	The properties like Young's modulus and yield strength of porous copper are directly proportional to its relative density; however, densification strains are indirectly proportional.

2.2.2 Non-Conventional Foaming Methods Based on Direct Foaming Technique

Traditional foaming methods are being improved through innovations aimed at lowering costs, increasing productivity, and controlling pore morphology. Metal foams produced through non-conventional methods are suitable and frequently preferred for various operational and architectural applications, with prosthetics, electrical, and thermal applications. Metal foams produced through non-conventional methods are versatile and stable. A brief review of non-conventional foaming methods based on the direct foaming technique is presented in sub-section 2.2.2.1.

2.2.2.1 Additive manufacturing (AM) methods

The additive manufacturing (AM) process involves layer-by-layer material deposition to obtain regular and intricate design objects by utilizing CAD models. AM of metal foams is performed through liquid-state and solid-state processing. The liquid-state AM process is versatile and yields higher productivity; however, the solid-state AM process is more complex, diverse, and renders low productivity. The AM process is expensive due to high initial setup and material costs *[15]*.

Literature suggests that AM can be accomplished by seven different processes *[31]*. This section deals with the additive manufacturing of metal foams, which can be accomplished through Powder Bed Fusion (PBF) and Direct Energy Deposition method (DED) by utilizing either a laser beam or an electron beam as a heat source *[32]*. PBF and DED methods can be accomplished by different processes such as Selective Laser Melting (SLM), Direct Metal Laser Sintering (DMLS), Direct Metal Printing (DMP), Laser Cusing (LaserCUSING), Electron Beam Melting (EBM), Laser Engineered Net Shaping (LENS), Direct Metal Deposition (DMD), Electron Beam Additive Manufacturing (EBAM) *[33]*. 3D printing, powder bed fusion (PBF), DED, and electron beam melting (EBM) are the liquid-state AM processes; however, binder jet additive manufacturing (BJAM) is a solid-state AM process.

In Laser Powder Bed Fusion (L-PBF) mixture of metal powder and the foaming agent is spread over the foaming bed in thin layers of 20 µm- 100 µm. Laser beam selectively heats powder bed layers, and foaming takes place. In Electron Beam Powder Bed Fusion (EB-PBF), foaming is accomplished through cyclic heating of powder bed with thickness ranging from 50 µm to 200 µm. While the L-PBF process is conducted in an inert gas environment, the EB-PBF process is carried out in a vacuum *[34]*.

Direct energy deposition method (DED) is an additive manufacturing method of metal foam production. It involves directing a blend of metallic powder and gas-releasing agent or carrier gas toward a base plate, with high-power irradiation of a laser beam *[35]*. Metal pool deposited on the base plate acquires

a porous structure during solidification due to gas-releasing agents. During solidification, gases like H_2, CO_2 etc. are released, which are entrapped inside the molten metal resulting in the porous structure. The schematic of Direct Energy Deposition is depicted in Fig. 2.4. Conventional methods of foam production are complicated and lengthy; however, direct energy deposition method proves to be a simple and advanced method of foam fabrication. Ingredients required in direct energy deposition (DED) methods for metal foam fabrication are tabulated in Table 2.3. Table 2.4 contains a brief literature review of additive manufacturing (AM) methods of metal foam fabrication.

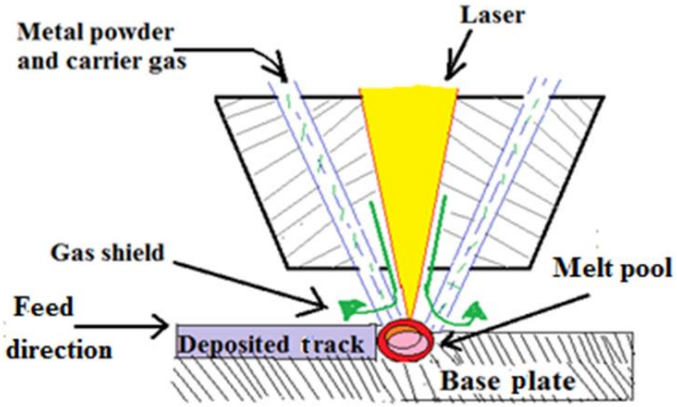

Fig. 2. 4: Schematic of direct energy deposition (DED) process *(Adapted [35])*

The quality of metal foams produced through the DED method is governed by various process variables, including laser power, laser beam spot size, powder or carrier gas flow rate, scanning speed, layer dimensions, and heat flow due to conduction and convective heat transfer phenomenon. The melt pool flow dynamics is mainly affected by the Marangoni effect due to surface tension which indirectly contributes towards porosity. The strength of the Marangoni

flow can be determined by the provided Eq. 2.4.

$$M_a = \frac{d\gamma}{dT}\frac{dT}{dx}\frac{L^2}{\eta\alpha} \qquad \text{Eq. 2.4}$$

Where, γ is surface tension, $\frac{dT}{dx}$ is a temperature gradient, L is characteristic length, η is the viscosity of molten metal, and α is the thermal diffusivity.

Table 2. 3: Ingredients required in direct energy deposition method *[35]*

Property of Sample	Single Layer	Six Layer
Laser power (w)	1200, 1600, 2000	800, 1200,1600
Powder supply (g/min)	18	18
Carrier gas supply (L/min)	6	6
Shield gas supply (L/min)	4	4
Nozzle feed rate (mm/min)	1000	1000
Titanium hydride (TiH_2) ratio wt. %	2, 10	4,6,8,10
Calcium oxide (CaO) ratio wt. %	0	1
Tellurium (Te) ratio wt. %	0	1

Table 2. 4: Brief literature review of additive manufacturing (AM) methods

Authors	Materials Used	Foaming Technique	Results & Findings
Liquid-State Additive Manufacturing			
Koike et al. [35]	Blend of Stainless steel & 6 wt. % of TiH_2 as Foaming agent Laser Beam	Direct Energy Deposition (DED)	Stainless steel foam of high porosity up-to 46% was produced when the melt was blended with calcium oxide and tellurium for single-layer deposition. The Porosity of the foam increased with a higher TiH_2 content ratio, and a similar effect was observed with increased laser power.

Koike et al. [36]	SUS316L and titanium-hydride (TiH_2) powder together. Laser Beam	Direct Energy Deposition (DED)	The energy absorption of foam produced by four-layer deposition was 185kJ, which is 7.7 times higher than that of average deposition.
Shim et al.[37]	Combination of Ti6Al4V powder and sodium carbonate (Na_2CO_3) An intense laser beam fuses the mixture with the substrate.	Direct energy deposition (DED) CO_2 gas is generated on fusion, due to which pores are formed.	The density of porous material can be adjusted by modifying process variables such as laser power, scanning speed, powder feed rate, and propellant mixing ratio. During compression, metal foam manufactured by DED collapsed due to internal fracture of cells followed by material densification and, finally, crumbling of the material. The metal foam produced effectively absorbed compression loads.
Shim et al.[38]	The mixture of Ti6Al4V powder and TiH_2 is sprayed on Ti6Al4V to form a substrate. High-power laser beam	Direct energy deposition (DED) process with a foaming agent($TiH_{2)}$	At 900 and 1100 W, the porosity of the porous structure was 20% and 11%, respectively. The porosity, as well as density of manufactured foam, was governed by varying laser power. The metal foam's compressive strength was demonstrated to be high.

Changdar et al.[39]	-	Direct Energy Deposition (DED)	Laser processing works such as forming, welding, cutting, and laser-based additive manufacturing of metal foams were discussed thoroughly.
Hernández-Nava, E., et al.[40]	Glass spheres, XCT, Ti6Al4V	Additive Manufacturing (AM) Electron beam melting (EBM)	Ti–6Al–4V foam samples were manufactured by EBM, having different relative densities. The mechanical properties of fabricated foam were better as compared to existing literature.
Kang, Boseok, et al.[41]	Copper formate Solution, UV pulse laser.	UV-pulsed laser deposition Additive manufacturing (AM)	Copper porous structures were manufactured by utilizing UV-pulsed laser deposition. No shielding gas is required in this AM technique. The produced copper foam finds its application in electrodes, filters, and heat exchangers etc.
Mustapha, K. A., et al.[42]	Nylon powder and plastic acid	3-D printing by utilizing tomography scanning	Open cell foam structure was produced by the additive manufacturing method. It was found that the surface finish and structural strength of produced foam depends on the printing process, the material used, and cell size.
Takeuchi, Toshihiro, et al.[43]	Stainless alloy powder and TiH_2	Direct Energy Deposition (DED)	Foam stainless alloy was produced through DED by adding TiH_2 as a foaming agent into metal powder. Optimum numbers of layers were found by varying TiH_2 particle size and the number of layers per line.

Moser, S., et al.[44]	Printing ink (15 ml dichloromethane,with 0.24g dibutyl phthalate, 0.88 g polystyrene, 1.2 g ethylene glycol monobutyl ether, and 4.66 g of Silicon submicron particles)	3D extrusion-printing of Silicon (Si) scaffolds using 3D Bioplotter	Hierarchical porous Silicon (Si) electrode scaffolds with different levels of filament porosity were produced. The filaments' open pores boosted the Si electrode capacity. The volumetric and gravimetric capacity of produced electrodes was higher than conventional graphite anodes.
Park, et al.[45]	Printing ink (Co_3O_4, NiO, and WO_3 powders, an elastomeric binder and solvents)	3D extrusion-printing and pack-cementation surface alloying	The mechanical properties of γ/γ′ cobalt-based precipitation-strengthened micro lattices measured at ambient temperatures were much superior to unalloyed cobalt micro lattices.
Song, et al. [46]	Printing ink (TiH_2+TiB_2 or TiH_2+TiC blends)	3D ink extrusion-printing and sintering	Ti-TiB and Ti-TiC composites were produced by dehydrogenation and *in situ* reaction. The crushing strength of TiB/TiC MMCs increased from 55 to 1019 MPa as the modeled lattice macro-porosity decreased from 71 to 24%.
Matheson, Kristoffer, et al.[47]	Aluminium 6061 alloy	Investment casting Laser powder bed	The global load-displacement responses of the investment cast and LPBF- produced foams showed significant variability, due to variations in

		fusion(LPBF)	the localized deformation behavior among individual ligaments.
Carpenter, Julia A., et al.[48]	Metal oxide particle-stabilized foams were used as self-assembling inks.	Extrusion-based 3D printing	The produced steel and iron foams exhibit ultrahigh porosity spread over three structured levels. This process allows for the production of iron and iron-based alloys with an elastic modulus greater than 300 MPa and a density under 1 g/cm^3, maintaining the mechanical performance anticipated for porous materials.
Valdez, Mario, et al.[49]	Nickel-based superalloy (Inconel) 718	Direct Metal Laser Sintering (DMLS) process	Processing-induced porosity effects on the mechanical properties of Inconel 718 were studied. Drop weight energy absorption capacity was reduced with induced porosity. The compression behavior of porosity-induced Inconel 718 resembled porous materials; yield strength decreased with density decrease.
Yang, Li, et al.[50]	Ti6Al4V alloy	Electron Beam Melting (EBM) additive manufacturing process.	EBM-produced Ti6Al4V alloy auxetic foams possessed excellent mechanical properties.
Kenel, C.,	Printing ink	Extrusion-	Hierarchically porous Fe or Ni

et al.*[51]*	(fine oxide powders Fe_2O_3 or NiO, <3 μm), coarse space-holder particles ($CuSO_4$, < 45 μm and a polymer binder within a solvent)	based 3D ink printing of powders followed by sintering	scaffolds were produced by 3D printing (a) Small size open channels are present in between the lattice of produced struts; (b) Open pores of 5-50 μm are found within the struts due to the removal of filler particles; (c) Submicron size closed-pores are present in the pore walls because of partial sintering of the metallic particles caused by reduction of the oxides. The porosity was dictated by sintering temperature, with the smallest pores being removed first. Sintering temperatures ranging between 873 and 1373 K resulted in strut porosities ranging from 38% to 19% in iron and 59% to 29% in nickel.
Xu, Chenyang, et al.[52]	Powder-based TiO_2 inks	Extrusion-based 3D printing	The printing method offers the following benefits: (a)The printing can be carried out in an open air environment without requiring in situ solidification, which offers greater control and flexibility over this method and is advantageous for cost-effective, and high volume production. (b) The 3D-fabricated materials exhibit hierarchical porosity at both the macro and micro scales.

			(c) The dimensions and shape of the printed structures can be easily modified by adjusting the printing variables
		Solid-State Additive Manufacturing	
Atwater, Mark A., et al.[53]	-	Review article	Liquid-state foaming creates porosity in molten metals, while solid-state foaming creates porosity in a solid metallic structure. Liquid-state foaming is commercially applied technique; however, solid-state foaming is complex and provides more control over pore morphology.
Mostafaei, Amir, et al.[54]	Ni-Mn-Ga ball-milled powder	Binder jet Additive manufacturing (BJAM) Sintering at 1020 °C for 4 hours in both vacuum and Argon environment.	The relative density of magnetic shape memory alloy foam prepared by BJAM was about 50-60%. Scanning electron microscopy with elemental analysis of argon sintered samples showed homogeneous composition. Producing a magnetic shape memory alloy through printing would allow for the manufacturing of intricately shaped components, which can be tailored for unique applications.
Miyanaji, Hadi, et al.[55]	Copper matrix containing copper oxides	Binder jet Additive manufacturing (BJAM) and sintering	The porosity, microstructural evolution, and volumetric shrinkage of produced foam samples were examined.

	Foam structures that were processed by sintering in air and subsequently annealing in a hydrogen environment exhibited greater porosity than those processed by sintering directly in a hydrogen environment. Annealing the components at 600 °C for 2 hours offered the maximum porosity of 59% and the minimum volumetric shrinkage of 5%.

2.3 Indirect Foaming Techniques

In the indirect foaming method of metal foam fabrication, the precursor material is prepared and foamed subsequently, or molten metal is poured over inorganic granulates. Metal foams can also be synthesized by using pre-processed foam templates through indirect foaming. The section 2.3.1 and 2.3.2 presents a brief review of conventional and technologically advanced methods of metal foam fabrication based on indirect foaming techniques, respectively.

2.3.1 Conventional Foaming Methods Based on Indirect Foaming Technique

A brief review of conventional foaming methods based on the indirect foaming technique is presented in Section 2.3.1.1 and 2.3.1.2.

2.3.1.1 Powder metallurgy (PM) process

Metal foams are fabricated through the PM process in two ways. The first one is

based on the compaction of powdered metals or metal alloys around the placeholders, hollow metallic spheres, etc., followed by sintering. In the second one, gas-releasing agent is added into the powdered metal or metal alloys. The mixture is pressed to produce pre-finished metal foam with uniformly dispersed foaming agent particles. This semi-finished foam is converted into various profiles, such as sheets and rods, by rolling or extrusion, etc. These processed sheets and rods are heated to temperatures above their melting point, and finally, finished metal foam is obtained. The mechanical behavior of processed foam could be managed by modifying the process variables, such as the amount of foaming agent, heating temperature, etc. The powder metallurgical process, also termed as sintering dissolution process, is more complex and costly than the liquid metallurgy method due to various factors such as pressure and synthesizing the precursor *[15]*. Fig. 2.5 shows the flow chart, which describes the steps for widely used powder metallurgical process, and Table 2.5 contains a review of powder metallurgical (PM) processes of metal foam fabrication.

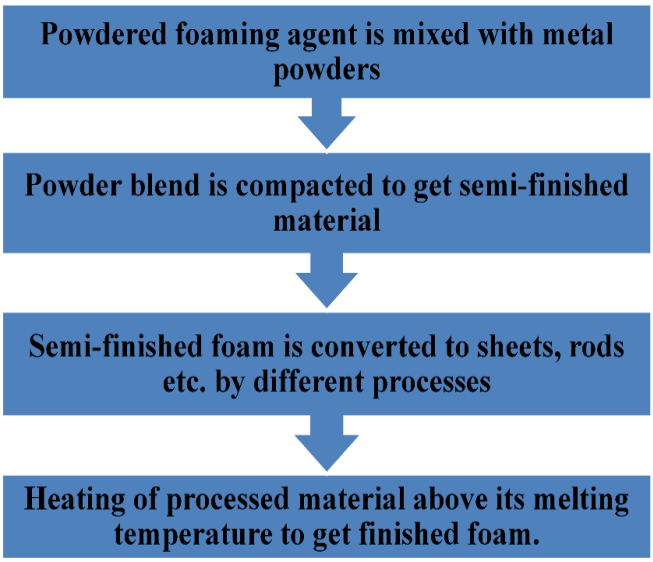

Fig. 2. 5: Flowchart for powder metallurgical (PM) process

Table 2. 5: Brief literature review of powder metallurgical (PM) processes

Authors	Materials Used	Foaming Technique	Results & Findings
Koizumi, Takuya, et al. [56]	Al-Si-Cu alloy Foaming agents $MgCO_3$, $CaMg(CO_3)_2$ and TiH_2	Powder Metallurgy (PM) Process.	Al-Si-Cu alloy foam was prepared through the PM process by utilizing $MgCO_3$, $CaMg(CO_3)_2$ and TiH_2 as foaming agents. The thermal decomposition effect of foaming agents on cell structure of produced foam was studied. $MgCO_3$, $CaMg(CO_3)_2$ were found more suitable for foaming Al-Si-Cu alloy.
Bram and Wazen et al. [57, 58]	Metal matrix Granulates as a placeholder (urea or ammonium hydrogen carbonate)	Powder metallurgy (PM) process. Heat treatment of sintered mixture results in foam production	The porosity of open cell structures depends upon the mixing ratio of metallic powders and the placeholder. If the placeholder volume is less in mixture, then its removal becomes difficult. The PM process is commonly employed for producing metallic foams with high melting points, like titanium alloy foam.

2.3.1.2 Reinforcement method of metal foam fabrication

In the reinforcement method of metal foam fabrication, micro sized ceramic particles, stabilizing agents, intermetallics, hollow filler particles, carbon nanotubes, multi walled carbon nanotubes, etc. are used as reinforcement. Reinforcement promotes foam stability and avoids non-uniformity in pore sizes. The reinforcement particles enhance the viscosity of the molten metal by

stabilizing bubbles formed during foaming at liquid-gas interface. The movement of ceramic particles to the liquid-gas interface is mainly caused by the difference in surface tensions of the solid and liquid phase present in the mixture. Schematic manufacturing methods for closed-pore aluminium foam with or without multi-walled carbon nanotubes (MWCNTs), Carbon Nano-tube/Aluminium (CNT/Al) foam, and aluminium composite foams reinforced by $MgAl_2O_4$ spinel whiskers are shown in Fig. 2.6, 2.7 and 2.8 respectively. Table 2.6 contains a review of reinforcement methods of metal foam fabrication.

Table 2. 6: Brief literature review of reinforcement methods

Authors	Materials Used	Foaming Technique	Results & Findings
Jin et al. [59]	Metal matrix Finely dispersed stabilizers (SiC and Al_2O_3 etc.) Gases (air, CO_2, inert gases, etc.)	Reinforcement method	The amount of stabilizer particles ranges between 5 to 15% of the total, with a preferred particle size range of 1 to 25 µm. Foam cell size is governed by regulating the flow rate of the gas, adjusting impeller's design and controlling impeller rotational movement. Cell size of the produced foam is typically less than 1mm, and the obtained foam is stable.
Thomas et al. [60]	Metal matrix (Al or Al alloy) Finely dispersed stabilizers	Reinforcement method	The foamed metal has improved crush and machining properties.

	(MgO) Gases (air, CO_2, inert gases, etc.)		
Zeppelin et al. [61]	Zinc powder & aluminium powders. TiH_2 ZrH_2, MgH_2 powders.	Reinforcement method	The time taken by titanium hydride to decompose depends on its heating environment. Vacuum heating leads to early decomposition, i.e. at 516 °C, whereas air heating delays the hydrogen evolvement, i.e.at 655 °C approximately. The best quality of foam was obtained by TiH_2, followed by ZrH_2 and MgH_2.
Gui et al. [62]	$AlSi_7Mg$ (A356) SiC particles Titanium hydride as blowing agent.	$AlSi_7Mg$ (A356) foam was produced by dispersing 20% SiC particles by volume and titanium hydride as a blowing agent.	The compressive strength test results describe mainly three regions: the linear elastic region, the collapse region, and the densification region. Low strain rates (<0.03) correspond to the linear elastic region, where the mechanical behavior can be characterized by the Ashby criterion. Crushing test results show the brittle nature of A356/SiCp composite foam, and the collapse region shows serration marks on the compression curves. The properties, such as damping capacity, of composite foam largely depend on its relative density.

Huang et al. [63]	Aluminium alloy scandium	Solid composite Al-foam was produced when a small amount of scandium was added to Al-alloy and then heat treatment.	Compressive strength of aluminium foam increases as the amount of scandium increases in its composition.
Yang et al. [64]	Stabilizer (Calcium) Foaming agent (TiH_2) Intermetallics (Mn)	The closed foam was produced by using a stabilizer and foaming agent. They used Calcium (Ca) stabilizer while titanium hydride (TiH_2) was used as foaming agent.	It was elaborated that manganese (Mn) was found to be consistent intermetallics in the form of reinforcement, which also enhances the mechanical properties.
Aguirre-Perales et al. [65]	Aluminium powder Intermetallics (cobalt, magnesium, manganese, nickel, and tin)	Powder metallurgy technique was employed for alloying, compacting, and foaming Al using Tin ($Sn \leq 5$ wt. %) as reinforcement.	It was deduced that low melting point of tin (Sn) and its immiscibility with molten aluminium resulted in an integral mixture with reduced surface tension and pore coalescence. The foam produced was more stable, and the number of pores increased with their sphericity. Pore shape and foam expansion mechanism were studied with the help of expansion maps and image analysis. Optimized process parameters

			were achieved with foam expansion up to 375% for 10 minutes at 2 to 3 wt. % addition of tin, hot pressing at 300˚C and foaming at 725 ˚C.
Rabiei et al. [66]	Aluminium alloy Steel hollow spheres	Metal foam composite material was processed by PM and gravity casting process.	The densities of Al-Fe composite foam were found to be 2.4 g/cm^3, whereas the density of iron foam was more significant and was estimated to be 3.2 g/cm^3. The average compressive strength of aluminium-iron composite foam was estimated to be 67 MPa in the region of 10 - 50% strain range. In contrast, the average compressive strength of steel foam fabricated by powder metallurgy (PM) process was found to be 45 MPa. Densification started at around 50% strain for the foams processed through casting and at 55% strain for the PM processed foam.
Prabhu and Du et al. [67, 68]	Aluminium matrix Reinforcement (Al_2O_3, SiC) Foaming agent(CaCO)	A powder metallurgy process was employed to fabricate 1% by volume SiC reinforced nano-SiC_p/Al composite foams and pure Aluminium foams with foaming agent $CaCO_3$.	It was deduced that pore size and pore shape directly depend on reinforcement since inclusion of nano-particles leads to the reduction in average pore size from a millimeter to a micrometer. It was found that the average pore size was reduced by 50.4%. It was found that adding 1 volume % SiC nano-particles into the melt reflects improvement in foam structure as well as enhanced the mechanical properties of the composite foam. An increase of 194.5% in yield stress and a 69.4% enhancement in energy

			absorption capacity was obtained in comparison to the base aluminium foams.
Zhang et al. [69]	Al-alloy Carbon nanotubes	Reinforcement melt foaming technique was employed to fabricate closed pore aluminium foam, in which multi-walled carbon nanotubes (MWCNTs) were used as reinforcement.	It was observed that during foaming, MWCNTs got embedded totally or partially in the cell wall, and in some cases, they were found exposed on the cell wall surface. The properties like yield strength, energy absorption capacity, and stiffness improves with increasing content up to a certain point, beyond which adverse effects are seen. It was deduced that metal foams having 0.5% of MWCNTs possessed optimal mechanical properties.
Wang et al. [70]	Al alloy Carbon nanotubes (CNTs)	Modified chemical vapor deposition method (CVD) using space holder technique	CNTs are uniformly distributed in the metal foams produced by this method; hence structurally uniform metal foams are obtained.
Liu et al. [71, 72]	Zn-22Al Reinforcement (Al_2O_3) Blowing agent($CaCO_3$)	Direct foaming method.	Closed pore zinc composite (Zn-22Al) foam was produced by direct foaming in which aluminium oxide (Al_2O_3) fibers were mixed in a volume ratio of 3%, and calcium carbonate was used as a blowing agent. It was observed that zinc composite foam exhibits better mechanical and physical properties such as compressive

			yield strength and energy absorbing properties etc.
Chakraborty et al. [73]	$AlMg_5$ alloy Melt Reinforcement (SiO_2)	Chemical synthesis	A new method was suggested for producing foamable precursor in which reinforcing nano-particles of (SiO_2) were synthesized inside the metal matrix ($AlMg_5$) with $MgAl_2O_4$ through a chemical reaction. The study suggested that the best foamable precursor was prepared by mixing 3.4% spinel particles ($MgAl_2O_4$) into the matrix.
Guo et al. [74]	Metallic melt Reinforcement ($MgAl_2O_3$ nano-whiskers) Space holder (NaCl)	Foams were produced by sintering and dissolution process using $MgAl_2O_3$ nano-whiskers as reinforcement and sodium chloride as a space holder.	The $MgAl_2O_3$ spinel whiskers generated during the fabrication may exists in three forms: fully inserted in the cell boundary slightly bulging through the cell boundary and piercing through micro-pores. Structural and mechanical properties of fabricated metallic foam in which spinels are entirely embedded in its cell wall are superior.

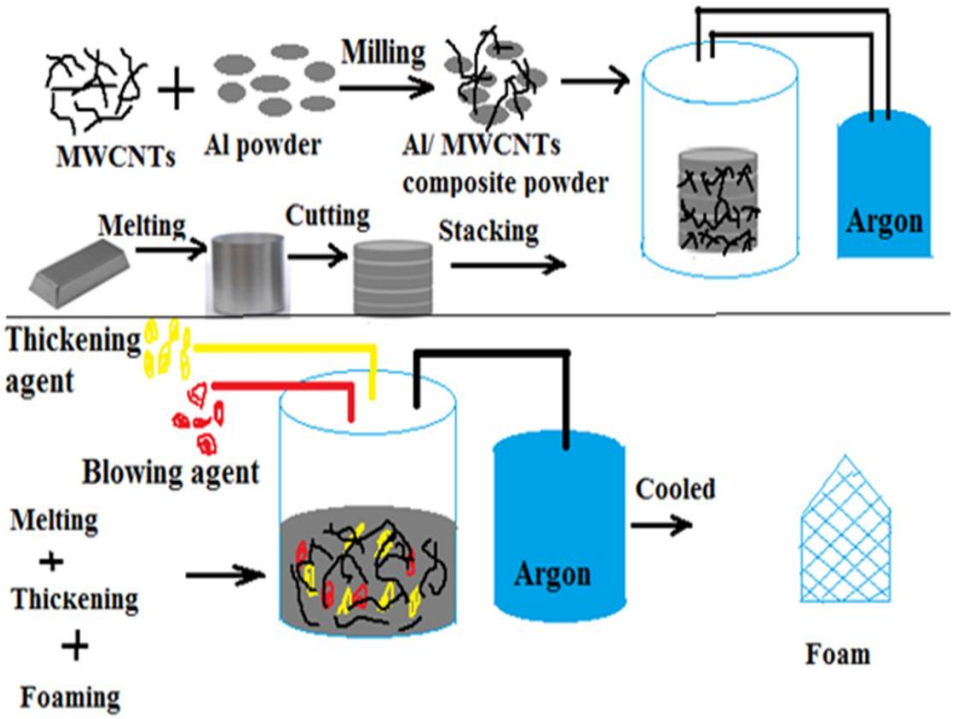

Fig. 2. 6: Manufacturing method of closed pore aluminium foams with and without MWCNTs *(Adapted [69])*

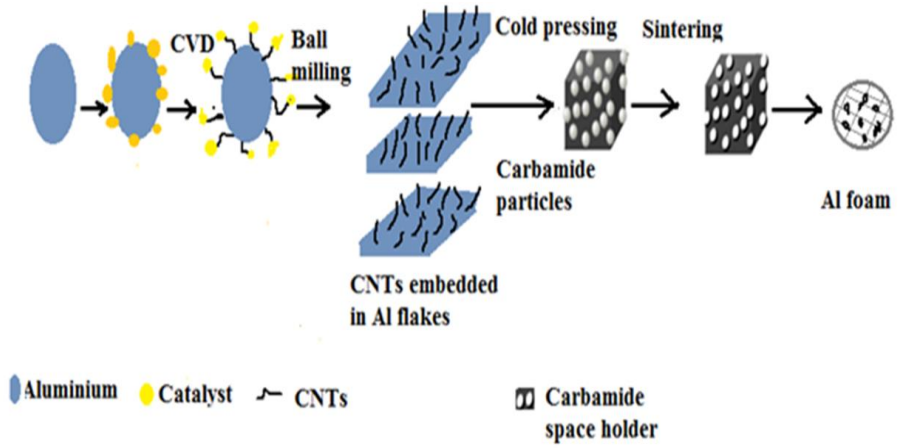

Fig. 2. 7: Manufacturing process for CNT/Al foam (*Adapted [70]*)

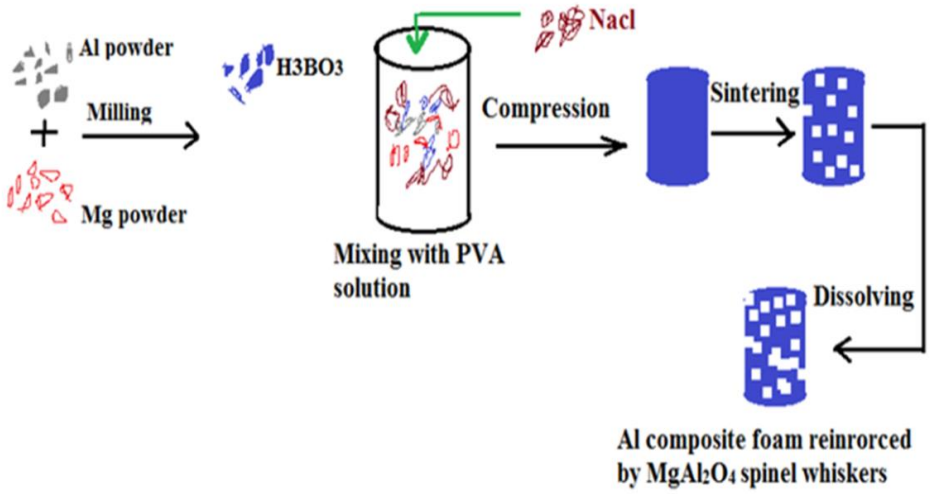

Fig. 2. 8: Fabrication of aluminium composite foam reinforced by $MgAl_2O_4$ spinel whiskers *(Adapted [74])*

2.3.2 Non-Conventional Foaming Methods Based on Indirect Foaming Technique

A brief review of non-conventional foaming methods based on the indirect foaming technique is presented in section 2.3.2.1, 2.3.2.2, 2.3.2.3, and 2.3.2.4.

2.3.2.1 Fabrication of metal foam by filament winding technology

The foamable precursor material is produced by extruding the mixture of metal powders and some foaming agents. Metal foam is manufactured by heating foamable precursor material in a mold. Finally, hybrid metal foam is obtained by depositing some material (epoxy/S2 glass) on previously produced metal foam through filament winding technology. The schematic for the hybrid metal foam fabrication process through filament winding technology is shown in Fig. 2.9.

The hybrid composite metal foam was produced through filament winding

technology by heating extruded foamable precursor made of Al-Si10 alloy powder and foaming agent (TiH_2) and depositing epoxy/S2 glass on its surface *[75]*. Compression and three-point bend tests were performed on samples of hybrid metal foam, metal foam cylinder, and epoxy glass tube with diameters and lengths of 32 mm and 235 mm. It was found that the load-resisting and energy absorption capacity of hybrid samples were slightly higher than the metal foam cylinder and epoxy glass tube.

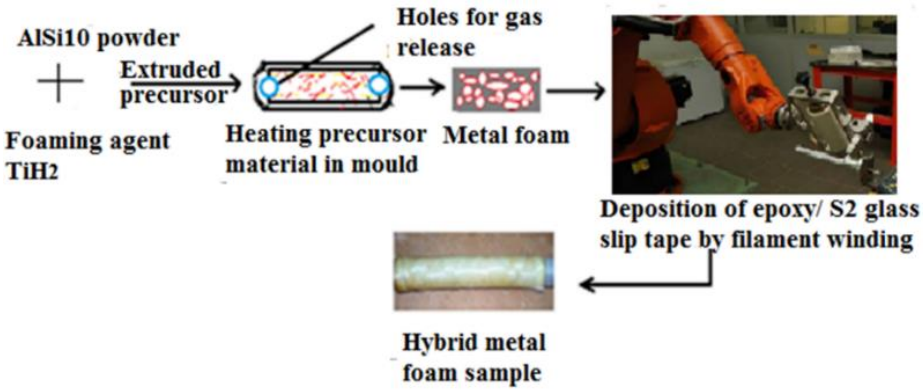

Fig. 2. 9: Metal foam fabrication by filament winding technology
(Adapted [75])

2.3.2.2 Novel methods of metal foam fabrication

Metal foams have been produced for decades conventionally; some researchers have focused on new methods which can be categorized as novel methods of foam fabrication. Conventional methods of metal foam fabrication are the main source of industrial metal foam production; however, non-conventional methods may find their application in the near future. Table 2.7 provides a brief review of some novel methods of metal foam fabrication.

Table 2. 7: Brief literature review of novel methods

Authors	Materials Used	Foaming Technique	Results & Findings
Drolet [76]	A slurry of aluminium powder and foaming agent (ortho-phosphoric acid with aluminium hydroxide or hydrochloric acid)	Novel method	A novel method of foam fabrication was suggested as the slurry of metal powder and the foaming agent starts to dry, gas starts to evolve and results in foaming of the metal matrix. The expanded slurry was dried completely with sufficient stabilizing measures, resulting in metal foam.
Kulkarni et al.[77]	A slurry of aluminium powder and foaming agent	Novel method	Metal foams obtained by this process have cracked with low strength and a relative density of approximately 7%
Product data sheet of (SEAC) [78]& Sumitomo Electric [79]	Metal-polymer foam with open pores.	Polymeric method of foam fabrication.	The polymer was removed after electroplating from the metal-polymer composite by the thermal treatment process. The pore size ranges from 2 to 30 cells per centimeter (2 to 70 pores per inch). This process prominently foams the nickel and nickel chrome alloys; however, fabrication of copper foams can also be done.
Paserin et al. [80]	Nickel tetra-carbonyl [$Ni(CO)_4$] Polymer	The coating of [$Ni(CO)_4$] was done by chemical vapor	Inco Company developed chemical vapor deposition (CVD) method for foam fabrication in Canada. Now, this technology is used by Alantum Company in China to produce iron and copper foams.

		deposition (CVD).	Nickel tetra-carbonyl [Ni (CO) $_4$] was deposited in the form of a coating on the polymer with further sintering and polymer removal. On heating, at temperatures around 150˚C to 200˚C, this coating of [Ni (CO) $_4$] decomposed to nickel and carbon monoxide. The foam produced by this method has high thermal and electrical conductivity.
Torres et al. [81]	Metal matrix Granulates as a placeholder (sodium chloride)	Placeholder method	The pore size and microstructure of the foam largely depend on the granulate morphology. The efficiency of placeholder removal decides the porosity of the foam. Aluminium alloy foams are produced using placeholder technique by many companies such as Exxentis, Switzerland, and Alveotec, France. Exxentis produced foam with pore sizes ranging from 0.14 to 3 mm in diameter.
Limper, Alexander, et al.[82]	Metal-polymer dispersions. Nickel particles NaCl pore formers	Novel fabrication method	Porous nickel electrodes were prepared through a combined novel approach involving pore formers and metal-polymer dispersions. The electrochemical surface area (ECSA) of the produced porous electrode was more than that of thick nickel foil and commercial nickel foam.

Yu, et al.[83]	Metal slurry	Template replication fabrication process	Partially open window morphology open-cell metallic foam was fabricated by a novel template replication method. It was observed that the flow resistivity and sound absorption coefficient of partially open window morphology foam were substantially increased.
Singh, R., et al.[84]	Porous oxide precursor	Gel casting method followed by electrochemical reduction.	A novel process for producing titanium foams was suggested for biomedical applications. The porosity of produced metal foam can be tailored independently, unlike traditional space-holder techniques. The obtained shear modulus, yield strength, and permeability values of produced titanium foam having 80% porosity were 1 GPa, 8 MPa, and 350 Darcies, respectively.

2.3.2.3 Investment casting method

In the investment casting method replica of polymeric open foam is utilized to process metallic foam. First of all, open cells, polymeric foam is processed, and the pores are filled with some heat-resisting material like mullite, calcium carbonate, phenolic acid, etc. After complete drying of slurry, the polymeric material is extracted by heating the mold in a furnace. Thus open cell structure of heat-resisting material is obtained. Molten metal is poured into the open cell structure. Finally, heat resisting material is also removed to get metal foam. The

steps for processing metal foam by investment casting method are shown in Fig. 2.10.

Aluminium alloy foam was produced through investment casting using open-cell polymeric foam as a pattern *[85]*. The pores of the pattern were filled with heat-resisting material (casting wax). After the complete drying of the slurry, polymeric material was extracted by heating the mold, resulting in an open-cell structure of casting wax. Molten aluminium alloy was poured into the open-cell structure. The casting wax was also extracted to get aluminium alloy foam. It was observed that the mechanical and thermal properties of produced aluminium alloy foam were superior to conventionally produced foam.

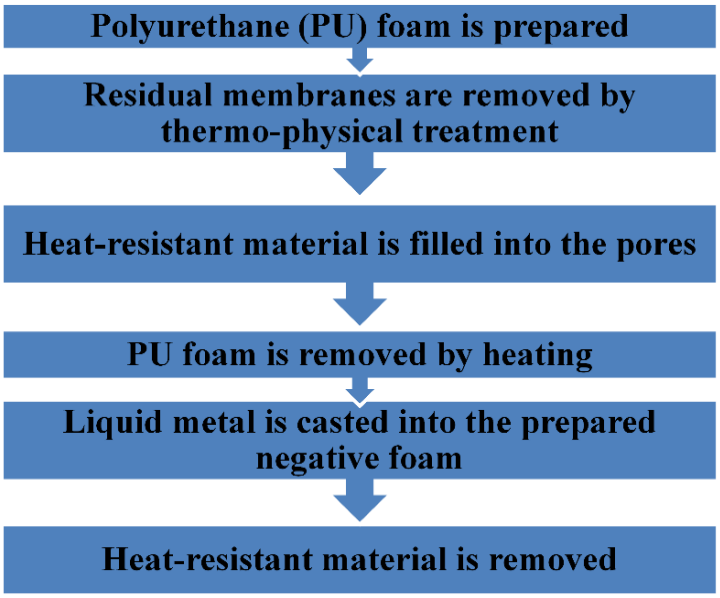

Fig. 2. 10: Flowchart for investment casting method

2.3.2.4 Functionally-graded metallic syntactic foam (MSFs) using filler materials

Syntactic and functionally graded metal syntactic foam is produced by using inorganic filler materials. In this process, foaming can be performed in two

ways: in one case, molten metal is poured over the filler particles, and in second, filler particles are introduced into molten metal matrix. Easy flow of molten metal is ensured across the bulk because of the low thermal conductance and thermal capacity of filler particles; however, the higher surface tension of the melt leads to incomplete filling of interstitial spaces. Filler particles used in this process are foamed aluminium oxide spheres, clay granules, etc. Various metals including aluminium, lead, tin, zinc, magnesium etc. can be easily foamed through this technique and products of predefined shape can be prepared with the help of required mold geometry. The schematic of the MSFs production process is shown in Fig. 2.11.

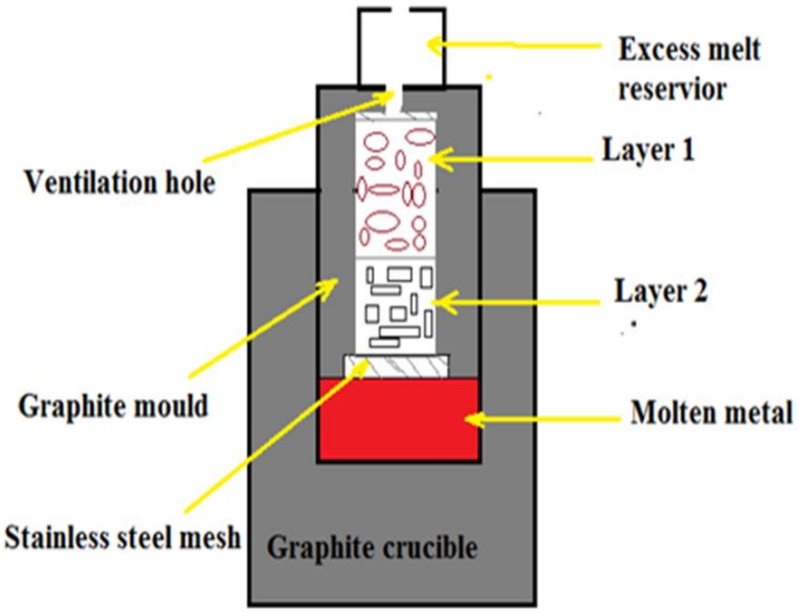

Fig. 2. 11: Schematic of the MSFs production process *(Adapted [86])*

The brief review of metal syntactic foams (MSFs) and metal matrix syntactic foams (MMSFs) fabrication methods is tabulated in Table 2.8.

Table 2. 8: Metal syntactic and metal matrix syntactic methods

Authors	Materials Used	Foaming Technique	Results & Findings
Movahedi et al. [86]	Metal melts EP(expanded perlite) and AC (activated carbon) is used as filler material.	EP-MSF AND AC-MSF Syntactic foam was processed by the syntactic method.	When tested, it was found that the density of the FG-MSF was 2.11to 2.15 g/cm^3 while the density of uniform EP-MSF was 2.02 g/cm^3 and of AC-MSF 2.15 g/cm^3. It was stated that FG-MSF exhibits more deformation at low strains and is limited in the EP layer. In contrast, deformation occurs at relatively high strains in the AC layer. Plateau stress of FG-MSFs is higher than uniform syntactic foams, and this higher plateau stress leads to higher volumetric energy absorption of FG-MSFs.
Thiele et al. [87]	They produced porous metals by using inorganic particles as filler material, such as foamed aluminium oxide spheres, clay granules, etc.	Syntactic metal foam fabrication.	The advantages of this technique are that a diverse array of metals like aluminium, lead, tin, zinc, magnesium etc. can be easily foamed and predefined shape products can be prepared with the help of required mold geometry.
Sánchez et al. [88]	Aluminium alloy Filler particles and	Infiltration casting technique.	Metal matrix syntactic foam was synthesized by infiltration casting technique. The porosity, plateau stress

	Foaming agent was taken from wastes of Spanish white marble quarries.		and energy absorption capacity of produced foam were found to be 41%, 37.65 MPa and 8.62 MJ/m^3 respectively at 35% of densification.
Bolat et al. [89]	Aluminium 7075 Hollow bubble alumina spheres.	Syntactic foam by recyclable pressure infiltration casting method	The porosity of produced metal syntactic foams was found in the 43.2% - 45.6% range. Smooth infiltration was obtained with alumina spheres of size 2 – 4 mm. Syntactic foam has a positive relationship of heat treatment with compressive strength.
Spratt et al. [90]	Aluminium alloy 4047 Glass particles were used as filler particles.	Additive manufacturing method.	Aluminium matrix syntactic foam was processed through an additive manufacturing method. It was deduced that floatation and fracture of microsphere in the molten composite during processing got diminished.
Rohatgi et al. [91]	-	Review on metal syntactic foams.	Published literature contains studies on syntactic foams of Aluminium, magnesium, lead, zinc, etc. It was deduced that metal matrix syntactic foams exhibit better energy absorption capability as compared to standard foams.

Spratt et al. [92]	Iron and aluminium based metal matrix. Glass microspheres.	Metal syntactic foam was manufactured by laser additive manufacturing process.	Microsphere segregation is a problem in this method of syntactic foam fabrication. They evaluated Vickers micro-hardness and performed microstructural analysis of produced syntactic foam.
Neville et al.[93]	Carbon steel and Stainless steel powder. Steel hollow spheres.	Powder metallurgy technique.	Two samples of carbon steel and one sample of stainless steel were prepared. Relative density ranges from 32.4 to 38.9%. The produced foams exhibited excellent compressive strength and energy absorption capability. Plateau strength to density ratio of carbon steel and stainless steel foams ranged from 12 to 31.9 MPa/ (g/cm^3) and 43.7 MPa/ (g/cm^3), whereas the energy absorption capability of carbon steel & stainless steel foam specimens lies between 18.9 - 41.7 MJ/m^3 and 67.8 MJ/m^3 respectively.
Rabiei et al.[94]	Aluminium alloy Steel hollow spheres.	Gravity casting technique.	The density and relative density of aluminium composite foam was reported to be 2.4 g/cm^3 and 41.5%, respectively. Composite foam showed a compressive strength of 67 MPa before densification strains, i.e. before 50%

			strain. The compressive strength at 50% strain was 30 MJ/m^3.
Rabiei, Afsaneh [95]	Metal matrix Hollow metallic spheres.	US patent	The composite metal foam was invented, which exhibited low density and high strength. This type of metal foam can be processed by filling the gaps between hollow spheres, which can be accomplished by powder metallurgy and casting technology.
Majlinger et al.[96]	AlSi12 matrix alloy. Monomodal Globocer (Al_2O_3 and SiO_2-based ceramic) and Globomet (pure Fe) were utilized as reinforcements.	Hybrid metal matrix syntactic foams (MMSFs) by pressure infiltration technique.	It was deduced that the composition and aspect ratio of reinforcements determines the mechanical and physical properties of hybrid metal foams. It was concluded that desired properties of hybrid metal syntactic foams can be achieved by utilizing different reinforcements.
Balint et al. [97]	Al99.5, AlSi12, AlMgSi1 and AlCu5 metal matrix. Iron hollow spheres as reinforcement.	Gas infiltration technique.	Microstructural investigation revealed some unwanted voids and an interface layer between reinforced spheres and metal matrix. The mechanical properties of produced foams were found to be better than the conventionally produced metal foams.

Orbulov et al. [98]	Al99.5 and AlSi9MgMn metal matrix. Light-expanded clay agglomerate Particles (LECAPs) of 4, 8, and 11 mm diameters were used as reinforcements.	MMSFs were prepared by low-pressure infiltration technique.	Low-cost MMSFs were developed by low-pressure infiltration. They investigated the structural and mechanical properties of produced foams. The density of produced MMSFs was found to be in the range of 1.38–1.53 g/cm^3. An exponential relationship was found between LECAPs and the strength of produced foams. Compression test reveals plastic collapse failure.

2.4 Literature Survey Analysis

Various conventional and non-conventional metal foam manufacturing processes based on direct and indirect foaming techniques have been identified. In the direct foaming method, non-metallic particles are mixed and dispersed uniformly into the molten metal pool. Foaming is done either by mixing the blowing agent or directly injecting the gases into the molten mixture. In indirect foaming, a precursor material is prepared initially, a mixture of aluminium matrix and uniformly dispersed blowing agent particles. On heating, this precursor expands, and foaming takes place. Conventional metal foaming processes are accomplished by injecting gases, admixing blowing agents and utilizing space holders in one way or another. Additive manufacturing, novel methods, and metal syntactic foaming techniques are the prominent non-conventional metal foaming processes. Metal foams can be produced efficiently

and economically using blowing agents and space holders.

Metal foam fabrication processes developed and adopted by various researchers and companies based on direct and indirect foaming techniques are shown in the pie charts in Fig. 2.12.

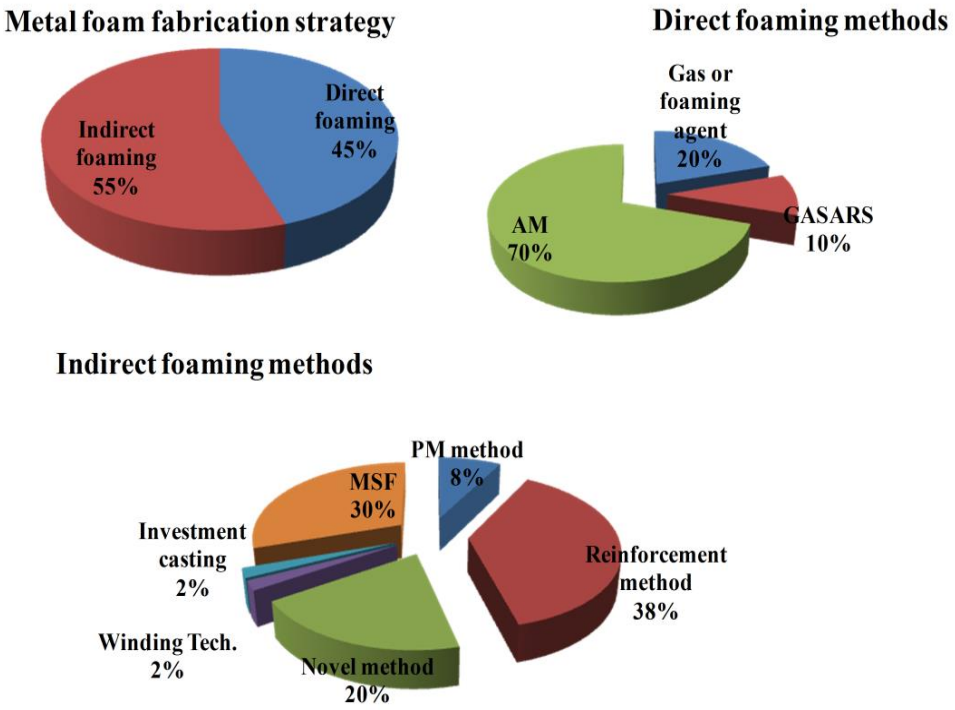

Fig. 2. 12: Metal foam fabrication strategy

Based on the literature review, it is concluded that 45% of metal foams are manufactured by direct foaming techniques which include additive manufacturing (AM) method 70%, foaming by gas injection or foaming agents 20%, and solid-gas eutectic solidification process of metal foam fabrication (GASARS) process 10%. Rest 55% of metal foams are manufactured by the indirect foaming techniques; which include, investment casting method 2%, winding technology 2%, metal syntactic foam (MSF) production with filler

materials 30%, reinforcement method of foam fabrication 38%, powder metallurgical (PM) process 8%, and novel methods 20%.

Direct foaming methods are cost-efficient regarding initial setup and material costs. Also, a large volume of foam with low densities can be continuously produced through direct foaming process. It is easy and cost-effective to fabricate metal foams through liquid metallurgy route based on the direct foaming technique. Metal matrix composite foams fabricated through liquid metallurgy route are more affordable and cost-effective than other porous metallic structures.

Foaming agents are essential components in the conventional foaming process as they impart better mechanical and physical properties. It is evident from the literature survey that $CaCO_3$, TiH_2, $CaMg(CaCO_3)_2$, and ZrH_2 are being abundantly utilized as foaming agents due to their wettability. Space holders provide better control of porosities, cell morphology, and stability of metal foams. A range of space holders like carbamide, ammonium hydrogen carbonate, sodium chloride, magnesium polypropylene carbonate (PPC), and polymethylmethacrylate (PMMA) are being utilized to produce porous structures. The reinforcing agents such as $CaCO_3$, B_4C, SiC, CNTs, and so on significantly improve the strength, stability, cell structure and pore size distribution when used for producing metal foams. Non-conventional metal syntactic foams are produced by using filler particles such as hollow metallic spheres, glass microspheres, hollow bubble alumina spheres, clay granules, foamed aluminium oxide spheres, expanded perlite, activated carbon, etc.

Metal foams have superior mechanical and physical properties such as stiffness, compressive strength, tensile strength, proof stress, sound absorption quality, specific energy absorption capacity, etc. Hence, they are being widely used in automotive, aerospace, and defense applications. Metal foam properties are influenced by the method of foam fabrication, type of foaming agent or space holder, reinforcing agent, and filler particle employed etc. Literature survey suggests that the compressive stress-strain behavior of metal foams largely depends on their density. Denser foam cells lead to more energy absorption during compression at lower stress levels. The plateau stress remains low for low-density metal foams and vice versa; however, the plateau stress is lower for high-density metals or their alloys.

2.5 Research Gaps

After thorough literature survey on aluminium alloy foams, following points are observed.

- Various researchers have worked on fabrication of aluminium alloy foam but only few researchers focused on fabrication of aluminium alloy foam economically through stir casting method based on direct foaming technique.
- There is an inadequate control on structure and morphology of aluminium alloy foams prepared through mixing of blowing agents.
- Few researchers focused on structural and mechanical properties evaluation, optimization, and characterization of aluminium alloy foams.

- Few researchers focused on the effects of porosity on the tribological properties of aluminium alloy foams.

2.6 Research Objectives

After thorough literature survey on fabrication and property analysis of aluminium alloy foams, following research objectives are decided.

- To employ economical method for the fabrication of aluminium alloy foam.
- To investigate the microstructure of fabricated aluminium alloy foam for ensuring proper distribution of blowing agent.
- To study the effects of blowing agent amount, blowing agent mixing temperature and stirring time on structural and mechanical properties of fabricated aluminium alloy foam.
- To study the mechanical and tribological properties of fabricated aluminium alloy foam experimentally.

Chapter 3
Materials and Methods

3.1 Materials and Methods

Al-6063 alloy foam was fabricated through stir casting, using Al-6063 alloy as the base metal and TiH_2 (specific gravity: 3.9 g/cc @ 12, melting point 400 °C, purity 99.4%) as a blowing agent. Al-6063 alloy was procured from Alloy Pipe Impex, Mumbai, India. Foaming agent TiH_2 was procured from N.B. Enterprises, Tikrapara Road, Bilaspur, Chhattisgarh, India. The foaming agent TiH_2 was preheated to 200 °C in a muffle furnace. The aluminium alloy foaming process is delayed, and a more uniform pore distribution is ensured using a preheated foaming agent *[99]*. Energy dispersive X-ray (EDX) analysis of the procured Al-6063 alloy presented in Fig. 3.1 confirmed the presence of aluminium and other alloying elements. A stir casting furnace with a stirring arrangement was used for melting and subsequent foaming of Al-6063 alloy.

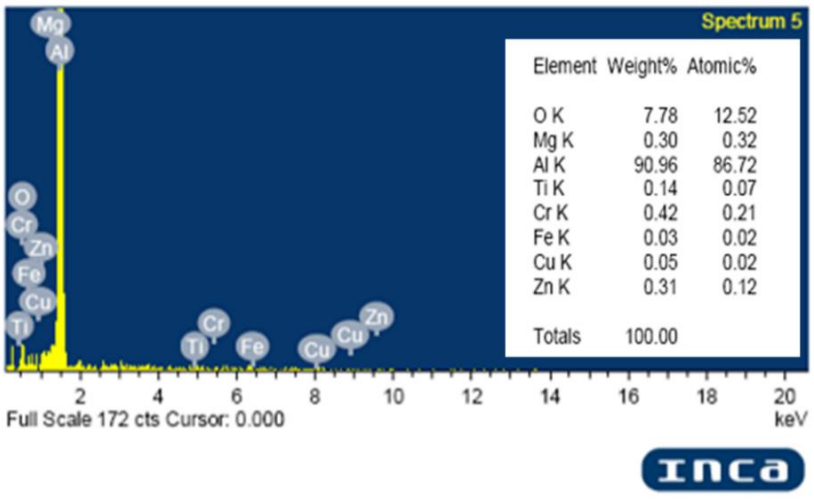

Fig. 3. 1: EDX spectra of Al-6063 alloy

3.2 Foam Fabrication Process

In this study, Al-6063 alloy foam was fabricated through the stir casting method using TiH_2 as a foaming agent, as per the published literature *[100–107]*. In order to fabricate Al-6063 alloy foam for mechanical properties evaluation and process optimization, 0.5 kg of Al-6063 alloy was melted in a graphite crucible inside a stir-casting furnace for each iteration. Based on Table 3.1, preheated foaming agent TiH_2 (1, 2, and 5 wt.%) was mixed into the melted Al-6063 alloy at mixing temperatures (600 °C, 650 °C, and 700 °C), and the mixture was stirred mechanically for 2, 5, and 8 minutes at 200 RPM. At a temperature of 400 °C, TiH_2 decomposition was initiated, due to which pure hydrogen (H_2) gas evolved, leaving behind titanium aluminide (Al_3Ti) as a precipitate in the metal composite. The chemical reaction is shown in Eq. 2.2. The molten metal composite expanded due to TiH_2 decomposition and the nucleation and growth of bubbles. The molten metal composite was cooled to room temperature to obtain porous Al-6063 alloy blocks. The stepwise fabrication process of Al-6063 alloy foam is shown in Fig. 3.2. The Al-6063 alloy was melted in a stir-casting furnace and cooled down to room temperature to fabricate the base Al-6063 alloy block.

Table 3. 1: Levels and factors for orthogonal design of experiments

	A	B	C
Factor / **Level**	Amount of TiH_2 (Wt.%)	TiH_2 mixing temperature (°C)	Stirring time (Mins.)
1	1	600	2
2	2	650	5
3	5	700	8

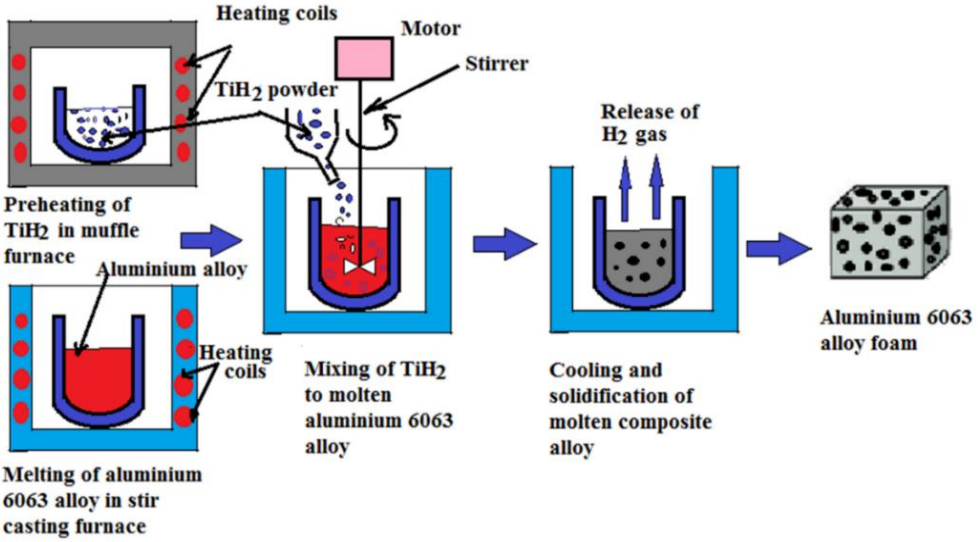

Fig. 3. 2: Fabrication process of Al-6063 alloy foam

3.3 Structural Properties Evaluation

The morphology, microstructure, and chemical composition of fabricated Al-6063 alloy foam were analyzed by performing scanning electron microscopy (SEM) with energy dispersive X-ray (EDX) analysis (Model No. JSM6510LV, made by JOEL, Japan). The Al-6063 alloy and foam samples of 25 mm cubic size (15.625 cm^3 volume) were cut using electrical discharge machining (EDM) from the fabricated Al-6063 alloy foam blocks, respectively. The finished specimens were weighed on a scale, and their mean masses (m) were noted. The mean mass evaluation process for Al-6063 alloy and its foam is demonstrated in Fig. 3.3. The density (ρ) and porosity (ϕ) of finished Al-6063 alloy and foam samples were calculated using Eq. 3.1 and Eq. 3.2, respectively, as per the published literature *[108–112]*.

$$\rho = \frac{m}{V_t}\ (g/cm^3) \qquad \text{Eq. 3.1}$$

$$\phi = [\frac{(\rho_a - \rho_f)}{\rho_a}]100\ (\%) \qquad \text{Eq. 3.2}$$

Where m is mean mass of the specimen, V_t is the total specimen volume (15.625 cm^3), ρ_a is the density of base Al-6063 alloy, and ρ_f is the density of the Al-6063 alloy foam sample.

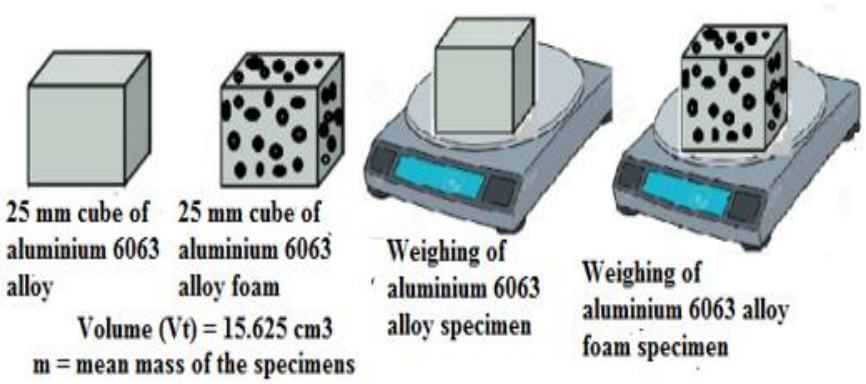

Fig. 3. 3: Mean mass measurement process for Al-6063 alloy and its foam

3.4 Mechanical Properties Evaluation

The Al-6063 alloy and foam samples of 25 mm cubic size and 75*30*15 mm cuboidal size were cut using electrical discharge machining (EDM) from the fabricated Al-6063 alloy and foam blocks. The samples of 25 mm cubic size were used to evaluate energy absorption capability, whereas the samples of 75*30*15 mm cuboidal size were used to evaluate flexural strength. The energy absorption capability and flexural strength of finished Al-6063 alloy and foam samples were evaluated by performing compression and three-point bending tests, as per the published literature *[113–116]*. Instron-8801 Universal Testing Machine (UTM) was used to perform compression and three point bending tests. The compression and bending tests were performed for three samples of

each type at a head speed of 0.01 mm/s at room temperature at room temperature of 30 °C in March 2022 AD. Compression tests were performed up to 80% sample deformation, and the bending of specimens was continued to their fracture limit. Mechanical properties such as plateau stress (σ_p), densification strains (ε_d), and energy absorption capabilities (W) were evaluated from the obtained compressive stress-strain curves. The flexural strength was evaluated from the obtained flexural stress-strain curves. Sample foam specimens and the mechanical property evaluation process are illustrated in Fig. 3.4.

Fig. 3. 4: Evaluation of Mechanical properties of Al-6063 alloy foam **(a)** Sample foam specimen for compression test **(b)** Sample foam specimens for bending test **(c)** Compression strength evaluation process **(d)** Flexural strength evaluation process

3.5 Multi-response Process Optimization Using Grey Relational Analysis

Dr. Taguchi developed an optimization method based on an orthogonal array, which provided much-reduced variance in experiments and optimal control parameters. In the Taguchi method, all problems are divided into static and dynamic categories. Dynamic problems have a signal factor; however, static problems do not have any signal factor. In dynamic problems, analysis is based on two types of S/N ratios: slope and linearity. In contrast, the static problems are analyzed based on three S/N ratios: the smaller the better, the larger the better, and the nominal the best. Eq. 3.3 and Eq. 3.4 represent the larger the better and the smaller the better criteria, respectively.

$$\left(\frac{S}{N}\right) ratio\ larger\ the\ better\ = -10log\frac{1}{n}\sum_{i=1}^{n}(1/R)^2 \qquad \text{Eq. 3.3}$$

$$\left(\frac{S}{N}\right) ratio\ smaller\ the\ better\ = -10log\frac{1}{n}\sum_{i=1}^{n}(R)^2 \qquad \text{Eq. 3.4}$$

Where n the number of observations, and R is the observed data for each response.

The Taguchi method can be effectively used for single-response optimization; however, the best-suited method for multi-response optimization is Taguchi coupled with grey relational analysis. In this research work, the foam fabrication process was optimized through the Taguchi method coupled with grey analysis as per the published literature *[117–119]*. Finally, the percentage contribution of each process parameter to the response variables (grades) was analyzed through ANOVA, and the correlation between process parameters and the response variable (grades) was established by regression modelling.

3.6 Tribological Properties Evaluation

In order to present a comparative microstructural and wear behavior analysis of stir-cast aluminium 6063 alloy and its foam, Al-6063 alloy foam was synthesized through stir casting using varying amounts of titanium hydride as a foaming agent. The foam fabrication process was based on the optimum process parameters established in previous section. Hence, 0.5 kg of Al-6063 alloy was melted in a graphite crucible inside a stir-casting furnace, preheated foaming agent TiH_2 (1, 2, and 5 wt.%) was mixed into the melted Al-6063 alloy at mixing temperatures (650 °C), and the mixture was stirred mechanically for 8 minutes at 200 RPM. TiH_2 decomposition inside the molten alloy resulted in pore generation. The molten composite alloy was cooled to room temperature to obtain porous Al-6063 alloy blocks.

3.6.1 Sample preparation and microstructure characterization

The Al-6063 alloy and foam samples of 30 mm height and 8 mm diameter were cut from the synthesized blocks through electro-discharge machining (EDM). Three samples of each type were ground with emery papers of 220 to 2000 grit size. Keller's reagent was used for etching the polished surfaces. The finished samples were weighed on a scale, and their mean masses were noted. Mean mass evaluation statistics for the finished samples are demonstrated in Table 3.2. The porosity of the base Al-6063 alloy was considered to be zero. Densities (ρ) and porosities (ϕ) of finished Al-6063 alloy foam samples were evaluated through Eqs. 3.1 and 3.2. The porosities of Al-6063 alloy foam samples synthesized by mixing 1 wt.%, 2 wt.%, and 5 wt.% amounts of TiH_2 were found to be 36.4%, 38.2%, and 53.03%, respectively.

Table 3. 2: Mean mass measurement statistics

Sample	Property	Mean	Minimum	Maximum	Std. deviation	Range
Al-6063 alloy	Mass(g)	4.023	3.490	4.380	0.384	0.890
Al-6063 alloy foam (1 wt.% TiH_2)	Mass(g)	2.560	2.290	2.860	0.233	0.600
Al-6063 alloy foam (2 wt.% TiH_2)	Mass(g)	2.490	2.420	2.540	0.050	0.120
Al-6063 alloy foam (5 wt.% TiH_2)	Mass(g)	1.890	1.830	1.920	0.042	0.090

The microstructural morphology and elemental composition of finished Al-6063 alloy and its stir-cast foam specimens were investigated with the help of a scanning electron microscope, Model No. JSM6510LV, made by JOEL, Japan.

3.6.2 Taguchi-based grey optimization

To optimize the impact of process variables on the tribological properties of stir-cast Al-6063 alloy foam, the $L_9 3^3$ orthogonal array (OA) was designed as a static problem, as shown in Table 3.3. Load (N), sliding speed (m/s), and porosity (%) of synthesized foam samples were considered as the independent input parameters that affect the responses, namely wear (microns), coefficient of friction (μ), and frictional force (N). The tribological properties of fabricated Al-6063 alloy foam samples were evaluated with the help of a high-temperature

rotary tribometer (TR-20L-PHM800-DHM850). Various low-carbon steel plates have been used as counter-disc for tribological investigation of aluminium foams, as per the published literature *[120-122]*. In this research work, an EN-32 steel disc of 100 mm diameter, 8 mm thickness, and 24-HRC hardness was used as a counter-disc for wear tests. Since EN-32 is a low carbon grade case hardened, readily machinable, and weldable steel suited for lightly stressed applications subjected to wear such as gears, spindles, and bushes. The foam samples were placed perpendicular to the counter-disc in a pin-on-disc arrangement. The working principle of the pin-on-disc tribometer is illustrated in Fig. 3.5. A high-temperature rotary tribometer, EN 32 steel counter-disc, and Al-6063 alloy foam sample are shown in Fig. 3.6.

Table 3. 3: L_9 orthogonal design of experiments for tribological properties

Factor	A	B	C
Level	Load (N)	Sliding speed (m/s)	Porosity (%)
1	20	0.52	36.4
2	30	0.65	38.2
3	40	0.78	53.03

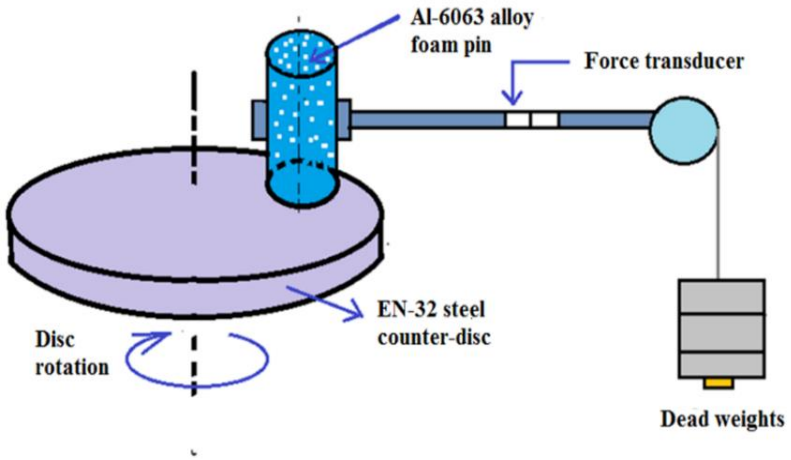

Fig. 3. 5: Schematic diagram of the pin-on-disc tribometer apparatus

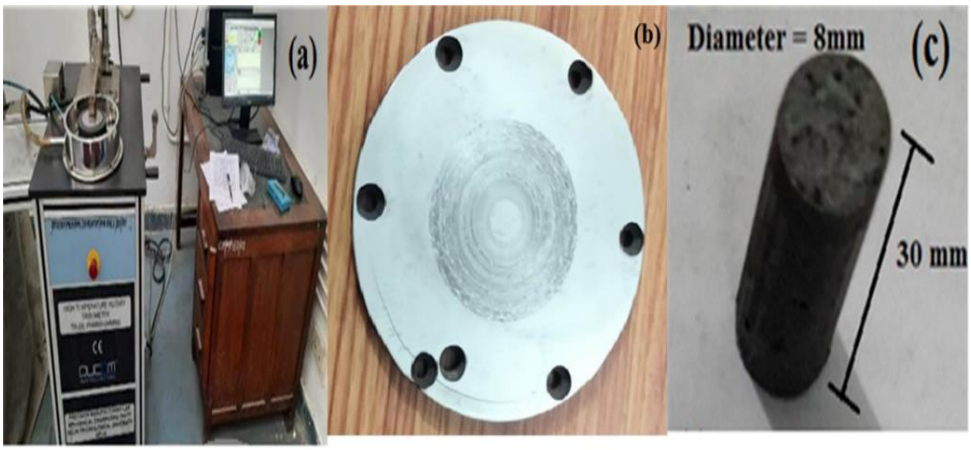

Fig. 3. 6: Tribological properties evaluation **(a)** Tribometer apparatus **(b)** EN 32 steel counter-disc **(c)** Al-6063 alloy foam specimen

The tribological tests were performed in dry sliding conditions at room temperature of 30 °C in March 2022 AD, keeping the sliding distance and rotational speed constant. It was assumed that the wear on the counter-disc was negligible. Other parameters were as follows: $sliding\ distance = \frac{\pi * D * N * T}{60000}$ =200 m (constant); rotational speed = 500 RPM (constant); rotational diameter of the pin (D) = 20 mm, 25 mm, and 30 mm; $rotation\ time\ (T) = \frac{200 * 60000}{\pi * D * N}$ = 382 sec, 305 sec, and 255 sec; $sliding\ speed(V) = \frac{\pi * D * N}{60000}$ = 0.52 m/s, 0.65 m/s, and 0.78 m/s.

3.6.3 Wear mechanism

The wear mechanism and surface morphology of worn-out surfaces of optimal parameter setting-based Al-6063 alloy and its foam samples were analyzed on a scanning electron microscope, Model No. JSM6510LV, made by JOEL, Japan.

Chapter 4
Results and Discussion

4.1 Results and Discussion

This chapter incorporates detailed discussion on microstructure characterization, structural and mechanical properties evaluation, and process optimization of stir-cast Al-6063 alloy foam. Also, in this chapter a detailed discussion on Taguchi-coupled grey optimization of wear parameters and the wear mechanism of stir-cast Al-6063 alloy and its foam is provided.

4.2 Foam Fabrication

In this research work, Al-6063 alloy foam was fabricated by the melt foaming process using TiH_2 as the foaming agent. The stir casting method employed for fabricating Al-6063 alloy foam is economical, as it is based on the direct foaming technique, as per the published literature *[5, 123, and 124]*. It is evident from the published literature *[125]* that aluminium alloy foams obtained using TiH_2, regardless of the base matrix, have more homogeneity in pore distribution, higher expansion at low temperatures, and a lower relative density. Also, it was established that the lowest amount of gases was exhibited by using $CaCO_3$ as a foaming agent *[126]*. The decomposition temperature of TiH_2 is close to the melting temperature range of aluminium alloys, and its decomposition rate is higher than that of other foaming agents as per the published literature *[127]*, which indicates that TiH_2 is a suitable foaming agent for aluminium alloys. During aluminium foaming through metal hydrides, hydrogen gas is evolved due to the decomposition of TiH_2 and absorbates,

which are present in base metal in the form of hydroxides.

The structure of Al-6063 alloy foam was generated within the foaming temperature range of 600-700°C, as per the published literature *[128, 129]*. The sample specimen of fabricated Al-6063 alloy foam block is shown in Fig. 4.1. Al-6063 alloy foam with 40 to 50 pores per inch and an average pore size of 3.5 mm was fabricated in this research work.

Fig. 4. 1: Sample specimen of the fabricated Al- 6063 alloy foam block

The pores generated are non-uniform in shape and size; the cells formed are closed, as shown in Fig. 4.2.

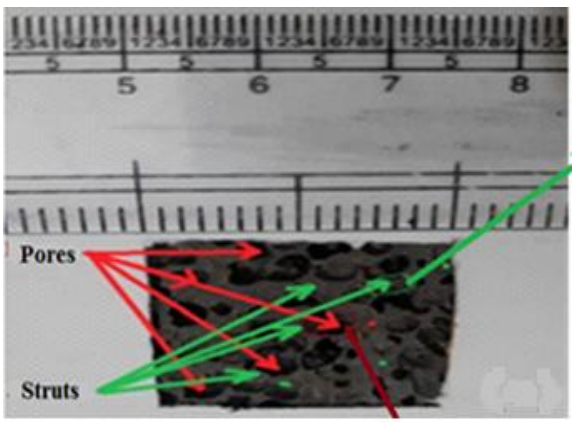

Fig. 4. 2: Schematic representation of the pores and strut in Al-6063 alloy foam

The uniform distribution of an average number of pores per inch in the fabricated Al-6063 alloy foam, as shown in Fig. 4.2, confirms the uniform distribution and decomposition of the blowing agent in the metal matrix. It is evident from published research *[130]* that inter-metallic compounds significantly affect melt viscosity.

4.3 Structural Properties

Density and porosity are fundamental properties that are related to each other. The ratio of the volume of voids to the total volume of the material as a whole is known as porosity. Materials exhibit micro and macro-porosity. In the case of metal foams, generally, macro-porosity is considered. Macro-porosity increases metal foams' effective surface area, making their utilization feasible in heat transfer, acoustic, and energy-absorbing applications.

The density and porosity of Al-6063 alloy foam fabricated by direct pouring method using TiH_2 as a foaming agent were 2.58 g/cm^3 and 9.15%, respectively *[131]*. The density, relative density, and porosity of aluminium 6061 alloy foam fabricated by the salt-sand mould method were 2.24 g/cm^3, 0.8313, and 16.86%, respectively *[109]*. The porosities of low-cost close and open-cell aluminium foams fabricated using $CaCO_3$ and polystyrene granules as foaming agents and space holders were 19.18% and 21.771%, respectively *[132]*.

The mean evaluated densities and porosities of finished Al-6063 alloy and foam samples are listed in Table 4.1. In this research work, fabricated foam's densities and porosities were 1.28–1.85 g/cm^3 and 35.20–57.64%, respectively. The fabricated foam is superior in density and porosity compared to the foams

published in the literature *[109, 131, and 132]*.

Table 4. 1: Structural properties of fabricated Al-6063 alloy foam

Sample specimen	Mean sample mass (m) g	Sample volume (V_t) cm^3	Mean sample density (ρ) g/cm^3	Mean porosity of foam sample (ϕ) %
Foam 1 (1 wt.% TiH_2, 600 °C, 2 mins.)	26.500	15.625	1.696	36.48
Foam 2 (1 wt.% TiH_2, 650 °C, 5 mins.)	26.234	15.625	1.679	37.12
Foam 3 (1 wt.% TiH_2, 700 °C, 8 mins.)	25.687	15.625	1.644	38.41
Foam 4 (2 wt.% TiH_2, 600 °C, 5 mins.)	17.671	15.625	1.131	57.64
Foam 5 (2 wt.% TiH_2, 650 °C, 8 mins.)	19.546	15.625	1.251	53.15
Foam 6 (2 wt.% TiH_2, 700 °C, 2 mins.)	19.812	15.625	1.268	52.51
Foam 7 (5 wt.% TiH_2, 600 °C, 8 mins.)	27.031	15.625	1.730	35.20
Foam 8 (5 wt.% TiH_2, 650 °C, 2 mins.)	24.093	15.625	1.542	42.25
Foam 9 (5 wt.% TiH_2, 700 °C, 5 mins.)	24.218	15.625	1.550	41.96
Al 6063 alloy	41.710	15.625	2.670	0.0

It has been observed that the porosity of aluminium alloy foams depends on their density. The plotted graph, density Vs porosity (%) of fabricated Al-6063 foam depicts that as porosity (%) decreases, there is an increase in density (g/cm^3) of the Al-6063 alloy, as shown in Fig. 4.3.

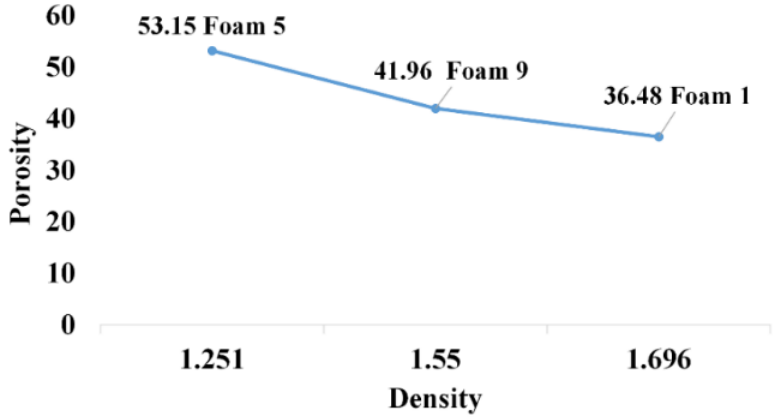

Fig. 4. 3: Density Vs. porosity graph

4.4 Mechanical Properties

Aluminium alloy foams exhibit desirable mechanical properties such as energy absorption capability, flexural strength, and impact absorption. Energy absorption and flexural strength of fabricated Al-6063 alloy and foam samples were evaluated by performing compression and three-point bending tests, respectively. Stress-strain curves were plotted from the load-displacement data obtained from the compression and bending tests through the software. The stress-strain curve provided in Fig. 4.4(a) clearly describes the deformation behavior of metal foams. The stress-strain curve comprises three different regions: the I linear elastic region, where the stress remains directly proportional to strain, and the cell walls of metal foams deform elastically; the II plateau stress region, where the cell walls deform plastically and start to collapse slowly; this region starts with the plateau stress (σ_p); and the III densification region, where cell walls start to collapse entirely under sharply rising stress; densification strain (ε_d) marks the beginning of the densification

region. The three regions of stress-strain curves for metal foams have been reported in the published literature *[133–136]*. Stress-strain curves obtained by compression loading of finished Al-6063 alloy Foam 1, Foam 5, and Foam 9 samples are provided in Fig. 4.4(b). The energy absorption capability (W) of fabricated foam was evaluated by integrating the area under the stress-strain curve up to the beginning of densification strain as given in Eq. 4.1. The obtained values of energy absorption capability are listed in Table 4.2 and range from 12.4 to 33.3 MJ/m^3. Pore structure and cell wall material greatly influence aluminium alloy foams' mechanical properties, as discussed in the published literature *[15, 137]*. It can also be deduced from the published literature *[111], [138]* that the energy absorption capability of fabricated Al-6063 alloy foam is better than the foams fabricated by other researchers.

$$\boldsymbol{W = \int_0^{\varepsilon_d} \sigma_p(\varepsilon) d\varepsilon} \qquad \text{Eq. 4.1}$$

Where, W is the energy absorption capability, σ_p is the Plateau stress, and ε is the densification strain.

Flexural strength is essential when aluminium alloy foams are utilized in structural applications. The flexural properties of aluminium alloy foams largely depend on their porosity and inhomogeneities in the cell wall metal matrix. Uniform porosity distribution positively impacts flexural strength; however, an increase in inhomogeneities in the metal matrix has a negative impact. In this research work, the flexural strength of the fabricated foam was evaluated. Stress-strain curves obtained by three-point bending of finished Al-6063 alloy Foam 1, Foam 5, and Foam 9 samples are provided in Fig. 4.4(c). The flexural

strength (σ) of fabricated foam was evaluated by Eq. 4.2. The obtained flexural strength values are listed in Table 4.2 and range from 4.76 to 25.97 MPa. During the three-point bending test, the foam structure remains intact up to the elastic limit. As the stress reaches the yield point, compression begins, and crack formation occurs at the tensile side of the specimen. Cracks propagate as strain increases, leading to fracture. Similar failure modes were noticed during the flexural property evaluation of aluminium syntactic foam *[139, 140]*.

$$\boldsymbol{\sigma = 3FL/2wd^2} \qquad \text{Eq. 4.2}$$

Where σ is the flexural strength, F is the maximum applied load, L is the span length, w is the width of the specimen, and d is the depth of the specimen.

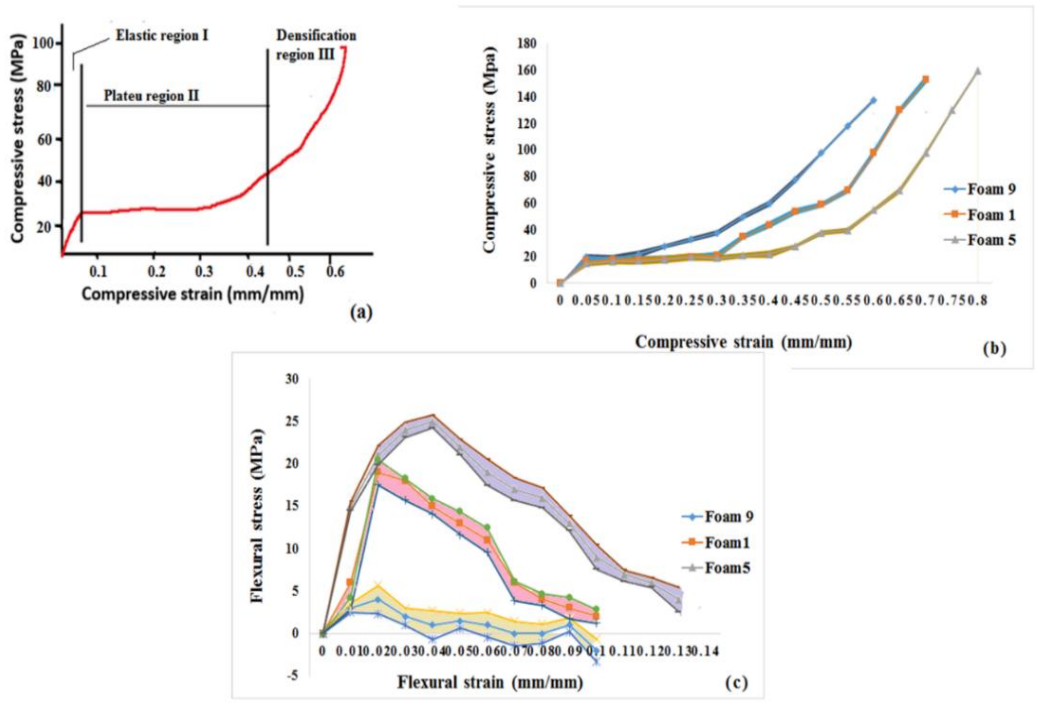

Fig. 4. 4: Stress-strain curves of fabricated Al-6063 alloy foam **(a)** Compressive stress-strain curve (adapted *[139]*) **(b)** Compressive stress-strain curve with standard deviation band **(c)** Flexural stress-strain curve for fabricated with standard deviation band

Table 4. 2: Mechanical properties of fabricated Al-6063 alloy foam

Sample specimen	Mean energy absorption capability $W = \int_0^{\varepsilon d} \sigma p(\varepsilon) d\varepsilon$ (MJ/m^3)	Mean flexural strength $\sigma = 3FL/2Wd^2$ (MPa)
Foam 1 (1 wt.% TiH_2, 600 °C, 2 mins.)	20.5	19.64
Foam 2 (1 wt.% TiH_2, 650 °C, 5 mins.)	22.6	18.24
Foam 3 (1 wt.% TiH_2, 700 °C, 8 mins.)	24.8	20.32
Foam 4 (2 wt.% TiH_2, 600 °C, 5 mins.)	27.5	23.48
Foam 5 (2 wt.% TiH_2, 650 °C, 8 mins.)	33.3	25.97
Foam 6 (2 wt.% TiH_2, 700 °C, 2 mins.)	25.5	24.53
Foam 7 (5 wt.% TiH_2, 600 °C, 8 mins.)	13.5	8.12
Foam 8 (5 wt.% TiH_2, 650 °C, 2 mins.)	15.6	6.78
Foam 9 (5 wt.% TiH_2, 700 °C, 5 mins.)	12.4	4.76
Al-6063 alloy	14.4	7.85

4.5 Multi-response Optimization of the foam fabrication process

The foam fabrication process was optimized through the Taguchi method coupled with grey relational analysis with the help of Minitab software based on the $L_9 3^3$ orthogonal array (OA) listed in Table 4.3.

Table 4. 3: $L_9 3^3$ Orthogonal array for structural and mechanical properties

Exp. number	Factors and levels			Porosity (%)	Energy absorption capability (MJ/m^3)	Flexural strength (MPa)
	A	B	C			
	Amount of TiH_2 (wt.%)	TiH_2 mixing temp. (°C)	Stirring time (mins.)			
1	1	600	2	36.48	20.5	19.64
2	1	650	5	37.12	22.6	18.24
3	1	700	8	38.41	24.8	20.32
4	2	600	5	57.64	27.5	23.48
5	2	650	8	53.15	33.3	25.97
6	2	700	2	52.51	25.5	24.53
7	5	600	8	35.20	13.5	8.12
8	5	650	2	42.25	15.6	6.78
9	5	700	5	41.96	12.4	4.76

The steps involved in grey relational analysis are discussed below.

Step 1: The first step is to calculate S/N ratios for porosity, energy absorption capability, and flexural strength, considering the larger the better criteria through Eq. 3.3. The obtained S/N ratios are provided in Table 4.4.

Table 4. 4: S/N ratios for structural and mechanical properties

S/N ratios		
Porosity (%)	**Energy absorption (MJ/m^3)**	**Flexural strength (MPa)**
31.241	26.235	25.863
31.392	27.082	25.220
31.689	27.889	26.158
35.214	28.787	27.414
34.510	30.449	28.289
34.405	28.131	27.794
30.931	22.607	18.191
32.517	23.862	16.625
32.457	21.868	13.552

Step 2: The second step is to normalize the obtained S/N ratios. The normalization for the larger the better characteristics for the present work is performed by Eq. 4.3. The normalized S/N ratios are listed in Table 4.5.

$$x_i(k) = \frac{y_i(k) - \min y_i(k)}{\max y_i(k) - \min yi\ (k)} \qquad \text{Eq. 4.3}$$

Where $x_i(k)$ is the normalized S/N ratio value, $y_i(k)$ is the evaluated S/N ratio value, $\min y_i(k)$ is the minimum value of $y_i(k)$, $\max y_i(k)$ is the maximum value of $y_i(k)$, i is the number of experiments, and k means the quality characteristics.

Table 4. 5: Normalized S/N ratios for structural and mechanical properties

Normalized S/N ratios		
Porosity (%)	**Energy absorption (MJ/m^3)**	**Flexural strength (MPa)**
0.072	0.509	0.835
0.108	0.608	0.792
0.177	0.702	0.855
1.000	0.806	0.941
0.836	1.000	1.000
0.811	0.730	0.966
0.000	0.086	0.315
0.370	0.232	0.208
0.356	0.000	0.000

Step 3: The third step is calculating grey relational coefficients from normalized S/N ratios. The grey relational coefficient expresses the relationship between the ideal and actual normalized S/N ratios. The grey relational coefficients calculated by Eq. 4.4 are listed in Table 4.6.

$$\epsilon_i(k) = \frac{\Delta \min + \omega \Delta max}{\Delta_{\circ i}(k) + \omega \Delta max} \qquad \text{Eq. 4.4}$$

Where $\epsilon_i(k)$ is the grey relational coefficient, Δmin and Δmax are the minimum and maximum values of the absolute difference($\Delta_{\circ_i}(k) = |x_{\circ_i}(k) - x_i(k)|$) of all comparing sequences, $x_{\circ_i}(k)$ is the best-normalized value of S/N ratios, which is equal to 1, and ω is the distinguishing coefficient defined in the range($0 \leq \omega \leq 1$). The value of ω is set to 0.5.

Table 4. 6: Grey relational coefficients, grade, and rank for structural and mechanical properties

Grey relational coefficients			Grey grade	Grade rank
Porosity (%)	**Energy absorption (MJ/m3)**	**Flexural strength (MPa)**		
0.350	0.504	0.752	0.4018	6
0.359	0.560	0.706	0.4063	5
0.378	0.626	0.776	0.4450	4
1.000	0.721	0.894	0.6536	2
0.753	1.000	1.000	0.6881	1
0.726	0.649	0.937	0.5780	3
0.333	0.354	0.422	0.2772	8
0.443	0.394	0.387	0.3060	7
0.437	0.333	0.333	0.2760	9
			Mean=0.4480	

Step 4: The fourth step is calculating grey relational grades from grey relational coefficients. The grey relational grade is calculated by Eq. 4.5.

$$\alpha_i = \frac{1}{n}\sum_{k=1}^{n} \in_i (k) \qquad \text{Eq. 4.5}$$

Where α_i is the grey relational grade for the i_{th} experiment, n is the number of performance characteristics (here n is 3). A higher grade means the trial outcome is getting closer to the ideal value. Therefore, the highest grey relational grade corresponds to the optimal process parameter combination.

Step 5: The fifth step is calculating grade ranks from grey relational grades. The highest value of the grey relational grade will be assigned a grade rank of one.

The grey relational coefficients, grey grade, and rank for all nine experiments are listed in Table 4.6. Rank 1 indicates the highest grey relational grade (0.6881), which will have better multi-performance characteristics. Table 4.6 shows that the 5^{th} experiment has the optimum process parameters for multi-response characteristics in terms of porosity, energy absorption capability, and flexural strength. Hence, the optimal process parameter setting for the foam fabrication process is 2 wt.% TiH_2 (Level 2), 650 °C TiH_2 mixing temperature (Level 2), and 8 minutes of stirring time (Level 3). Table 4.7 shows the response table for means of the grey relational grade for structural and mechanical properties of fabricated Al-6063 alloy foam. Table 4.7 shows that the amount of mixed TiH_2 has the maximum delta value (0.3535). Therefore, it is inferred that the amount of TiH_2 mixed during the Al-6063 alloy foaming process is the most influential process parameter, followed by stirring time (delta value 0.0415) and TiH_2 mixing temperature (delta value 0.0339). The effects of process parameters on grey relational grade for structural and mechanical properties of fabricated Al-6063 alloy foam are shown in Fig. 4.5. From Fig. 4.5, the optimal process parameter combination for foam fabrication through the stir casting method is 2 wt.% TiH_2 (Level 2), 650 °C TiH_2 mixing temperature (Level 2), and 8 minutes of stirring time (Level 3).

Table 4.7: Response table for means of grey relational grade

Level	Amount of TiH_2 (wt.%)	TiH_2 mixing temp. (°C)	Stirring time (mins.)
1	0.4177	0.4442	0.4286
2	0.6399	0.4668	0.4453
3	0.2864	0.4330	0.4701
Delta	0.3535	0.0339	0.0415
Rank	1	3	2

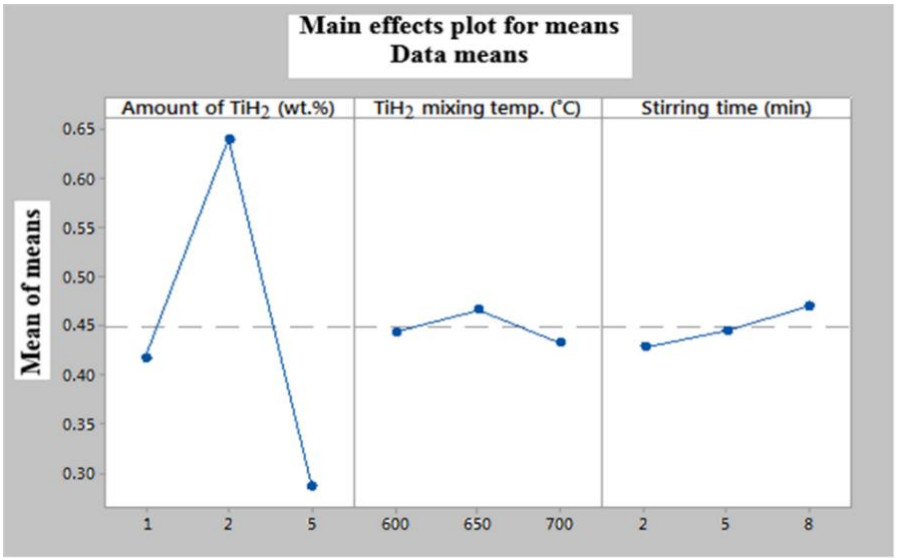

Fig. 4. 5: Effects of process parameters on grey relational grade

4.5.1 Analysis of variance (ANOVA)

An analysis of variance (ANOVA) for the grey relational grade was carried out assuming a 95% confidence level, where sources with a p-value more than 0.05 were considered statistically insignificant on response parameters otherwise significant. The percentage contribution of all process parameters to the structural and mechanical properties of fabricated foam samples was calculated

individually by dividing the individual Adj SS by the Total Adj SS, recorded in Table 4.8. From Table 4.8, it is observed that the amount of TiH_2 mixed during the foaming process is the most significant parameter (contributing 95.96%), followed by stirring time (contributing 1.31%) and TiH_2 mixing temperature (contributing 0.89%).

Table 4. 8: Analysis of variance for grey relational grades of structural and mechanical properties

Source	DF	Adj SS	Adj MS	F-value	P-value	Percentage contribution (%)
Amount of TiH_2 (wt.%)	2	0.191595	0.095798	52.46	0.019	95.96
TiH_2 mixing temp. (°C)	2	0.001786	0.000893	0.49	0.672	0.89
Stirring time (min.)	2	0.002618	0.001309	0.72	0.582	1.31
Error	2	0.003652	0.001826			1.82
Total	8	0.199651				100

DF: Degree of freedom; Adj SS: Adjusted sum of squares; Adj MS: Adjusted mean squares

The percentage contributions of process parameters and the modal summary for ANOVA of structural and mechanical properties of fabricated Al-6063 alloy foam are shown in Fig. 4.6 and Table 4.9, respectively.

Table 4. 9: Modal summary (ANOVA) analysis

S	R-sq	R-sq(adj)	R-sq(pred)
0.0427333	98.17%	92.68%	62.96%

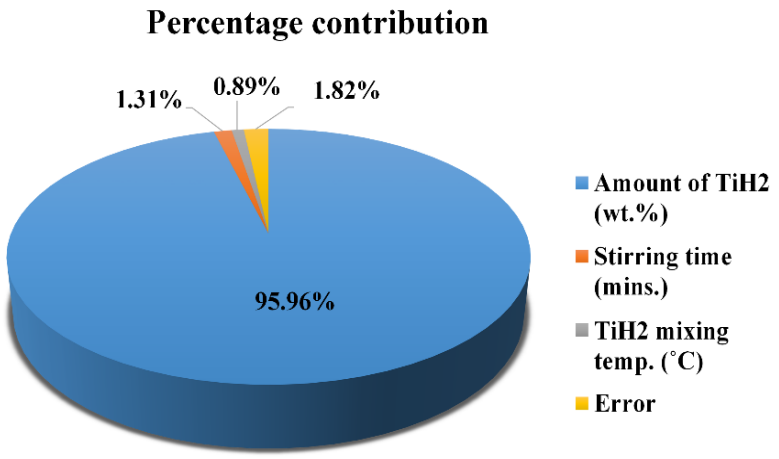

Fig. 4. 6: Percentage contributions of process parameters on foaming process

4.5.2 Confirmation test

A confirmation test was performed to verify the optimal results obtained from grey relational analysis with the help of the predicted grey relational grade. The predicted grey relational grade is expressed by Eq. 4.6.

$$\boldsymbol{\alpha_p = \alpha_\circ + \sum_{i=1}^{n}(\alpha_m - \alpha_\circ)} \qquad \text{Eq. 4.6}$$

Where α_p is the predicted grey relational grade, $\alpha_\circ$ is the total mean of the grey relational grade (here 0.4480), and α_m is the grey relational grade at an optimal level (here, $\alpha_{m1} = 0.6399$, $\alpha_{m2} = 0.4668$ and $\alpha_{m3} = 0.4701$). The predicted grey relational grade calculated from Eq. 4.6 is 0.6808. From Table 4.10, it is deduced that the percentage error between the predicted and experimental grey relational grades is 1.06%, which is under the acceptable range.

Table 4. 10: Confirmation test for process optimization

		Optimal process parameters
	Predicted	**Experimental**
Combination levels	**A2B2C3**	**A2B2C3**
Grey relational grade	**0.6808**	**0.6881**

Percentage error between predicted and experimental grey relational grade is 1.06%.

4.5.3 Regression analysis

Multiple regression analysis was also carried out to correlate the response parameters (grey relational grade) with the process parameters involved in the foaming process. The regression equation is shown in Eq. 4.7. Residual plots were also obtained to verify the significance of coefficients in the predicted regression models. The straight-line graph shown in Fig. 4.7 signifies that the residual errors are normally distributed, and the coefficients in the models are significant. Also, the residuals fall near the line; hence, it is deduced that the model coefficients are significant.

Regression Equation

$$Grade = -1.55 - 0.638\ amount\ of\ TiH_2(wt.\%) + 0.00285\ TiH_2\ mixing\ temp.(^{\circ}C) + 0.945\ stirring\ time(min.) + 0.00100\ amount\ of\ TiH_2(wt.\%) * TiH_2\ mixing\ temp.(^{\circ}C) - 0.0209\ amount\ of\ TiH_2(wt.\%) * stirring\ time(min.) - 0.001336\ TiH_2\ mixing\ temp.(^{\circ}C) * stirring\ time(min.) \quad \text{Eq. 4.7}$$

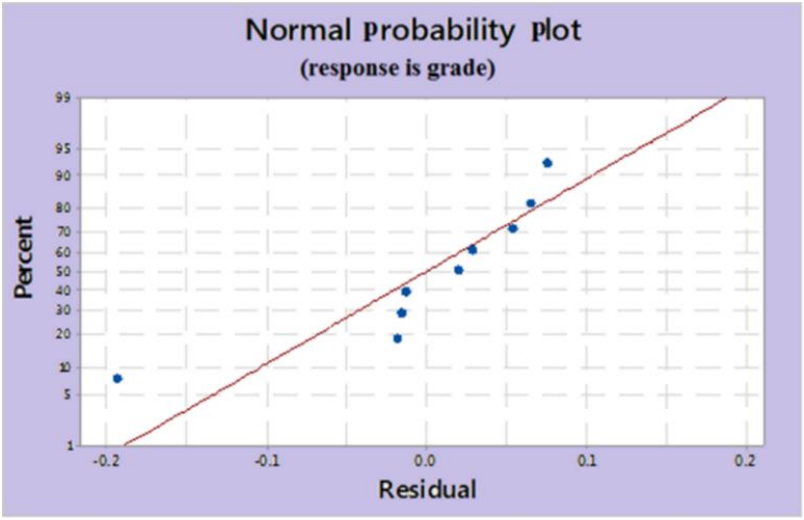

Fig. 4. 7: Normal probability plot for grey relational grade

4.6 Microstructure characterization

The scanning electron micrograph (SEM) technique was employed for the surface identification of finished Al-6063 alloy foam samples. During foaming, titanium combines with aluminium to form titanium aluminide (Al_3Ti) precipitate, an inter-metallic compound. Aluminium undergoes an oxidation process during the melting and solidification processes; hence, aluminium oxide (Al_2O_3) is also present in the Al-metal matrix. Al-matrix, Ti thickening phase, and aluminium oxides are present in the cell wall, as evident from SEM images of Foam 5 (optimal parameter setting) provided in Fig. 4.8(b). The presence of Al_3Ti in the Al-matrix during the foaming process increases the melt viscosity. Due to the combined effect of the aluminide (Al_3Ti) and oxide (Al_2O_3) phases present in the Al-matrix, the merging of bubbles is prevented, and stability of the foaming process is ensured.

The elemental composition of finished Al-6063 alloy foam samples was investigated by energy dispersive X-ray analysis (EDX). EDX analysis of the

Al-6063 alloy foam (Foam 5) sample provided in Fig. 4.9 confirms the presence of the elements aluminium (Al), titanium (Ti), silicon (Si), manganese (Mn), and zinc (Zn), and others.

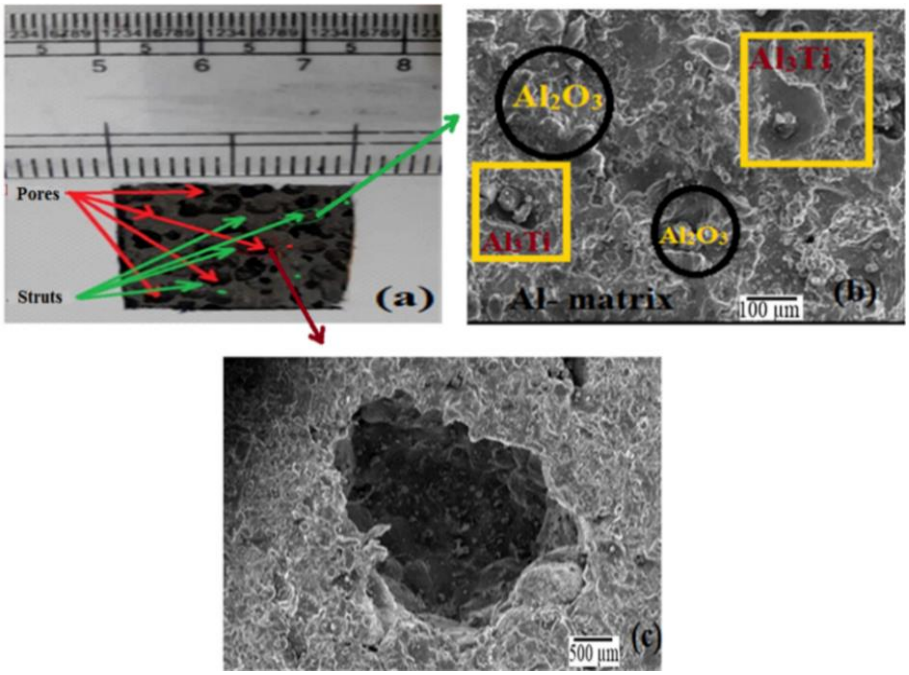

Fig. 4. 8: Microstructural analysis of fabricated Al-6063 alloy foam **(a)** Schematic view of pores and strut in fabricated Al-6063 alloy foam **(b)** SEM image of Al-6063 alloy foam Strut **(c)** SEM image of Al-6063 alloy foam pore (Foam 5)

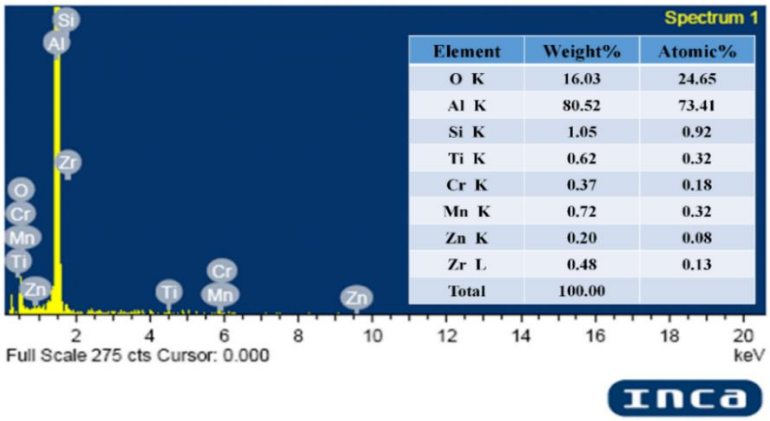

Fig. 4. 9: EDX spectra of fabricated Al-6063 alloy foam (Foam 5)

4.7 Tribological properties

A detailed discussion on microstructure characterization, Taguchi-coupled grey optimization of wear parameters, and the wear mechanism of stir-cast Al-6063 alloy and its foam is provided in section 4.7.1, 4.7.2, and 4.7.3, respectively.

4.7.1 Microstructure characterization

Scanning electron micrographs (SEM) with energy dispersive x-ray (EDX) profiles of Al-6063 alloy and its stir-cast foam samples are provided in Fig. 4.10. The SEM/EDX profile of Al-6063 alloy in Fig. 4.10(a) shows the Al-matrix with major alloying elements such as chromium (Cr), zinc (Zn), magnesium (Mg), etc. The SEM/EDX profile of stir-cast Al-6063 alloy foam samples containing 1 wt.%, 2 wt.%, and 5 wt.% of titanium hydride (TiH_2) are shown in Figs. 4.10(b), (c), and (d), respectively. Several micro and major pores are seen in the micrographs of stir-cast Al-6063 alloy foam samples; however, pores are absent in the micrograph of Al-6063 alloy.

SEM/EDX analysis was performed to identify the different phases present in the matrix *[141, 142]*. The stir-cast Al-6063 alloy and its foam samples contain oxygen (O) in a combined state as aluminium oxide (Al_2O_3). During the foaming of Al-6063 alloy, titanium (Ti) combines with aluminium (Al), which results in the formation of titanium aluminide (Al_3Ti) precipitate. Fig. 4.10(a) shows that Al-matrix and oxide phases are present in the Al-6063 alloy. Fig. 4.10(b), (c), and (d) show that Al-matrix, oxide, and aluminide phases are present in stir-cast Al-6063 alloy foam. The presence of oxide and aluminide phases as intermetallic compounds ensures the stability of aluminium alloy foams *[130]*.

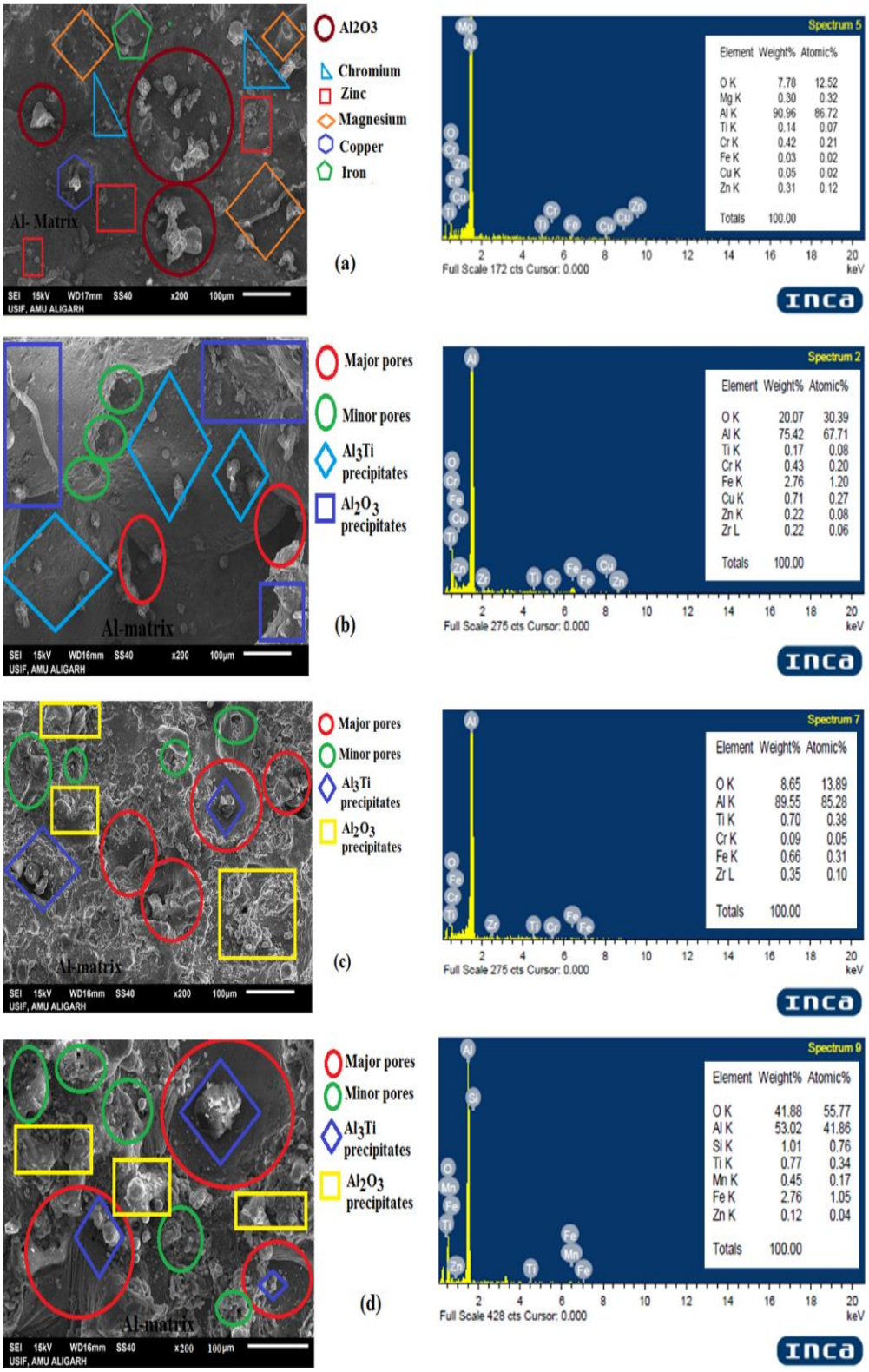

Fig. 4. 10: SEM/EDX images **(a)** Al-6063 alloy **(b)** Al-6063 alloy foam having 36.4% porosity **(c)** Al-6063 alloy foam having 38.2% porosity **(d)** Al-6063 alloy foam having 53.03% porosity

It is also evident from Figs. 4.10(b), (c), and (d) that the titanium hydride powder is uniformly distributed in the stir-cast foam matrix, and there are no clusters either of Al-matrix or of titanium hydride powder. The uniform distribution of TiH_2 powder ensures homogeneous pore distribution. The stir-cast Al-6063 alloy foam exhibits an isotropic nature similar to syntactic foams *[143]*.

4.7.2 Taguchi-based grey optimization for tribological properties

The stir-cast Al-6063 alloy foam wear parameters were optimized through Taguchi-coupled grey relational analysis with the help of Minitab software. The optimization process was based on the $L_9 3^3$ orthogonal array (OA), as listed in Table 4.11.

The Taguchi method can be effectively used for single-response optimization; however, the best-suited method for multi-response optimization is Taguchi coupled with grey relational analysis. In this research work, the grey relational analysis was performed through MS Excel to convert multi-responses into a single response, i.e., grey grades.

Finally, the stir-cast Al-6063 alloy foam wear parameters were optimized through the Taguchi method with the help of Minitab software, considering grey grades as the single response. Moreover, the fourth row of data in Table 4.12, Table 4.13, and Table 4.14 has been highlighted because it corresponds to the first rank, i.e., optimal tribological properties.

Table 4. 11: $L_9 3^3$ orthogonal array for tribological properties

Ex. No.	Factors and levels			wear (microns)	Coefficient of friction (COF)	Frictional force (N)
	A	B	C			
	Load (N)	Sliding speed (m/s)	Porosity (%)			
1	20	0.52	36.4	177	0.28	5.7
2	20	0.65	38.2	43	0.26	5.2
3	20	0.78	53.03	34	0.24	4.8
4	30	0.52	38.2	49	0.29	8.6
5	30	0.65	53.03	283	0.18	5.3
6	30	0.78	36.4	36	0.29	5.7
7	40	0.52	53.03	220	0.22	7.6
8	40	0.65	36.4	26	0.31	4.8
9	40	0.78	38.2	30	0.21	8.6

The steps involved in grey relational analysis are discussed below.

Step 1: The first step is to calculate S/N ratios for wear (microns), coefficient of friction (COF), and frictional force, considering smaller the better criteria using Eq. 3.4. The obtained S/N ratios are tabulated in Table 4.12.

Table 4. 12: S/N ratios for tribological properties

S/N ratios		
Wear (microns)	**COF**	**Frictional force (N)**
-44.959	11.057	-15.117
-32.669	11.701	-14.320
-30.630	12.396	-13.625
-33.804	10.752	-18.690
-49.036	14.895	-14.486
-31.126	10.752	-15.117
-46.848	13.152	-17.616
-28.299	10.173	-13.625
-29.542	13.556	-18.690

Step 2: The second step is to normalize the obtained S/N ratios. The normalization for smaller the better characteristics for the present work is performed by Eq. 4.8. The normalized S/N ratios are tabulated in Table 4.13.

$$x_i(k) = \frac{\max y_i(k) - y_i(k)}{\max y_i(k) - \min y_i(k)} \quad \text{Eq. 4.8}$$

Where, $x_i(k)$ is the normalized S/N ratio value, $y_i(k)$ is the evaluated S/N ratio value, $\min y_i(k)$ is the minimum value of $y_i(k)$, $\max y_i(k)$ is the maximum value of $y_i(k)$, i is the number of the experiments, and k means the quality characteristics.

Table 4. 13: Normalized S/N ratios for tribological properties

Normalized S/N ratios		
Wear (microns)	**COF**	**Frictional force (N)**
0.803	0.813	0.295
0.211	0.676	0.137
0.112	0.529	0.000
0.265	0.877	1.000
1.000	0.000	0.170
0.136	0.877	0.295
0.895	0.369	0.788
0.000	1.000	0.000
0.060	0.284	1.000

Step 3: The third step is calculating grey relational coefficients from normalized S/N ratios. The grey relational coefficient expresses the relationship between the ideal and actual normalized S/N ratios. The grey relational coefficients calculated by Eq. 4.4 are tabulated in Table 4.14.

Table 4. 14: Grey relational coefficients, grade, and rank for tribological properties

Grey relation coefficients			Grey grade	Grade rank
Wear (microns)	**COF**	**Frictional force (N)**		
0.718	0.728	0.415	0.620	3
0.388	0.607	0.367	0.454	8
0.360	0.515	0.333	0.403	9
0.405	0.803	1.000	0.736	1
1.000	0.333	0.376	0.570	5
0.367	0.803	0.415	0.528	7
0.826	0.442	0.702	0.657	2
0.333	1.000	0.333	0.556	6
0.347	0.411	1.000	0.586	4
			Mean= 0.568	

Step 4: The fourth step is calculating grey relational grades from grey relational coefficients. The grey relational grades are calculated by Eq. 4.5. A higher grade means that the experimental result is getting closer to the normalized value. Therefore, the higher the grey relational grade, the closer the corresponding process parameter combination is to the optimal.

Step 5: The fifth step is calculating grade ranks from grey relational grades. The highest value of the grey relational grade will be assigned a grade rank of one.

Table 4.14 shows all nine iterations' grey relational coefficients, grades, and ranks. Rank 1 indicates the highest grey relational grade (0.736), which will have better multi-performance characteristics. It is clear from Table 4.14 that the fourth experiment has the optimum process parameters for multi-response characteristics in terms of wear, coefficient of friction, and frictional force. Hence, the optimal wear parameter setting for the tribological properties is 30 N load (Level 2), 0.52 m/s sliding speed (Level 1), and 38.2% porosity (Level 2).

Table 4.15 shows the response table for Taguchi optimized means of the grey relational grade for tribological properties. Table 4.15, shows that the sliding speed has the maximum delta value (0.1653). Therefore, it is inferred that the sliding speed is the most influential process parameter, followed by load (delta value 0.1190) and porosity of Al-6063 alloy foam (delta value 0.0487). The effects of process parameters on grey relational grade for tribological properties are shown in Fig. 4.11. Hence, from Fig. 411, it is also observed that the optimal process parameter combination that affects the tribological properties of Al-6063 alloy foam is 30 N load (Level 2), 0.52 m/s sliding speed (Level 1), and 38.2% porosity (Level 2).

Table 4. 15: Response table for means of grey relational grades

Level	Load	Sliding speed	Porosity
1	0.4923	0.6710	0.5680
2	0.6113	0.5267	0.5920
3	0.5997	0.5057	0.5433
Delta	0.1190	0.1653	0.0487
Rank	2	1	3

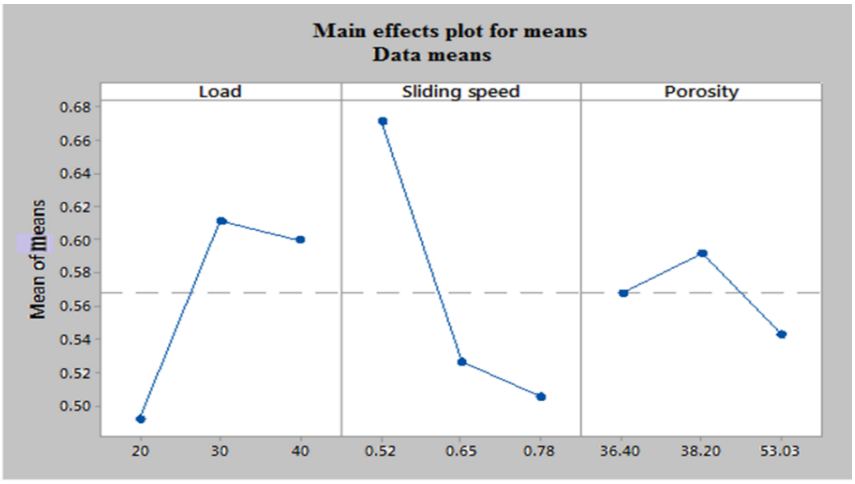

Fig. 4. 11: Effect of process parameters on grey relational grade

A confirmation test was performed to verify the optimal results obtained from grey relational analysis with the help of the predicted grey relational grade. The predicted grey relational grade calculated from Eq. 4.6 is 0.7383. From Table 4.16, it is deduced that the percentage error between the predicted and experimental grey relational grades is 0.32%, which is under the acceptable range.

Table 4. 16: Confirmation test results for tribological properties

		Optimal process parameters
	Predicted	**Experimental**
Combination levels	**A2B1C2**	**A2B1C2**
Grey relational grade	**0.7383**	**0.7360**

Percentage error between predicted and experimental grey relational grade is 0.32%.

4.7.3 Wear mechanism during wear test

Initially, adhesive wear results from relative motion between the surfaces of stir-cast Al-6063 alloy pin and the EN-32 steel disc. As the relative motion advances, the abrasive effect of fragmented adhesive wear debris causes a significant increase in wear rate. The schematic wear mechanism of stir-cast Al-6063 alloy foam is shown in Fig. 4.12. The relative motion between the softer Al-6063 foam pin and more arduous EN-32 steel disc increases the interface temperature. Al-6063 foam deforms plastically at elevated temperatures. The foam strut experiences adhesive wear, and debris accumulates in the pores. Due to the temperature rise and accumulation of wear debris in the pores, an adhesive wear layer is generated at the pin and disc interface. The generated

adhesive layer comprises Al-matrix, oxide, and aluminide phases of aluminium. The adhesive layer gets fragmented into tiny abrasive particles due to continuous sliding. As the sliding continues, newer pores are subjected to abrasive wear. The surface of stir-cast Al-6063 alloy foam wears due to the combined effect of sliding, adhesive, and abrasive wear phenomena. The Al-6063 alloy foam shows improved wear resistance due to the low interaction area between the matrix and counter-surface and more heat conduction due to its porous structure as per the published literature *[144, 145]*.

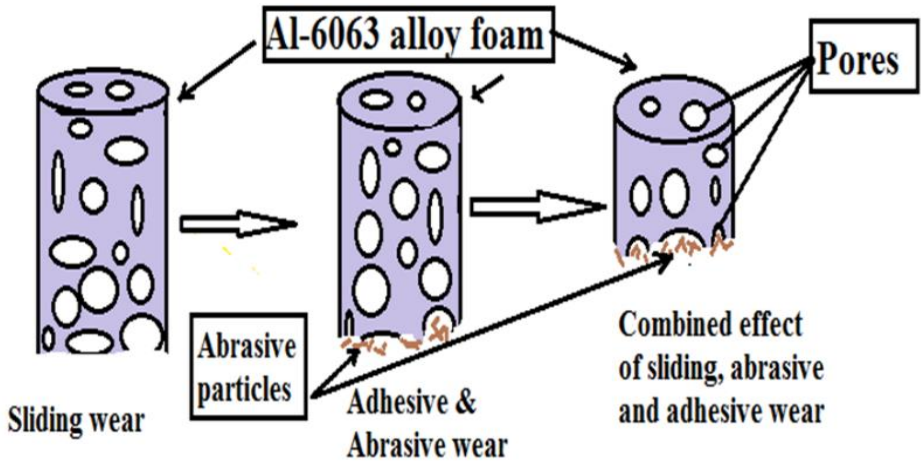

Fig. 4. 12: Wear mechanism of fabricated Al-6063 alloy foam

The surface morphology of worn-out surfaces of Al-6063 alloy and stir-cast foam at optimal parameter settings was analyzed with the help of a scanning electron microscope (SEM). The micrographs of worn-out surfaces of Al-6063 alloy and stir-cast foam samples at optimal parameter settings are shown in Figs. 4.13(a) and (b), respectively. Micrograph of Al-6063 alloy provided in Fig. 4.13(a) shows the combined effect of adhesive and abrasive wear in addition to some material uplift. Broader and deeper wear grooves are seen on

the surface of the Al-6063 alloy. The micrographs of stir-cast Al-6063 alloy foam at optimal parameter setting, provided in Fig. 4.13(b), show the combined effect of sliding, adhesive, and abrasive wear with shear deformation marks similar to those of A356/SiC foam and co-continuous ceramic foam/aluminium alloy interpenetrating composites *[146, 147]*.

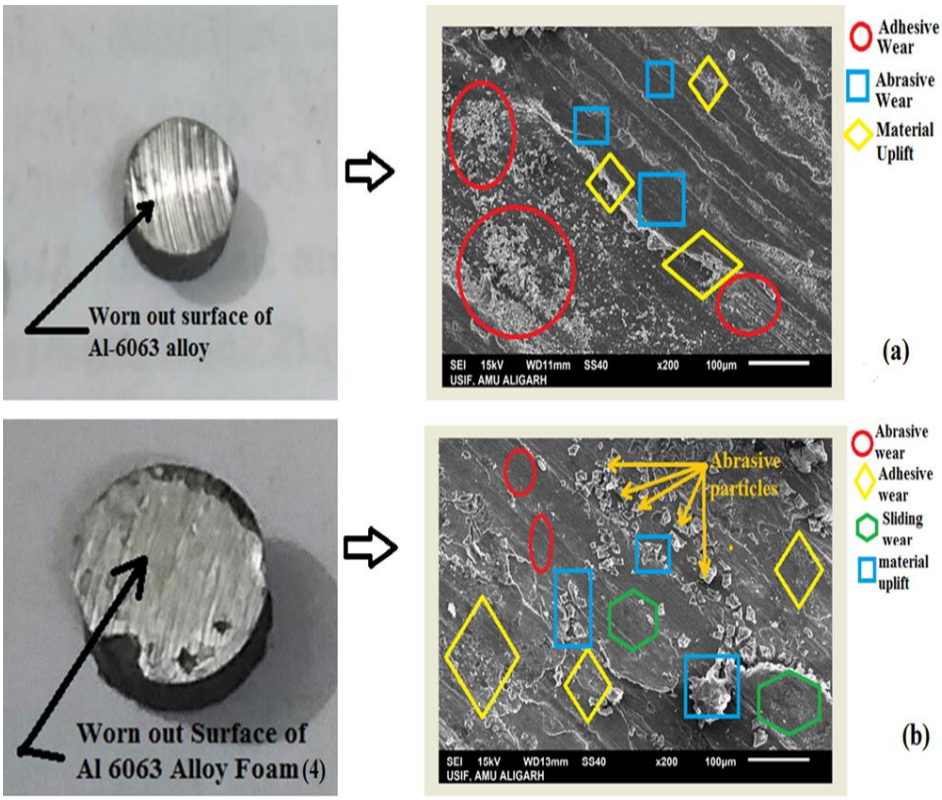

Fig. 4. 13: SEM images of worn-out surfaces **(a)** Al-6063 alloy **(b)** Al-6063 alloy foam at optimal parameter setting (4th iteration)

The maximum wear of stir-cast Al-6063 alloy foam at optimal parameter setting occurred in the vicinity of pores, similar to hybrid aluminium matrix syntactic foams (AMSFs) *[122]*. It is evident from the micrograph in Fig. 4.13(b) that abrasive wear is dominant in the stir-cast Al-6063 alloy foam at optimal parameter settings.

4.8 Comparison between the Tribological Properties of Al-6063 Alloy and its Foam

The tribological properties of the Al-6063 alloy sample (8mm in diameter and 30 mm in height) were evaluated experimentally at 30 N load and 0.52 m/s sliding speed by performing a pin-on-disc wear test in dry sliding conditions. The tests were performed at ambient temperature of 30 °C in March 2022 AD, keeping the sliding distance constant. It was assumed that the wear on the counter-disc was negligible. Other parameters were as follows: $sliding\ distance = \frac{\pi * D * N * T}{60000}$ = 200 m (constant); rotational speed = 500 RPM (constant); rotational diameter of pin (D) = 20 mm; $rotation\ time\ (T) = \frac{200 * 60000}{\pi * D * N}$ = 382 seconds; $sliding\ speed (V) = \frac{\pi * D * N}{60000}$ = 0.52 m/s.

A computer-aided data acquisition system was used to simultaneously record height loss (microns), frictional force (N), and coefficient of friction. The tribological properties of stir-cast Al-6063 alloy foam at optimal parameter settings are tabulated in Table 4.11 in experiment number four. The specimen height loss (h) was converted into volume loss (V) by using the interactive cross-sectional area of the specimens. Wear rate (W_r) was evaluated by finding the ratio of volume loss and sliding distance. Wear resistance (W_R) is defined as the reciprocal of wear rate; however, specific wear (W_S) rate is defined as the load-bearing ability of the material. The equations for volume loss, wear rate, wear resistance, and specific wear rate are illustrated in Eq. 4.9, Eq. 4.10, Eq. 4.11, and Eq. 4.12, respectively. The experimentally evaluated optimal tribological properties of Al-6063 alloy and its foam samples are listed in Table

4.17. The sliding interface area for Al-6063 alloy is πr^2 whereas the sliding interface area for Al-6063 alloy foam is (100-38.2 = 61.8% of πr^2).

$$Volume\ loss\ (V) = \pi r^2 \mathrm{h} \qquad \text{Eq. 4.9}$$

$$Wear\ rate\ (W_r) = \frac{Volume\ loss\ (V)}{Sliding\ distance} \qquad \text{Eq. 4.10}$$

$$Wear\ resistance\ (w_R) = \frac{1}{wear\ rate\ (W_r)} \qquad \text{Eq. 4.11}$$

$$Specific\ wear\ rate\ (W_s) = \frac{Wear\ rate\ (W_r)}{Normal\ Load\ (L)} \qquad \text{Eq. 4.12}$$

Table 4. 17: Optimal tribological properties of fabricated Al-6063 alloy and its foam

Load (N)	Sample specimen porosity (%)	Coefficient of friction(μ)	Frictional force (N)	Wear (microns)	Volume loss (mm^3)	Wear rate (mm^3/m)	Specific wear rate (mm^3/N-m)
30	Al-6063 alloy (0%)	0.92	27.6	169	8.49	0.043	0.0014
	Al-6063 alloy foam (38.2%)	0.29	8.6	49	1.51	0.0076	0.00025

The bar charts provided in Fig. 4.14 show the trends of coefficient of friction (COF), frictional force, and specific wear rate of Al-6063 alloy and its stir-cast foam samples at optimal parameter settings. It is evident from the bar charts provided in Fig. 4.14 that the values of coefficient of friction (COF), frictional force, and specific wear rate of stir-cast Al-6063 alloy foam are lower than those of the Al-6063 alloy. Indeed, the presence of different precipitates in the synthesized foam and several other factors, such as porosity, affect the tribological properties of the synthesized foam. The decreasing trends in tribological properties are partially attributed to decreased surface contact area

due to induced porosity, as per the published literature *[148]*.

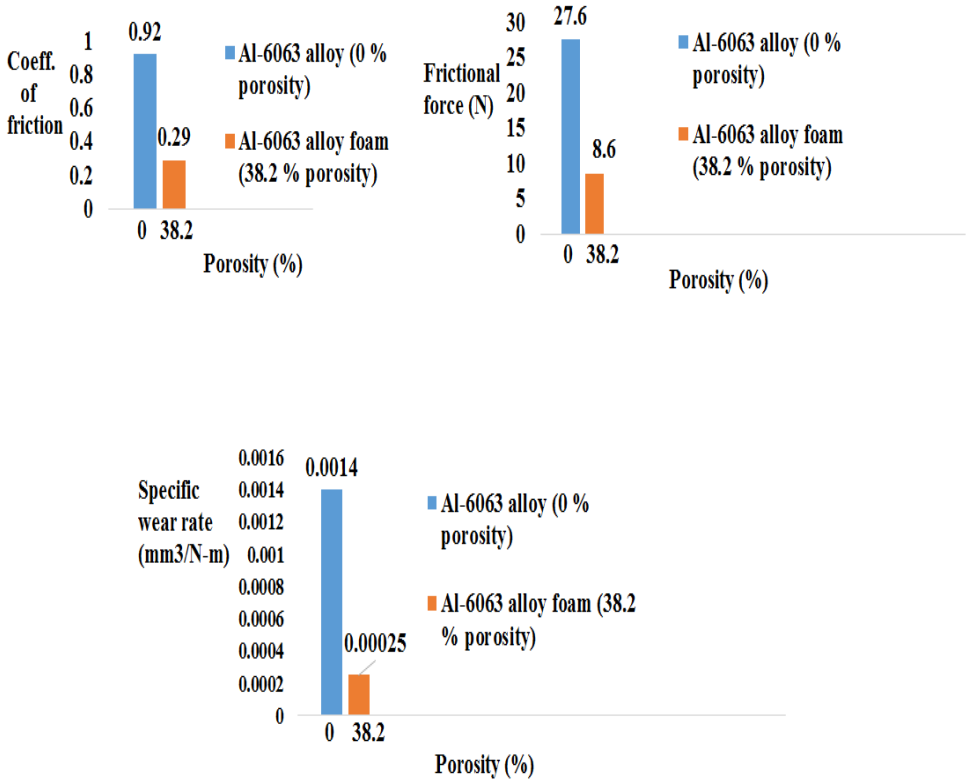

Fig. 4. 14: Bar charts of tribological properties of fabricated Al-6063 alloy and its foam at optimal parameters

A comparative literature survey of tribological properties of metal foams synthesized through different foaming routes with their base alloy/composite is presented in Table 4.18. It is evident from Table 4.18 that the tribological properties of stir-cast Al-6063 alloy foam are comparable to the other foams synthesized through different techniques, with some exceptions. The coefficient of friction of stir-cast Al-6063 alloy foam is less than that of the base Al-6063 alloy, as supported by the published literature *[120, 149, 122, 143, and 146]*.

Table 4. 18: Literature survey of tribological properties (Dry sliding wear)

S. No	Sample name	Tribological properties			References
		Coefficient of friction (μ)	**Wear rate (mm^3/m) * 10^-3**	**Specific wear rate ($mm^3/N-m$) * 10^-4**	
1	Al-syntactic foam	0.04-0.12	0.5 - 9.5	-	*[120]*
	Al-SiC composite	0.6	0.4 – 3.0	-	
2	A-356/SiC foam composite	0.31-0.39	4- 25	-	*[146]*
	A-356 alloy	0.37-0.59	5 - 28	-	
3	Cenosphere filled ASF	0.06-0.08	0.8-2.2	-	*[149]*
	10 wt.% SiC AMC	0.5-0.8	1.4-2.5	-	
4	AMSFs	0.07-0.54	85 -180	-	*[122]*
	AlSi12 matrix material	0.16-0.40	12.7	-	
5	Cenosphere reinforced epoxy foam	0.172 - 0.644	1.10-7.30	-	*[143]*
	Epoxy matrix	Higher than (0.172-0.644)	Lower than (1.10-7.30)	-	
6	Stir-cast Al-6063 alloy foam	0.18-0.31	4.01-33.4	1.037-14.1	Present study
	Stir-cast Al-6063 alloy	0.83-0.93	38-68	11-26	

Chapter 5
Conclusions and Future Scope

5.1 Conclusions

Aluminium alloy foams play a vital role in the automotive, aviation, marine, and defense sectors as they are light in weight and have better mechanical, physical, and tribological properties. The automotive industry has the greatest potential for the application of aluminium alloy foams due to their high strength-to-weight ratio. The present study was performed to analyze the microstructure, wear behavior, mechanical, and tribological properties of stir-cast aluminium 6063 alloy and its foam. Aluminium 6063 alloy is considered a structural aluminium alloy; hence, the fabricated Al-6063 alloy foam can be utilized in structural works requiring a high strength-to-weight ratio. The fabricated aluminium 6063 alloy foam is the effective replacement for solid materials used in vehicle frames to achieve improved drivability, stability, crashworthiness, and mileage. The synthesized aluminium 6063 alloy foam is also the suitable replacement for solid materials used in loading and unloading packaged goods in the shipping industry, which involves sliding and rubbing with other surfaces. The following conclusions are drawn from the above study:

1. Aluminium 6063 alloy foam was successfully produced via stir casting, utilizing different concentrations of titanium hydride as a foaming agent.
2. The density and porosity of fabricated aluminium 6063 alloy foam were 1.28–1.85 g/cm^3 and 35.20–57.64%, respectively.
3. Fabricated aluminium 6063 alloy foam's energy absorption capability

and flexural strength were 12.4–33.3 MJ/m^3 and 4.76–25.97 MPa, respectively.

4. The stir casting method of aluminium 6063 alloy foam fabrication was optimized and statistically modelled through the Taguchi method coupled with grey relational analysis based on $L_9 3^3$ orthogonal design. The optimal process parameter setting for the foam fabrication process is 2 wt.% TiH_2 (Level 2), 650 °C TiH_2 mixing temperature (Level 2), and 8 minutes of stirring time (Level 3). The corresponding values of the optimized response variables were 53.15% porosity, 33.3 MJ/m^3 energy absorption, and 25.97 MPa flexural strength.
5. It was observed through ANOVA analysis that the amount of TiH_2 mixed during the foaming process was the most significant parameter (contributing 95.96%), followed by stirring time (contributing 1.31%) and TiH_2 mixing temperature (contributing 0.89%).
6. It was observed from the confirmation test that the percentage error between the predicted and experimental grey relational grade is 1.06%, which is under a reasonable degree of approximation.
7. The correlation between the process parameters (amount of TiH_2 in wt.%, TiH_2 mixing temperature in ˚C, and stirring time in minutes) involved in the foaming process, and the response variables (porosity, energy absorption capability, and flexural strength) was successfully obtained.
8. The microstructures of stir-cast aluminium 6063 alloy and its foam were

studied by performing scanning electron microscopy. The uniform distribution of titanium hydride powder in the metal matrix ensures homogeneous pore distribution, which leads to the isotropic nature of stir-cast aluminium 6063 alloy foam.

9. Al-matrix and oxide phases are present in stir-cast aluminium 6063 alloy; however, Al-matrix, oxide, and aluminide phases are present in stir-cast aluminium 6063 alloy foam. The presence of oxide and aluminide phases as intermetallic compounds in the stir-cast aluminium 6063 alloy foam ensured the stability of the synthesized foam.

10. The wear parameters of stir-cast aluminium 6063 alloy foam were optimized using Taguchi-coupled grey relational analysis, based on the $L_9 3^3$ orthogonal design. The optimal wear parameter setting for the tribological properties is 30 N load, 0.52 m/s sliding speed, and 38.2% porosity. The corresponding optimal tribological properties are 0.29 coefficient of friction, 8.6 N frictional force, and 0.00025 mm^3/N-m specific wear rate.

11. Taguchi optimization revealed that sliding speed (with a delta value of 0.1653) is the most significant wear parameter, followed by load (delta value 0.1190) and porosity (delta value 0.0487) of stir-cast aluminium 6063 alloy foam.

12. Stir-cast aluminium 6063 alloy wears due to the combined effect of adhesive wear, abrasive wear, and material uplift. During sliding, the

surface of the aluminium 6063 alloy developed larger and deeper wear grooves. Stir-cast aluminium 6063 alloy foam shows the combined effect of sliding, adhesive, and abrasive wear with shear deformation marks. The maximum wear in stir-cast Al-6063 alloy foam occurs in the vicinity of pores.

13. The tribological properties of stir-cast aluminium 6063 alloy foam are better than those of aluminium 6063 base alloy and comparable to several other aluminium foams mentioned in the literature.

14. It can be concluded that better-quality aluminium 6063 alloy foam can be fabricated by following the established optimum process parameters through stir casting using TiH_2 as a foaming agent.

5.2 Future Scope

1. Advanced Optimization Techniques: Researchers have modeled the mechanical behavior of metallic foams; however, theoretical and numerical models for metal foam processing are unavailable. There needs to be more control over the structure and morphology of metal foams. Hence, existing methods should be improved and numerically modeled. The process parameters should be optimized by employing advanced optimization techniques like genetic algorithms or machine learning models to obtain good-quality foams.
2. Material diversification: Future studies can explore other aluminium alloys or different metals to understand the broader applicability of the findings.

3. Scale-up studies: Conducting studies on scaling up the foam manufacturing process to industrial levels and addressing the challenges associated with it.
4. Cost-benefit analysis: Cost-effective methods should be employed for metal foam fabrication suited for a high volume mass production. Cost-efficient metal foams can be obtained by adopting a recycling material strategy and using scrap material as the base metal. A comprehensive cost-effectiveness analysis may be performed to evaluate the economic feasibility of the proposed manufacturing method.
5. Applications in different sectors: Exploring the use of aluminium alloy foam in various sectors like biomedical, aerospace, and automotive for different applications. Mechanical properties of metallic foams can be enhanced by coating metallic or inorganic materials on their surface. Hence, new and technologically advanced metal foam coating methods and materials should be developed to obtain application-specific metal foams.
6. Search for admixing particles: Search for more effective foaming agents, reinforcing particles, space holders, and filler particles should be continued. Efforts should be made to develop methods for a more uniform distribution of reinforcing agents.

REFERENCES

[1] De Meller, M. A. "Produit métallique pour l'obtention d'objets laminés, moulés ou autres, et procédés pour sa fabrication." *French Patent* 615.147 (1925): 1926.

[2] Banhart, John. "Light-metal foams—history of innovation and technological challenges." *Advanced Engineering Materials* 15.3 (2013): 82-111.

[3] Baumeister, J. "Verfahren zur Herstellung poröser Metallkörper." *German Patent* 40.18 (1991): 360.

[4] Baumeister, J., and H. Schrader. "Verfahren zur Herstellung aufschäumbarer Metallkörper und Verwendung derselben." *German Patent* 41.01 (1992): 630.

[5] Banhart, John. "Manufacture, characterisation and application of cellular metals and metal foams." *Progress in materials science* 46.6 (2001): 559-632.

[6] Banhart, John, M. Ashby, and N. Fleck. "Metal foams and porous metal structures." *Conference on Metal Foams and Porous Metal Structures* 14 (1999).

[7] Banhart, John, M. Ashby, and N. Fleck. "International Conference on Cellular Metals and Metal Foaming Technology." (2001).

[8] Binks, Bernard P., and Tommy S. Horozov, eds. *Colloidal particles at liquid interfaces*. Cambridge University Press, 2006.

[9] Degischer, Hans-Peter, and Brigitte Kriszt. *Handbook of cellular metals* 71 (2002). Wiley-VCH, Weinheim.

[10] Gibson, Lorna J. "Cellular solids." *Mrs Bulletin* 28.4 (2003): 270-274.

[11] Banhart, John, and Denis Weaire. "On the road again: metal foams find favor." *Physics Today* 55.7 (2002): 37-42.

[12] Banhart J, Norman AF, Mortensen A. Proceedings of the International Conference on Cellular Metals: Manufacturing, Properties, Applications (*MetFoam'03).* 2003.

[13] Du, Ran, et al. "Engineering self-supported noble metal foams toward electrocatalysis and beyond." *Advanced Energy Materials* 10.11 (2020): 1901945.

[14] Atwater, Mark A., et al. "Solid state porous metal production: A review of the capabilities, characteristics, and challenges." *Advanced Engineering Materials* 20.7 (2018): 1700766.

[15] Zhao, Biao, et al. "A review on metallic porous materials: pore formation, mechanical properties, and their applications." *The International Journal of Advanced Manufacturing Technology* 95 (2018): 2641-2659.

[16] Jung, Anne, and Stefan Diebels. "Micromechanical characterization of metal foams." *Advanced Engineering Materials* 21.8 (2019): 1900237.

[17] Ashby, Michael F., and Lorna J. Gibson. "Cellular solids: structure and properties." *Press Syndicate of the University of Cambridge, Cambridge, UK* (1997): 175-231.

[18] Kiser, M., M. Y. He, and F. W. Zok. "The mechanical response of ceramic microballoon reinforced aluminum matrix composites under compressive loading." *Acta Materialia* 47.9 (1999): 2685-2694.

[19] Rohatgi, Pradeep K., et al. "The synthesis, compressive properties, and applications of metal matrix syntactic foams." *Jom* 63 (2011): 36-42.

[20] Jin, Iljoon, Lorne D. Kenny, and Harry Sang. "Method of producing lightweight foamed metal." U.S. Patent No. 4,973,358. 27 Nov. 1990.

[21] Kenny, Lorne D., and Martin Thomas. "Process for shape casting of particle stabilized metal foam." U.S. Patent No. 5,281,251. 25 Jan. 1994.

[22] Ruch, W., and B. Kirkevag. "International Patent Application PCT/NO90/00115 (1990)." (1991): 91-01387.

[23] Lloyd, David J., et al. "Melt process for the production of metal-matrix composite materials with enhanced particle/matrix wetting." U.S. Patent No. 5,028,392. 2 Jul. 1991.

[24] Prakash, O., H. Sang, and J. D. Embury. "Structure and properties of Al□ SiC foam." *Materials Science and Engineering: A* 199.2 (1995): 195-203.

[25] Akiyama, Shigeru, et al. "Foamed metal and method of producing same." U.S. Patent No. 4,713,277. 15 Dec. 1987.

[26] Miyoshi, Tetsuji, et al. "ALPORAS aluminum foam: production process, properties, and applications." *Advanced engineering materials* 2.4 (2000): 179-183.

[27] Schwartz, Daniel S., et al. "Porous and cellular materials for structural applications." *MRS Symp. Proc*. Vol. 521. 1998.

[28] Shapovalov, Vladimir I. "Method for manufacturing porous articles." U.S. Patent No. 5,181,549. 26 Jan. 1993.

[29] Zheng, Y., S. Sridhar, and K. C. Russell. "Advances in porous materials." *MRS Symp. Proc*. Vol. 371. 1995.

[30] Simone, A. E., and L. J. Gibson. "The compressive behaviour of porous copper made by the GASAR process." *Journal of materials science* 32 (1997): 451-457.

[31] ISO, ASTM. "ISO/ASTM 52900: 2015 additive manufacturing–general principles–terminology." *ASTM F2792-10e1* 1 (2015): 1-19.

[32] Du Plessis, Anton, et al. "Properties and applications of additively manufactured metallic cellular materials: A review." *Progress in Materials Science* 125 (2022): 100918.

[33] Milewski, John O., and John O. Milewski. "Understanding metal for additive manufacturing." *Additive Manufacturing of Metals: From Fundamental Technology to Rocket Nozzles, Medical Implants, and Custom Jewelry* (2017): 49-83.

[34] Murr, Lawrence E., et al. "Metal fabrication by additive manufacturing using laser and electron beam melting technologies." *Journal of Materials Science & Technology* 28.1 (2012): 1-14.

[35] Koike, Ryo, et al. "A basic study on metal foam fabrication with titanium hydride in direct energy deposition." *Procedia*

Manufacturing 18 (2018): 68-73.

[36] Koike, Ryo, et al. "Fabrication method for stainless steel foam block in directed energy deposition." *CIRP Annals* 69.1 (2020): 173-176.

[37] Shim, Do-Sik, et al. "Additive manufacturing of porous metals using laser melting of Ti6Al4V powder with a foaming agent." *Materials Research Express* 5.8 (2018): 086518.

[38] Shim, Do-Sik, and Ja-Ye Seo. "Fabrication of porous metals layered by laser-assisted melting of sprayed Ti6Al4V powder and foaming agent mixture." *Materials Letters* 219 (2018): 243-246.

[39] Changdar, Anirban, and Shitanshu Shekhar Chakraborty. "Laser processing of metal foam-A review." *Journal of Manufacturing Processes* 61 (2021): 208-225.

[40] Hernández-Nava, E., et al. "The effect of density and feature size on mechanical properties of isostructural metallic foams produced by additive manufacturing." *Acta Materialia* 85 (2015): 387-395.

[41] Kang, Boseok, et al. "3D porous metal structure manufacturing using UV pulsed laser and copper formate solution." *Applied Physics A* 124 (2018): 1-5.

[42] Mustapha, K. A., et al. "Production of open-cell foam using additive manufacturing method and porous morphology effects." *International Conference and Exhibition on Sustainable Energy and Advanced Materials*. Singapore: Springer Nature Singapore, 2021.

[43] Takeuchi, Toshihiro, et al. "Basic study of fabrication conditions for

foam stainless in directed energy deposition." *Proceedings of International Conference on Leading Edge Manufacturing in 21st century: LEM21 2021.10*. The Japan Society of Mechanical Engineers, 2021.

[44] Moser, S., et al. "3D ink-printed, sintered porous silicon scaffolds for battery applications." *Journal of Power Sources* 507 (2021): 230298.

[45] Park, Hyeji, Heeman Choe, and David C. Dunand. "Microstructure and compressive properties of 3D-extrusion-printed, aluminized cobalt-based superalloy microlattices." *Materials Science and Engineering: A* 815 (2021): 141262.

[46] Song, Binna, Christoph Kenel, and David C. Dunand. "3D ink-extrusion printing and sintering of Ti, Ti-TiB and Ti-TiC microlattices." *Additive Manufacturing* 35 (2020): 101412.

[47] Matheson, Kristoffer, et al. "Comparison of conventional open-cell aluminum foam and its additively manufactured twin." *Materials Science and Technology Conference and Exhibition 2016, MS and T 2016*. Vol. 2. 2016.

[48] Carpenter, Julia A., et al. "3D Printing of Hierarchical Porous Steel and Iron-Based Materials." *Advanced Materials Technologies* 8.3 (2023): 2200971.

[49] Valdez, Mario, et al. "Induced porosity in Super Alloy 718 through the laser additive manufacturing process: Microstructure and mechanical properties." *Journal of Alloys and Compounds* 725 (2017): 757-764.

[50] Yang, Li, et al. "Non-stochastic Ti–6Al–4V foam structures with negative Poisson's ratio." *Materials Science and Engineering: A* 558 (2012): 579-585.

[51] Kenel, C., et al. "Hierarchically-porous metallic scaffolds via 3D extrusion and reduction of oxide particle inks with salt space-holders." *Additive Manufacturing* 37 (2021): 101637.

[52] Xu, Chenyang, et al. "3D printing of powder-based inks into functional hierarchical porous TiO2 materials." *Advanced Engineering Materials* 22.3 (2020): 1901088.

[53] Atwater, Mark A., et al. "Solid state porous metal production: a review of the capabilities, characteristics, and challenges." *Advanced Engineering Materials* 20.7 (2018): 1700766.

[54] Mostafaei, Amir, et al. "Microstructural evolution and magnetic properties of binder jet additive manufactured Ni-Mn-Ga magnetic shape memory alloy foam." *Acta Materialia* 131 (2017): 482-490.

[55] Miyanaji, Hadi, et al. "Binder jetting additive manufacturing of copper foam structures." *Additive Manufacturing* 32 (2020): 100960.

[56] Koizumi, Takuya, et al. "Foaming agents for powder metallurgy production of aluminum foam." *Materials transactions* 52.4 (2011): 728-733.

[57] Bram, M., et al. "Preparation and characterization of high-porosity titanium, stainless steel, and superalloy parts." *Metal Foams and Porous Metal Structures* (1999).ISBN 3-9805748-7-3:197-202.

[58] Wazen, Rima M., et al. "Initial evaluation of bone ingrowth into a novel porous titanium coating." *Journal of Biomedical Materials Research Part B: Applied Biomaterials* 94.1 (2010): 64-71.

[59] Jin, I., L. D. Kenny, and H. Sang. "Lightweight foamed metal and its production." *International Patent Application WO91/03578* 21 (1991).

[60] Thomas, M., and L. D. Kenny. "Production of particle-stabilized metal foams." *PCT Patent WO* 94.017218 (1994): 21.

[61] Von Zeppelin, F., et al. "Desorption of hydrogen from blowing agents used for foaming metals." *Composites Science and Technology* 63.16 (2003): 2293-2300.

[62] Gui, M. C., et al. "Deformation and damping behaviors of foamed Al–Si–SiCp composite." *Materials Science and Engineering: A* 286.2 (2000): 282-288.

[63] Huang, Li, et al. "Effects of scandium additions on mechanical properties of cellular Al-based foams." *Intermetallics* 28 (2012): 71-76.

[64] Yang, Dong-Hui, et al. "Compression properties of cellular AlCu5Mn alloy foams with wide range of porosity." *Journal of materials science* 44 (2009): 5552-5556.

[65] Aguirre-Perales, Lydia Y., In-Ho Jung, and Robin AL Drew. "Foaming behavior of powder metallurgical Al–Sn foams." *Acta Materialia* 60.2 (2012): 759-769.

[66] Rabiei, A., Adrian T. O'Neill, and Brian P. Neville. "Processing and development of a new high strength metal foam." *MRS Online*

Proceedings Library (OPL) 851 (2004): NN11-4.

[67] [67] Prabhu, B., et al. "Synthesis and characterization of high volume fraction Al–Al2O3 nanocomposite powders by high-energy milling." *Materials Science and Engineering: A* 425.1-2 (2006): 192-200.

[68] Du, Y., et al. "Enhancement of the mechanical strength of aluminum foams by SiC nanoparticles." *Materials Letters* 148 (2015): 79-81.

[69] Zhang, Zan, et al. "Fabrication and characterization of closed-cell aluminum foams with different contents of multi-walled carbon nanotubes." *Materials & Design* 88 (2015): 359-365.

[70] Wang, Jiwei, et al. "A novel approach to obtain in-situ growth carbon nanotube reinforced aluminum foams with enhanced properties." *Materials Letters* 161 (2015): 763-766.

[71] Liu, Jiaan, et al. "Effect of Al2O3 short fiber on the compressive properties of Zn–22Al foams." *Materials Letters* 62.21-22 (2008): 3636-3638.

[72] Liu, J. A., et al. "Deformation and energy absorption characteristic of Al2O3f/Zn–Al composite foams during compression." *Journal of alloys and compounds* 506.2 (2010): 620-625.

[73] Vinod Kumar, G. S., et al. "Foamability of MgAl 2 O 4 (Spinel)-reinforced aluminum alloy composites." *Metallurgical and materials transactions A* 42 (2011): 2898-2908.

[74] Guo, Cheng, et al. "Compressive properties and energy absorption of

aluminum composite foams reinforced by in-situ generated MgAl2O4 whiskers." *Materials Science and Engineering: A* 645 (2015): 1-7.

[75] Carrino, Luigi, et al. "Mechanical performance analysis of hybrid metal-foam/composite samples." *The International Journal of Advanced Manufacturing Technology* 60 (2012): 181-190.

[76] Drolet, J. P. "A novel production method of metal foam." *Int. J. Powder Met* 13 (1977): 223-227.

[77] Kulkarni, S. B., and P. Ramakrishnan. "Foamed aluminium." *J Powder Metall.* 9.1(1973): 41–45.

[78] Product data sheet of SEAC B.V., Netherlands; 1986.

[79] Product data sheet of Sumitomo Electric, Japan; 1986

[80] Paserin, Vladimir, et al. "CVD technique for Inco nickel foam production." *Advanced engineering materials* 6.6 (2004): 454-459.

[81] Torres, Y., et al. "Processing, characterization and biological testing of porous titanium obtained by space-holder technique." *Journal of Materials Science* 47 (2012): 6565-6576.

[82] Limper, Alexander, et al. "Two-level porosity electrodes from metal-polymer dispersions." *Electrochemistry Communications* 135 (2022): 107205.

[83] Yu, Xiang, Zhenbo Lu, and Wei Zhai. "Enhancing the flow resistance and sound absorption of open-cell metallic foams by creating partially-open windows." *Acta Materialia* 206 (2021): 116666.

[84] Singh, R., et al. "Hierarchically structured titanium foams for tissue

scaffold applications." *Acta biomaterialia* 6.12 (2010): 4596-4604.

[85] Dmitruk, Anna, H. Kapłon, and K. Naplocha. "Mechanical and Thermal Properties of Aluminum Foams Manufactured by Investment Casting Method." *Archives of Foundry Engineering* (2022): 37-42.

[86] Movahedi, Nima, et al. "Functionally graded metal syntactic foam: Fabrication and mechanical properties." *Materials & Design* 168 (2019): 107652.

[87] Thiele, K-H. "A contribution to the chemistry of organotransition metal halides." *Pure and Applied Chemistry Fifth* 30.3-4 (1972): 575-586.

[88] Sánchez de la Muela, A. M., et al. "New aluminum syntactic foam: synthesis and mechanical characterization." *Materials* 15.15 (2022): 5320.

[89] Bolat, Çağın, Cem Bekar, and Ali GÖKSENLİ. "Mechanical and physical characteristics of bubble alumina reinforced aluminum syntactic foams made through recyclable pressure infiltration technique." *Gazi University Journal of Science* 35.1 (2022): 184–196.

[90] Spratt, M., Joseph William Newkirk, and K. Chandrashekhara. "Aluminum Matrix Syntactic Foam Fabricated with Additive Manufacturing." (2017): 242.

[91] Rohatgi, Pradeep K., et al. "The synthesis, compressive properties, and applications of metal matrix syntactic foams." *Jom* 63 (2011): 36-42.

[92] Spratt, M., Joseph William Newkirk, and K. Chandrashekhara. "Fabrication of metal matrix syntactic foams by a laser additive

manufacturing process." *Mater Sci Technol Conf Exhibit. 2016; 2* (2016): 1319-1326.

[93] Neville, B. P., and A. Rabiei. "Composite metal foams processed through powder metallurgy." *Materials & Design* 29.2 (2008): 388-396.

[94] Rabiei, A., and At T. O'Neill. "A study on processing of a composite metal foam via casting." *Materials Science and Engineering: A* 404.1-2 (2005): 159-164.

[95] Rabiei, Afsaneh. "Composite metal foam and methods of preparation thereof." U.S. Patent No. 9,208,912. 8 Dec. 2015.

[96] Májlinger, Kornél, and Imre Norbert Orbulov. "Characteristic compressive properties of hybrid metal matrix syntactic foams." *Materials Science and Engineering: A* 606 (2014): 248-256.

[97] Bálint, Attila, and Attila Szlancsik. "Mechanical properties of iron hollow sphere reinforced metal matrix syntactic foams." *Materials Science Forum*. Vol. 812. Trans Tech Publications Ltd, 2015.

[98] Orbulov, Imre Norbert, et al. "Compressive mechanical properties of low-cost, aluminium matrix syntactic foams." *Composites Part A: Applied Science and Manufacturing* 135 (2020): 105923.

[99] Matijasevic-Lux, B., et al. "Modification of titanium hydride for improved aluminium foam manufacture." *Acta Materialia* 54.7 (2006): 1887-1900.

[100] Nawaz, A., and Rani, S. "Fabrication and evaluation of percent

porosity and density reduction of aluminium alloy foam." *Materials Today: Proceedings* 47 (2021): 6025-6029.

[101] Rajak, D. K., L. A. Kumaraswamidhas, and S. Das. "Investigation and characterisation of aluminium alloy foams with TiH2 as a foaming agent." *Materials Science and Technology* 32.13 (2016): 1338-1345.

[102] Li, Da-Wu, et al. "Preparation and characterization of aluminum foams with ZrH2 as foaming agent." *Transactions of Nonferrous Metals Society of China* 21.2 (2011): 346-352.

[103] Karuppasamy, R., et al. "Investigation on the effect of aluminium foam made of A413 aluminium alloy through stir casting and infiltration techniques." *International Journal of Materials Engineering Innovation* 11.1 (2020): 34-50.

[104] Nawaz, A., and Rani, S. "Fabrication methods and property analysis of metal foams–a technical overview." *Materials Science and Technology* (2023): 1-26.

[105] Asadi Zeidabady, M., M. Tajally, and E. Emadoddin. "Manufacturing of copper foams through accumulative roll bonding (ARB) process: structure and damping capacity behavior." *Canadian Metallurgical Quarterly* 54.2 (2015): 198-204.

[106] Ip, S. W., S. W. Wang, and J. M. Toguri. "Aluminum foam stabilization by solid particles." *Canadian metallurgical quarterly* 38.1 (1999): 81-92.

[107] Madgule, Mahadev, et al. "Influence of foaming agents on mechanical

and microstructure characterization of AA6061 metal foams." *Proceedings of the Institution of Mechanical Engineers, Part E: Journal of Process Mechanical Engineering* (2022): 09544089221097534.

[108] Kosenko, Alexandra, et al. "Structural, electrical, and mechanical properties investigation of open-cell aluminum foams obtained by spark plasma sintering and replication on polyurethane template." *Materials* 15.3 (2022): 931.

[109] Yadav, Raja Yateesh, and E. S. Prakash. "Experimental determination of relative density and percentage porosity of open cell aluminum foam produced from sand salt mould method." *International journal of engineering research & technology (IJERT)* 4.5 (2016).

[110] Gopinathan, Arun, et al. "Investigation of the relationship between morphology and thermal conductivity of powder metallurgically prepared aluminium foams." *Materials* 14.13 (2021): 3623.

[111] Shi, Tong, et al. "Foaming process and properties of 6063 aluminum foams by melt foaming method." *Materials Transactions* 58.2 (2017): 243-248.

[112] Fernández-Morales, P., L. Marulanda-Zapata, and M. Vásquez-Rendón. "Microstructural and corrosion study of aluminum foams obtained by space holder process using low-cost removable preforms." *Journal of applied research and technology* 19.3 (2021): 202-216.

[113] Rathore, Ram Krishna, et al. "Mechanical properties of lightweight aluminium hybrid composite foams (AHCFs) for structural applications." *Advances in Materials and Processing Technologies* 8.4 (2022): 4194-4208.

[114] Youn, S. W., and C. G. Kang. "Evaluation of mechanical properties of porous 6061 alloys fabricated by the powder compression and induction heating process." *Metallurgical and Materials Transactions A* 35 (2004): 2419-2426.

[115] Byakova, Alexandra, et al. "The Mechanical Performance of Aluminum Foam Fabricated by Melt Processing with Different Foaming Agents: A Comparative Analysis." *Metals* 12.8 (2022): 1384.

[116] Nisa, Sharaf U., Sunil Pandey, and P. M. Pandey. "A review of the compressive properties of closed-cell aluminum metal foams." *Proceedings of the Institution of Mechanical Engineers, Part E: Journal of Process Mechanical Engineering* 237.2 (2023): 531-545.

[117] Surace, Rossella, et al. "Application of Taguchi method for the multi-objective optimization of aluminium foam manufacturing parameters." *International journal of material forming* 3 (2010): 1-5.

[118] Surace, R., et al. "Multi-objective optimization of aluminium foam manufacturing parameters." *International journal of simulation modelling* 8.2 (2009): 81-89.

[119] Patel, GC Manjunath, Prasad Krishna, and Mahesh B. Parappagoudar. "Optimization of squeeze cast process parameters using Taguchi and

grey relational analysis." *Procedia Technology* 14 (2014): 157-164.

[120] Mondal, D. P., S. Das, and Nidhi Jha. "Dry sliding wear behaviour of aluminum syntactic foam." *Materials & Design* 30.7 (2009): 2563-2568.

[121] Idriss, AN Md, and S. Kasolang. "The dry sliding wear behaviour of open cell aluminum foam against mild steel." *IOP Conference Series: Materials Science and Engineering*. Vol. 1244. No. 1. IOP Publishing, 2022.

[122] Májlinger, Kornél, et al. "Tribological properties of hybrid aluminum matrix syntactic foams." *Tribology International* 99 (2016): 211-223.

[123] Fu, Wensheng, and Yanxiang Li. "Fabrication, processing, properties, and applications of closed-cell aluminum foams: a review." *Materials* 17.3 (2024): 560.

[124] Hassan, Ahmed, and Ibrahim Abdullah Alnaser. "A Review of Different Manufacturing Methods of Metallic Foams." *ACS omega* 9.6 (2024): 6280-6295.

[125] Grgić K, Lela B, Jozić S, et al. "Aluminium foams made of various aluminium alloys scrap and various foaming agents." Paper presented at the *Mechanical Technology and Structural Materials* (2022):37-42.

[126] Nová, Iva, et al. "Theoretical calculations of the foaming properties of powder agents for the production of aluminium foams." *Manufacturing Technology* 19.1 (2019): 118-122.

[127] Koizumi, Takuya, et al. "Foaming agents for powder metallurgy

production of aluminum foam." *Materials transactions* 52.4 (2011): 728-733.

[128] Hur, Bo Young, Soo Han Park, and Arai Hiroshi. "Viscosity and surface tension of Al and effects of additional element." *Materials Science Forum*. Vol. 439. Trans Tech Publications Ltd, (2003): 51-56.

[129] Matijasevic, Biljana, and John Banhart. "Improvement of aluminium foam technology by tailoring of blowing agent." *Scripta Materialia* 54.4 (2006): 503-508.

[130] Babcsán, N., D. Leitlmeier, and J. Banhart. "Metal foams—high temperature colloids: Part I. Ex situ analysis of metal foams." *Colloids and Surfaces A: Physicochemical and Engineering Aspects* 261.1-3 (2005): 123-130.

[131] Nikitha DS, Karthik SB, Kishore. "Development and evaluation of density and porosity of aluminium foams." *International Journal of Research in Engineering and Technology* (2015); ISSN: 2321-7308.

[132] Kumar, B. Ashok, C. Naga Kumar, and V. Chengal Reddy. "Production of low cost aluminium foams." *International Journal of Current Engineering and Technology, INPRESCO, ISSN* 2277 (2014): 4106.

[133] Xia, Xingchuan, et al. "Compressive properties of closed-cell aluminum foams with different contents of ceramic microspheres." *Materials & Design (1980-2015)* 56 (2014): 353-358.

[134] Xia, Xingchuan, et al. "Effect of homogenizing heat treatment on the

compressive properties of closed-cell Mg alloy foams." *Materials & Design* 49 (2013): 19-24.

[135] Yang, Wei Han, et al. "Mechanical properties and energy absorption capability of closed-cell Al alloy foam." *Advanced Materials Research* 450 (2012): 325-328.

[136] Farahani, Mohammad Reza, Hamid Reza Rezaei Ashtiani, and S. H. Elahi. "Effect of zinc content on the mechanical properties of closed-cell aluminum foams." *International Journal of Metalcasting* 16.2 (2022): 713-722.

[137] Shi, Tong, et al. "Microstructure and compressive properties of aluminum foams made by 6063 aluminum alloy and pure aluminum." *Materials transactions* 59.4 (2018): 625-633.

[138] El Sayed, Ziad, Mohamed Abd-Alrazzaq, and M. Hamed Ahmed. "Experimental investigation of infiltration casting process parameters to produce open-cell Al-A356 alloy foams for functional and mechanical applications." *The International Journal of Advanced Manufacturing Technology* 119.9-10 (2022): 6761-6774.

[139] Rajak, D. K., L. A. Kumaraswamidhas, and S. Das. "Investigation and characterisation of aluminium alloy foams with TiH2 as a foaming agent." *Materials Science and Technology* 32.13 (2016): 1338-1345.

[140] Omar, Mohammed Yaseer, et al. "Data characterizing flexural properties of Al/Al2O3 syntactic foam core metal matrix sandwich." *Data in Brief* 5 (2015): 564-571.

[141] Rabiei, Afsaneh, et al. "Processing and characterization of a new composite metal foam." *Materials transactions* 47.9 (2006): 2148-2153.

[142] Hu, Lei, et al. "Characterization of as-cast microstructure of aluminum foams by melt foaming method." *Materials Letters* 308 (2022): 131112.

[143] Manakari, Vyasaraj, et al. "Dry sliding wear of epoxy/cenosphere syntactic foams." *Tribology International* 92 (2015): 425-438.

[144] Shukla, Amarish Kumar, and J. Dutta Majumdar. "Studies on wear behavior of aluminium foam developed by spray forming route." *Materials Today: Proceedings* 19 (2019): 532-535.

[145] Mondal, D. P., et al. "Cenosphere filled aluminum syntactic foam made through stir-casting technique." *Composites Part A: Applied Science and Manufacturing* 40.3 (2009): 279-288.

[146] Cree, D., and Martin Pugh. "Dry wear and friction properties of an A356/SiC foam interpenetrating phase composite." *Wear* 272.1 (2011): 88-96.

[147] Liu, Jing, Jon Binner, and Rebecca Higginson. "Dry sliding wear behaviour of co-continuous ceramic foam/aluminium alloy interpenetrating composites produced by pressureless infiltration." *Wear* 276 (2012): 94-104.

[148] Harders, Harald, Knut Hupfer, and Joachim Rösler. "Influence of cell wall shape and density on the mechanical behaviour of 2D foam

structures." *Acta materialia* 53.5 (2005): 1335-1345.

[149] Jha, Nidhi, et al. "Sliding wear behaviour of aluminum syntactic foam: A comparison with Al–10 wt% SiC composites." *Tribology International* 44.3 (2011): 220-231.

LIST OF PUBLICATIONS AND THEIR PROOFS

Research Papers Published/ Accepted In Journals

[1] Nawaz, Ali, and Sushila Rani. "Fabrication methods and property analysis of metal foams–a technical overview." *Materials Science and Technology* (2023):1-26. DOI:10.1080/02670836.2023.2186068. **(SCIE Indexed Journal)**.

[2] Nawaz, Ali, and Sushila Rani. "Fabrication, properties evaluation, and process optimization of aluminium 6063 alloy foam: Fabrication, évaluation des propriétés et optimisation du procédé de mousse en alliage d'aluminium 6063." *Canadian Metallurgical Quarterly* (2023): 1-16. DOI: 10.1080/00084433.2023.2233737. **(SCIE Indexed Journal)**.

[3] Nawaz, Ali, and Sushila Rani. "Microstructure and Wear Behavior Characterization of Stir-Cast Aluminium 6063 Alloy and its Foam: A Comparative Study." *Surface Review and Letters* (2024): https://doi.org/10.1142/S0218625X24500707. **(SCIE Indexed Journal)**.

Research Papers Presented in International Conferences

[1] Ali Nawaz, Sushila Rani. A review on fabrication methods and analysis of mechanical properties of metal foams. "2nd International Conference on Recent Trends in Engineering and Scientific Technology" held on 21St March 2020 at Rathinam Technical Campus, Coimbatore, India.

[2] Ali Nawaz, Sushila Rani. Fabrication and evaluation of percent porosity and density reduction of aluminium alloy foam. 1st International Conference on "Technology Innovation in Mechanical Engineering" (TIME-2021) organized by the Department of Mechanical Engineering, Sagar Institute of Science & Technology, Gandhi Nagar, Bhopal, India during 10-11 May 2021.

MATERIALS SCIENCE AND TECHNOLOGY
https://doi.org/10.1080/02670836.2023.2186068

I·M3 Institute of Materials, Minerals & Mining

Taylor & Francis

Fabrication methods and property analysis of metal foams – a technical overview

Ali Nawaz and Sushila Rani

Department of Mechanical Engineering, Delhi Technological University, Delhi, India

ABSTRACT

In recent years, metal foams have emerged as the most advanced materials for structural, thermal, and sound insulation purposes. Metal foams have more exciting properties than other lightweight materials, such as higher deformation resistance, compressive strength, and crashworthiness. This review article highlights various conventional and non-conventional manufacturing methods of metal foams under direct and indirect foaming techniques. Non-conventional methods of metal foam fabrication, such as additive manufacturing, novel methods, and metal syntactic foaming have been described in detail. A detailed review of foaming agents, space holders, and filler particles utilised in the metal foaming process is provided. Recent advancements in the metal foam coating process and coating materials have also been discussed.

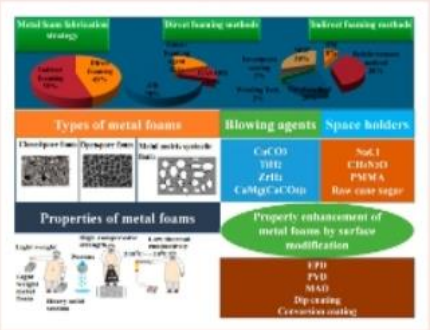

ARTICLE HISTORY
Received 13 October 2022
Revised 22 February 2023
Accepted 25 February 2023

KEYWORDS
Metal foam; precursor; investment casting; foaming agent; mechanical properties; metal foam coatings; additive manufacturing

Introduction

At the beginning of twentieth century, researchers paid their attention to porous composite materials, and the patent by French researchers in 1925AD initialised the path towards the fabrication of porous materials [1]. From the 1950s to the 1970s, a large number of patents were issued, and various types of foaming processes were discovered and proposed [2]. In the late 1980s, researchers re-established some of the old techniques of metal foam fabrication and discovered new ones. In the beginning, many companies conducted in house research in their laboratories and published their work. In 1990, Fraunhofer-Institute in Bremen worked in the field of metal foam fabrication and re-established old powder-based foam fabrication technique [3,4]. The advent of twenty-first century brought new advancements in metal foam fabrication techniques. It was established that the foremost fabrication methods of metal foams are based on liquid state, solid state, vapour deposition, and electro-deposition processing techniques [5]. It was suggested that the quality of metal foams depends on many factors such as porosity, density, cell structure and distribution, grain size and distribution and foaming process involved, and so on [6,7]. The main problem encountered was to understand how metal foams are stabilised and how their stability can be enhanced to produce reliable metal foams. The stabilisation mechanism of metal foams during foaming is studied under the term high-temperature colloid chemistry in the field of aqueous foam physics [8]. Recent developments, applications, new methods of metal foam characterisation, and property analysis have been discussed in detail [9].

CONTACT Ali Nawaz alinawaz_2k18phdme502@dtu.ac.in; aliamu200@gmail.com Department of Mechanical Engineering, Delhi Technological University, Delhi, 110042, India

CANADIAN METALLURGICAL QUARTERLY
https://doi.org/10.1080/00084433.2023.2233737

Fabrication, properties evaluation, and process optimization of aluminium 6063 alloy foamFabrication, évaluation des propriétés et optimisation du procédé de mousse en alliage d'aluminium 6063

Ali Nawaz and Sushila Rani

Department of Mechanical Engineering, Delhi Technological University, Delhi, India

ABSTRACT

Aluminium alloy foams can be fabricated through various conventional and non-conventional foaming methods. In this research work, aluminium 6063 alloy foam was fabricated through stir casting using aluminium 6063 alloy as the base metal and varying amounts of titanium hydride as a foaming agent. The structural and mechanical properties of the fabricated foam were evaluated experimentally. The foam fabrication process was optimised through the Taguchi method coupled with grey relational analysis. The optimised process parameter setting for the foam fabrication was 2 wt.% titanium hydride, 650°C titanium hydride mixing temperature, and 8 min of stirring time. The corresponding values of the optimised response variables were 53.15% porosity, 33.3 MJ/m^3 energy absorption, and 25.97 MPa flexural strength.

On peut fabriquer les mousses en alliage d'aluminium par diverses méthodes de moussage conventionnelles et non conventionnelles. Dans ce travail de recherche, on a fabriqué une mousse en alliage d'aluminium 6063 par coulée avec agitation en utilisant un alliage d'aluminium 6063 comme métal de base et diverses quantités d'hydrure de titane comme agent moussant. On a évalué expérimentalement les propriétés structurelles et mécaniques de la mousse fabriquée. On a optimisé le procédé de fabrication de la mousse à l'aide de la méthode de Taguchi couplée à l'analyse relationnelle grise. Le réglage optimisé des paramètres du procédé pour la fabrication de la mousse incluait 2% en poids d'hydrure de titane, température de mélange de l'hydrure de titane de 650°C et durée d'agitation de 8 minutes. Les valeurs correpondantes des variables de la réponse optimisées étaient une porosité de 53.15%, une absorption d'énergie de 33.3 MJ/m^3 et une résistance à la flexion de 25.97 MPa.

ARTICLE HISTORY
Received 12 April 2023
Accepted 2 July 2023

KEYWORDS
Aluminium 6063 alloy foam; stir casting; titanium hydride; metal foam porosity; multi-response optimisation

1. Introduction

The metal foam market is expanding rapidly, and its demand is rising sharply worldwide. Aluminium alloy foams are fabricated mainly through direct and indirect foaming techniques based on the melt route method. A broad review of metal foam fabrication methods, property analysis, and applications in different sectors was presented [1]. It was suggested that direct or indirect foaming methods could be employed for the liquid-state processing of metal foams; however, gaseous or ionised processing can be employed by electro-deposition or metal vapour deposition methods. A detailed review of the pore formation mechanism, pore-generating agents, mechanical property analysis, and applications of porous materials was presented [2]. They deduced that closed or open-cell metallic foams could be fabricated using different foaming agents through the powder metallurgy (PM) process.

Aluminium alloy foam was fabricated using aluminium powder with a foaming agent through mould foaming [3]. It was observed that the relative density of the fabricated foam varied from 0.2 to 0.3 depending on the steel pipe cooling rate. The aluminium foam fabricated by the mould foaming method has high compressive resistance. Closed-cell Al-Mg alloy foam was fabricated by the PM process, in which intermetallics were formed due to aluminium addition [4]. They found that the foaming temperature and time for uniform pore generation were 620°C and 150 s, respectively. It was also found that the mechanical properties of fabricated foam were better than those of aluminium-base foams. However, the formation of intermetallics adversely affected the yielding strength of the resultant foam. ADC12 Al–Si-Cu aluminium foam sandwiches were fabricated using ADC6 Al-Mg as face plates through a friction stir welding process using ADC12 Al–Si-Cu as precursor material [5]. ADC12

CONTACT Ali Nawaz alinawaz_2k18phdme502@dtu.ac.in, aliamu200@gmail.com Department of Mechanical Engineering, Delhi Technological University, Main Bawana Road, Shahbad Daulatpur Village, Rohini, New Delhi, Delhi 110042

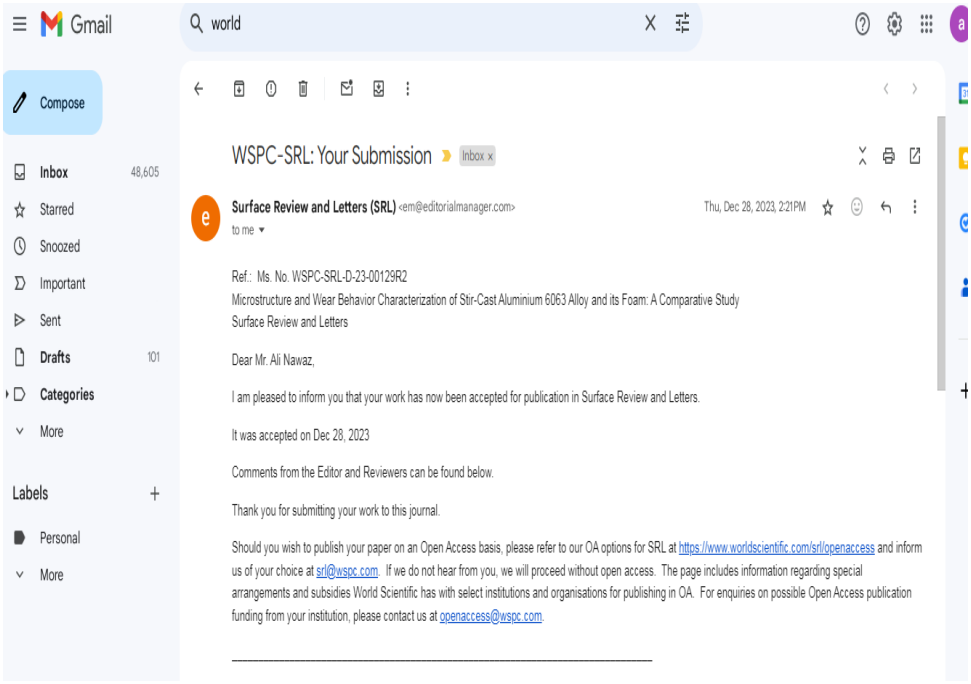
Gmail
world
Compose
Inbox 48,605
Starred
Snoozed
Important
Sent
Drafts 101
Categories
More
Labels
Personal
More
WSPC-SRL: Your Submission
Inbox x
Surface Review and Letters (SRL) <em@editorialmanager.com>
to me
Thu, Dec 28, 2023, 2:21PM
Ref.: Ms. No. WSPC-SRL-D-23-00129R2
Microstructure and Wear Behavior Characterization of Stir-Cast Aluminium 6063 Alloy and its Foam: A Comparative Study
Surface Review and Letters
Dear Mr. Ali Nawaz,
I am pleased to inform you that your work has now been accepted for publication in Surface Review and Letters.
It was accepted on Dec 28, 2023
Comments from the Editor and Reviewers can be found below.
Thank you for submitting your work to this journal.
Should you wish to publish your paper on an Open Access basis, please refer to our OA options for SRL at https://www.worldscientific.com/srl/openaccess and inform us of your choice at srl@wspc.com. If we do not hear from you, we will proceed without open access. The page includes information regarding special arrangements and subsidies World Scientific has with select institutions and organisations for publishing in OA. For enquiries on possible Open Access publication funding from your institution, please contact us at openaccess@wspc.com.

2nd International Conference on recent Trends in Engineering and Scientific Technology - 2020

ORGANIZED BY

RATHINAM TECHNICAL CAMPUS

(Affiliated to Anna University, approved by AICTE and Recognized UGC under section 2(f))

RATHINAM SCHOOL OF ARCHITECTURE

Rathinam Techzone, Pollachi Main Road, Eachanari, Coimbatore, India.

IN ASSOCIATION WITH

ORGANIZATION OF SCIENCE & INNOVATIVE ENGINEERING AND TECHNOLOGY (OSIET), CHENNAI, INDIA.

Certificate of Presentation

This is to certify that Ali Nawaz from Delhi Technological University has presented a paper titled A review on fabrication methods and analysis of mechanical properties of metal foams in the "2nd International Conference on recent Trends in Engineering and Scientific Technology" held on 21st March 2020

Dr. P. Aravinthan, M.E., Ph.D
Technical Lead OSIET
Secretary

Dr. S.Vijayakumar, M.Tech., Ph.D
Vice-Chairman
IEEE Product Safety Engineering Society, Madras Chapter

Dr. K.Shivkumar, M.E., Ph.D
Principal
Rathinam Technical Campus

TIME-2021

Lecture Notes in Mechanical Engineering

Certificate of Participation

This is to Certify that

Ali Nawaz

Participated and presented a paper titled "Fabrication and evaluation of percent porosity and density reduction of aluminium alloy foam " in the 1st International Conference on "Technology Innovation in Mechanical Engineering" (TIME-2021) organized by the Department of Mechanical Engineering, Sagar Institute of Science & Technology, Gandhi Nagar, Bhopal, India during 10th-11th May 2021.

Prof. Mousam Sharma, Coordinator | Dr. Rashmi Dwivedi, Coordinator | Dr. Prem Chaurasiya, Organizing Secretary | Dr. Ravishanker V Choudri, HOD, ME Dept.,SISTec | Dr. Keshavendra Choudhary, Principal, SISTec

DELHI TECHNOLOGICAL UNIVERSITY

(Formerly Delhi College of Engineering)
Shahbad Daulatpur, Main Bawana Road, Delhi-42

PLAGIARISM REPORT

Title of the Thesis: Characterization and Tribo-Mechanical Analysis for Fabricated Aluminium Alloy Foam

Total Pages:

Name of the Scholar: ALI NAWAZ

Supervisor: Dr. SUSHILA RANI

Department: Mechanical Engineering, DTU, Delhi, India

This is to report that the above thesis was scanned for similarity detection. Process and outcome is given below:

Software used: **Similarity Index:** **Total Word Count:**

Date:

Candidate's Signature **Signature of Supervisor**

(Ali Nawaz) **(Dr. Sushila Rani)**

CURRICULUM VITAE

MR. ALI NAWAZ has obtained his B.E (Mechanical Engineering) and M.Tech (Industrial & Production Engineering) Degrees from Aligarh Muslim University, Aligarh, Uttar Pradesh, India. He has worked as Lecturer in Glocal University, Saharanpur, Uttar Pradesh, India. He has four year of Teaching Assistantship experience at undergraduate and post graduate levels. He is currently working as Guest Lecturer in Department of Mechanical Engineering, Delhi Technological University, Delhi, India. He is actively engaged in teaching and research activities. He has published four research papers in International Journals. He has also presented five research papers at International Conferences. He is currently working in the area of Metal foams, Metal Matrix Composites, Process Optimization, and Optimization Techniques.